university of groningen

University Medical Center Groningen

University of Groningen

Distinguishing and connecting self and others

Cui, Fang

IMPORTANT NOTE: You are advised to consult the publisher's version (publisher's PDF) if you wish to cite from it. Please check the document version below.

Document Version
Publisher's PDF, also known as Version of record

Publication date:
2013

Link to publication in University of Groningen/UMCG research database

Citation for published version (APA):
Cui, F. (2013). *Distinguishing and connecting self and others: a social neuroscience perspective*. s.n.

Copyright
Other than for strictly personal use, it is not permitted to download or to forward/distribute the text or part of it without the consent of the author(s) and/or copyright holder(s), unless the work is under an open content license (like Creative Commons).

The publication may also be distributed here under the terms of Article 25fa of the Dutch Copyright Act, indicated by the "Taverne" license. More information can be found on the University of Groningen website: https://www.rug.nl/library/open-access/self-archiving-pure/taverne-amendment.

Take-down policy
If you believe that this document breaches copyright please contact us providing details, and we will remove access to the work immediately and investigate your claim.

Downloaded from the University of Groningen/UMCG research database (Pure): http://www.rug.nl/research/portal. For technical reasons the number of authors shown on this cover page is limited to 10 maximum.

Download date: 11-12-2022

DISTINGUISHING & CONNECTING

Self Other

FANG CUI
崔 芳

Distinguishing and Connecting Self and Others

A social neuroscience perspective

Fang Cui

Groningen, December 9th 2013

rijksuniversiteit groningen

Distinguishing and Connecting Self and Others

A social neuroscience persepective

Proefschrift

ter verkrijging van het doctoraat in de

Medische Wetenschappen

aan de Rijksuniversiteit Groningen

op gezag van de

Rector Magnificus, dr. E. Sterken,

in het openbaar te verdegigen op

maandag 9 december 2013

om 11:00 uur

door

Fang Cui

geboren op 26 augustus 1982

te Shanxi, China

Promotor	:	Prof. dr. C.M. Keysers
Copromotor	:	Dr. V. Gazzola

Beoordelingscommissie	:	Prof. dr. T. Singer (Max Planck Institut Leipzig)
		Prof. dr. M. Brass (University Gent)
		Prof. dr. C. Lamm (University of Vienna)

ISBN printed version: 978-90-367-6551-0
ISBN digital version: 978-90-367-6550-3

Table of Contents

Introduction

Aristotle said: “Man is by nature a social animal; an individual who is unsocial naturally and not accidentally is either beneath our notice or more than human.” To successfully perform in daily social interactions, we need two “opposite” skills: to distinguish between oneself and others and to connect oneself with others. Lack of either of them will result in chaos or dysfunction in social life. In this thesis, together with my collaborators, I first examined the aspect of distinguishing self and other by examining how human brains distinguish between active movements and passive movements, or, in other words, how the brain identifies if a body movement is generated by its own motor command or by external forces. Then, I examined how people connect by examining how our brain shares the actions and emotions (pain) of others and how certain factors modulate these vicarious feelings.

Who makes me move?

A common experience to most of you is that you can be tickled but you cannot tickle yourself. When your hand prepares to tickle, the motor command generated in the premotor cortex (PM) in your brain is sent to the body parts performing the action. At the same time, this motor command will also be sent to the somatosensory cortices as an efference-copy, where the forward internal models will predict the expected sensory consequences. This efference-copy is thought to be sent by the supplementary motor areas (SMA) (Haggard and Whitford, 2004). So when you try to tickle yourself, the efference-copy that reaches your somatosensory cortex makes your brain predict the sensory consequences of the coming action. Then, the predicted sensory outcome will be cancelled (Blakemore et al., 2000;Wolpert, 1997;Blakemore et al., 1998;Tsakiris and Haggard, 2003). However, if the tickling is done by others, there will not be an efference-copy send to the somatosensory cortex, so the sensory outcome of the tickling will not be cancelled. Because of this mechanism, we can distinguish whether a sensation is caused by actions performed by ourselves or by others.

Another important distinction is whether a body part is moved actively by our own will or passively by outside forces. The somatosensory evoked potentials (SEPs) produced by electrical stimulation of the median nerve were found to be reduced during active movements but not during passive movements (Lee and White, 1974). However, another study found no difference between active and passive finger movements on the following SEP components: N11, N13 and later cerebral SEP component (Abbruzzese et al., 1981). One explanation for these results is that the modifications of SEPs observed during movement are likely to depend mainly on the activation of muscle spindle endings that sense the stretching of the muscle, irrespectively of whether the stretch was active or passive (Abbruzzese et al., 1981). Another study used positron emission tomography (PET) to compare the regional cerebral blood flow (rCBF) during active and passive flexion of the elbow. Differences in activation were found only in the basal ganglia and the cingulated gyrus, but no differences were found in the primary sensorimotor cortex, SMA and inferior partial cortex (Weiller et al., 1996). Another PET study compared brain activation between an auditory-cued active finger movement and a servo-motor driven passive finger movement. The authors report that active movement was associated with activation of the contralateral primary sensorimotor cortex, PM, SMA, bilateral secondary somatosensory areas and basal ganglia and the ipsilateral cerebellum. In contrast, only the contralateral primary and secondary somatosensory areas were activated by the passive movement (Mima et al., 1999). It has also been argued that the differences in brain activation evoked by active and passive movements are too small for consistent detection using PET (Weiller et al., 1996). In functional magnetic resonance imaging (fMRI) studies on this topic, significant activation of contralateral rolandic regions, SMA, the PMC, and the ipsilateral cerebellum are usually found during voluntary movements (Ball et al.,

1999;Freund, 2002;Newton et al., 2005;Kapreli et al., 2006). One fMRI study found that compared to active movement, passive movement only activated somatosensory areas but not the motor, PM and cerebellar areas (Agnew and Wise, 2008). In order to further address this question, in the first study presented in this thesis, Blood-Oxygen-Level-Dependent (BOLD) signals and electromyogram (EMG) data were recorded simultaneously in order to allow a quantitative comparison of brain activity (fMRI) as a function of how active the movement was (EMG). We asked the participants to squeeze a ball made of soft materials actively, and in a different condition, to let the experimenter squeeze the participant's hand so as to squeeze the ball passively. We found that the EMG signal, which works as a proxy of motor activity (and hence the efference-copy), predicted the BOLD activity in the primary somatosensory regions, mainly Brodmann area (BA) 2. It can be inferred from this result that active and passive movements can be distinguished by our brain. Additional connectivity analyses identified a stronger signal from the motor cortices as a significant force contributes to the differential BA2 activation during active movement and passive movement. We can tell from the results that the crosstalk between motor and sensory regions helps us distinguish sensations caused by our own body movements from those caused by external forces (Chapter 2).

Mirror Neurons: from Monkey to Human being

Based on our daily experience, when we perceive another person's actions we can often instantly understand what they are doing and predict what they are going to do next with high accuracy. This ability is necessary for our own survival because it allows us to process information from others' behaviour and to adjust our own behaviour accordingly. "What neural mechanism underlies this ability?" has been a question for neuroscientists for years.

The discovery of mirror neurons in monkeys

In 1992, a research paper published in the journal Experimental Brain Research shed new light onto this mystery (di Pellegrino et al., 1992). In this study, neurons in area F5 in the brains of macaques were found to activate both when the monkey grasped an object and when the monkey observed the experimenter performing the same action. In following years, this result has been strongly confirmed and these neurons' properties were studied in depth (Gallese et al., 1996;Rizzolatti et al., 1996;Kohler et al., 2002;Keysers et al., 2003;Ishida et al., 2010). These neurons, that discharge both during action execution and action observation in monkeys, were named "mirror neurons" because through them, the brain of the observer "mirrors" the activity in the brain of the observed (Gallese et al., 1996). It has been proposed that the discharges of mirror neurons represent the neuronal correlate of an internal representation of the observed motor actions; this representation is mapping the observed motor action onto the observer's own motor repertoire. By activating during action observation the same neurons that discharge during self-actions, we match the visual representation of this observed action onto its motor representation and it has been proposed that that would lead to understanding the visual stimulus quickly and precisely (Gallese et al., 1996;Rizzolatti et al., 1999;Rizzolatti et al., 1996). The discovery of mirror neurons in monkey offers strong neurophysiologic support for simulation theories which propose that we understand other people by transforming their actions into our own motor-representation of the respective action. Thereby, we internally simulate doing this action (Gallese and Sinigaglia, 2011;Gallese and Goldman, 1998;Gallese, 2007;Casile, 2013).

Mirror neurons in the human brain

These results make us wonder if this mechanism also exists in humans. Do mirror neurons also exist in human brains and enable us to understand and predict the actions of others? Since single-unit neuron recordings are not typically performed on humans, most evidence that support the existence of a functionally analogous system to the macaque mirror neurons in the human brain comes from indirect measures (Iacoboni and Mazziotta,

2007;Iacoboni et al., 1999;Iacoboni et al., 2005;Oberman et al., 2007;Dinstein et al., 2007;Gazzola and Keysers, 2009;Rizzolatti et al., 2009;Perlovsky and Ilin, 2013). The majority of studies, that target on mirror neurons in the human brain, use fMRI or Electroencephalography (EEG).

In a typical paradigm used in fMRI studies studying mirror neuron, subjects are presented with visual stimuli showing a person executing an action in one session (action observation) and instructed to perform an equivalent action in the scanner in a second session (action execution). The actions usually involve relatively simple hand actions like reaching or grasping an object. Then the brain activation during action execution and observation are compared. The voxels that activated during both conditions compared to respective control conditions are seen as candidate locations for mirror neurons and sometimes called “shared voxels” (sVx) (Gazzola and Keysers, 2009;Grezes et al., 2003;Dinstein et al., 2007;Iacoboni et al., 2005;Arnstein et al., 2011). Shared voxels were found in the ventral premotor cortex, the human equivalent to area F5 in macaques (Gallese et al., 1996;Rizzolatti et al., 1996), but also in a number of other brain regions, including the dorsal premotor cortex, the SMA, SI, the inferior parietal cortex and the cerebellum (see Gazzola and Keysers, 2009; and Caspers et al. 2010 for a meta-analysis (Caspers et al., 2010)). Each voxel consists of thousands of neurons, the activation of one sVx may thus be caused by the same neurons during action observation and execution (mirror neurons); it may however also be caused by the activation of different neurons during action observation and execution, that simply occupy space within the same voxel. Therefore, the sVx found in fMRI studies cannot directly prove the existence of mirror neurons in the human brain (Gazzola and Keysers, 2009)

Another technique widely used is EEG. EEG typically quantifies the activity of the mirror neuron system (MNS) using the modulation of a ~10 Hz rhythm (usually named mu/μ rhythm, although it actually is the lower mu-rhythm – a higher frequency my-rhythm in the beta range also exists) recorded over the sensorimotor cortex. Mu is measured while participants observe hand actions and while repeatedly executing the same action themselves (Pineda et al., 2000;Oberman et al., 2005;Southgate et al., 2009). Mu power is found to decrease during both action observation and execution (Perry et al., 2011;Oberman et al., 2008;Warreyn et al., 2013;Muthukumaraswamy and Johnson, 2004;Muthukumaraswamy et al., 2004). The suppression of the mu rhythm during action observation akin to that found during execution is thought to reflect the activation of the mirror neuron system (MNS) (Salmelin et al., 1995;Ohara et al., 2000;Oberman et al., 2005;Oberman et al., 2007;Caetano et al., 2007). However, whether the sVx of fMRI experiments are the cause of the mu-suppression measured using EEG in the human brain remained unclear. In order to answer this question, we simultaneously measured EEG and fMRI during action observation and action execution and then correlated the mu suppression in the EEG with the BOLD effect in the fMRI signal. Our results suggest that mu suppression EEG indeed measures activity of regions associated with the MNS, including the inferior partial lobule and the dorsal premotor cortex but not BA44 as suggested by earlier studies. This study is the first to combine the two techniques to study the MNS and offers much-needed support for the fact that the two measures probe at least overlapping brain regions (Arnstein et al., 2011) (Chapter 3).

It is worth mentioning that Mukamel et al. (Mukamel et al., 2010) provide the critical direct electrophysiological evidence that humans have mirror neurons (Keysers and Gazzola, 2010). This study offers direct and powerful evidence to the existence of mirror neurons at least in some locations of the human brain, although that study cannot detail where humans have mirror neurons

In monkeys, mirror neurons have been proposed to facilitate action understanding (Rizzolatti and Craighero, 2004). In humans, it is suggested that the MNS not only represents the physical aspects of the actions but also the underlying intentions, thoughts and feelings that motivated that action (Rizzolatti and Sinigaglia, 2007). It is thought to be at the basis of many social functions such as imitation (Iacoboni et al., 1999;Caspers et al., 2010), action prediction (Cooper, 2006;Kilner et al., 2007;Lamm et al., 2007b), language learning (Perlovsky and Ilin, 2013;Hamzei et al., 2003;Cooper, 2006;Chen and Yuan, 2008;Knapp and Corina, 2010), theory of mind (Agnew

et al., 2007) and, as we will see in the next section, that similar neurons in limbic and somatosensory cortices could form the neural basis of empathy for sensation and emotions (Keysers et al., 2004;Blakemore et al., 2005;Morrison et al., 2004;Singer et al., 2004;Jackson et al., 2005;Lamm et al., 2007c;Morrison et al., 2012).

Expanding the mirror: from action to sensation and emotion

As social animals, successful social interactions not only require us to understand and to predict other's action. We also need to understand their sensations and emotions. The ability to share the feelings of others is sometimes loosely referred to as "empathy" (Singer, 2006). The discovery of MNS for actions inspired research towards understanding of the neural basis of empathy. The simulation theory that suggests that attributors use their own mental mechanisms to calculate and predict the mental processes of others may also be applicable to empathy (Gallese, 2003;Gallese et al., 2004;Preston and de Waal, 2002). We might empathically share the states of others because seeing their affective states triggers representations of corresponding states in our own brain. In other words, we may also recruit brain regions responsible for our own sensations and emotions while we perceive those of others (Keysers and Gazzola, 2009).

Mirroring other's sensations

Results from fMRI studies seem to support this hypothesis. The patter of brain activation when participants are being touched and when the participants observe someone else being touched were compared. The results show that some of the voxels that got activated in the first condition also got activated in the second condition. These sVx, found during touch experience and observation of touch, are mainly located in SII and sometimes also SI (mainly BA2). This is true while observing legs, hands or faces being touched (Blakemore et al., 2005;Ebisch et al., 2008;Keysers et al., 2004). A special case found in approximately 1% of the population also indirectly supports how strong the observation of tactile sensations can recruit the somatosensory cortices: this mirror-touch-synaesthete report literally feeling touch on their own skin when they see other people being touched. This results a in difficulties to judge where they are being touched when they see other people being touched on a different body part simultaneously (Banissy and Ward, 2007).

Mirroring others emotions

The definition of the word "Empathy" varies a lot amongst researchers. A broad definition given by Preston and De Waal states that "empathy is a super-ordinate category that includes all sub-classes of the phenomena that share the same mechanism, it includes emotional contagion, sympathy, cognitive empathy, helping behaviour, etc" (Preston and de Waal, 2002). R.J.R. Blair also states that empathy subsumes a variety of associated neuro-cognitive processes, including cognitive, motor and emotional empathy (Blair, 2005). Some narrower definitions only focus on the emotional aspect of the "broader empathy". For example, Tania Singer defined empathy as the process by which an individual infers the affective state of another person by generating an isomorphic affective state, while retaining knowledge that the cause of the affective state is the other person (de Vignemont and Singer, 2006;Singer et al., 2004). The operational definition of empathy used in this thesis is close to Singer's definition, although we do not explicitly assess the knowledge that the cause of the affective state is the other person (Singer et al., 2004;de Vignemont and Singer, 2006)

Studies in empathy also support the "shared representation" assumption. In addition to the case of pain, which will be reviewed in next section, in a fMRI study on disgust, the anterior insula (AI) and the anterior cingulated cortex (ACC) were activated both while the participants inhaled odorants producing a strong feeling of disgust and when they observed video clips showing the emotional facial expression of disgust (Wicker et al., 2003). Similarly, the observation and experience of pleasant tastes activate the AI (Jabbi et al., 2007). During a complex emotion like embarrassment, it has been found that the ACC and left AI were strongly implicated in experiencing other's embarrassing misfortunes (Krach et al., 2011).

Studies on empathy that include an emotion experience condition in addition to the observation of other people's emotions provide proof that observing affective states in others activates brain networks also involved in the first-hand experience of these states. This confirms that empathy is, in part, based on shared networks (Preston and de Waal, 2002;de Vignemont and Singer, 2006;Keysers and Gazzola, 2007;Bernhardt and Singer, 2012). In other word, just like observing hand actions activates the observer's motor representation of that action, observing an emotion or a sensation also activates the neural representation of that emotion or sensation (de Vignemont and Singer, 2006;Wicker et al., 2003;Keysers and Gazzola, 2009).

Empathy for pain: shared circuits and social modulation

Pain Matrix

Pain is defined as "a somatic perception containing (1) a bodily sensation with qualities like those reported during actual or potential tissue damaging stimulation; (2) an experienced threat associated with this sensation; and (3) a feeling of unpleasantness or other negative emotion based on this experienced threat" (Price DD, 1999). We can tell from this definition that pain is a complex experience consisting of sensory-discriminative and affective-motivational dimensions. In the past 30 years, researchers have intensively studied which brain areas respond to pain experience using fMRI, EEG, Positron emission tomography (PET). Several brain regions including primary (SI) and secondary (SII) somatosensory cortices, insula and posterior anterior and anterior medial cingulate cortices (pACC/aMCC) are consistently found to respond to pain stimulation. These regions constitute the so-called "Pain Matrix", i.e., a network of cortical areas "mediating pain experience itself" (Chen et al., 1998;Apkarian et al., 1999;Hudson, 2000;Laurent et al., 2000;Chen, 2001;Chen, 2009;Iannetti and Mouraux, 2010;Mouraux et al., 2011). There are two functional sub-regions in the Pain Matrix: the sensory-discriminative aspects of pain perception are processed in SI and SII, constitute the so-called "lateral pain system" or "somatosensory node" while the affective aspects of pain perception are processed in medial brain structures such as the ACC and insula and constitute the "medial pain system" or "affective node" (Schnitzler and Ploner, 2000;Derbyshire et al., 1997;Melzack, 2001;Iannetti and Mouraux, 2010;Mouraux et al., 2011).

Empathy for pain

An influential hypothesis guiding empathy research is that the neural bases of empathy are based on shared networks: observing the affective states in others activates brain networks that are also involved in the first-hand experience of pain. In order to test this hypothesis, efforts have been put into research on the neural basis of empathy ranging from the vicarious experience of disgust, reward, joy and embarrassment to pain (Singer, 2006;Jabbi et al., 2008;Suzuki, 2010;Wicker et al., 2003;Keysers and Gazzola, 2009;Krach et al., 2011;Singer et al., 2004).

The majority of empathy studies focus on empathy for pain. There are several reasons for that: (1) Testing the "shared network" theory of empathy requires triggering first-hand and second-hand experience of the same emotion. Compared to basic emotions like happiness, sadness, fear and anger, pain is much easier to trigger, measure, control and repeat in both conditions. (2) The neural basis of first-hand pain experience is well studied and established. As mentioned above, the Pain Matrix is a specific neural circuit that response to pain experience; (3) Pain experience is a multi-dimensional process which includes both sensory and affective aspects (Derbyshire, 2000;Melzack, 2001;Iannetti and Mouraux, 2010). The results from fMRI studies in empathy for pain support the "shared network" hypothesis. Shared activations very robustly include insular and cingulate regions (for a meta analysis see (Lamm et al., 2011)). Morrison and Downing studied fMRI signals of individual subjects in native anatomical space, minimizing confounds introduced by image pre-processing. They observed activation overlaps in 6 of 11 subjects in aMCC, activated by direct and vicariously felt pain (Morrison and Downing, 2007). However, testing the shared network in empathy for pain using fMRI has the same shortcoming as testing the

existence of mirror neuron system in action observation: the activation of the same voxel does not necessarily mean that the same neurons are activated. A recent multivoxel patter analysis found that the bilateral AI exhibited a similar spatial distribution of cortical fMRI activity when seeing another person in pain compared to first-hand pain, providing additional evidence for similar neuronal populations involved in pain experience and empathy for pain (Corradi-Dell'Acqua et al., 2011). Recently, two meta-analyses, summarizing the published neuroimaging studies on empathy for pain found that the AI and pACC/aMCC were consistently involved in both pain experience and empathy for pain (Lamm et al., 2011;Fan et al., 2011). However, certain paradigms also show overlapping activations in somatosensory cortices during pain observation and experience, if a local somatic cause is graphically obvious (Keysers et al., 2010)

Social modulation of empathy for pain

Empathy is thought to be a crucial contributor to successful social interaction, because it enables one to understand and predict others feelings and behaviours. Empathy also promotes the building of inter-individual relationship and prosocial behaviour (Hoffman, 1977;Eisenberg and Miller, 1987;Eisenberg, 2007;Singer and Lamm, 2009;Hein et al., 2011). Despite its adaptive value, empathy is not obligatory (Engen and Singer, 2012). In our daily experience, even when we are surrounded by emotions and feelings from people around us, we do not constantly switch our own emotional states based on what we perceive in others. For example, when you are passing by a crying stranger you might feel curious but you will not necessarily empathize with her sadness and feel sad yourself. Why do we not empathize with everyone all the time? From a developmental perspective, with continuing maturation of the prefrontal cortex, development of a sense of self and more complex forms of cognitive abilities, humans exhibit more advanced and flexible levels of empathy, which allow human beings to empathize with other's more precisely and more specifically. From an evolutionary point of view, it is not adaptive to extend one's empathy to everyone. If we consistently empathize with all emotional stimuli around us, there is no room for our own emotions and proper social functions will be harmed.

In our real life, we empathize with other people to varying degrees. Various situational and interpersonal variables influence the processes involved in empathy (Hein and Singer, 2008). Empathic traits can modulate empathic responses. There are individual differences in the ability and sensitivity to empathize with others. This difference can be measured using several relatively reliable self-report questionnaires, such as the Interpersonal Reactivity Index (IRI) (Davis MH, 1983), the Balanced Emotional empathy Scale (BEES) (Mehrabian A, 1997) and the Empathy Quotient (EQ) (Baron-Cohen and Wheelwright, 2004). In one of the earliest studies focusing on empathy for pain, Singer and colleagues reported that scores on the IRI "Empathic Concern" sub-scale correlate with AI and dACC activity during empathizing with others' pain (Singer et al., 2004). Another study from Keysers' group found that several IRI sub-scales were correlated with fronto-insular activation while observing disgusted and pleased facial expression (Jabbi et al., 2007). More evidences for the modulation of empathy by empathic traits come from the studies on alexithymia in autistic patients and healthy controls. It has been found that empathic brain responses to the suffering of others were associated with increased activation in left anterior insula and the strength of this signal was predictive of the degree of alexithymia in both autistic and control groups (Bird et al., 2010).

The interpersonal relationship between the empathizer and pain-receiver can also modulate the empathic response. An fMRI study reports that when we observe pain of a fair player in a money-related game (the person we like) a stronger empathic brain response was triggered compared to activation when we observe the pain of an unfair player (the person we do not like) (Singer et al., 2006). Another study found that stronger empathic responses were evoked when we observe pain of an in-group member compared to an out-group member and this brain activation was also correlates with prosocial behaviours (Hein et al., 2010). It has been reported that

empathy with friends relies on emotion sharing and self-processing mechanisms, whereas empathy for strangers' social suffering relies more heavily on metalizing systems (Meyer et al., 2012). These results indicate that the emotionally closer the pain-receiver is to the empathizer and the more the empathizer likes the pain-receiver, the stronger the empathic brain response.

Contextual factors also strongly modulate empathic responses. In one study from Decety's group, the empathizer was instructed to empathize with AIDS patients' pain. In some patients they were infected due to blood transfusion (not their own fault) while others were due to drug use (their own fault). Results showed that stronger empathic response happened when empathizing with innocent patients than with drug users (Decety et al., 2010). In another study, subjects watched a series of needle injections and were informed that the injections were administered to normal, pain-sensitive or anesthetized hands. It turned out that this prior knowledge modulated hemodynamic response in regions relevant for empathy including AI and ACC (Lamm et al., 2007a). In one recent fMRI study an increased brain empathic response to others in pain was observed when they received no rather than a large reward, with different level of activations in the ACC, aMCC, insula and postcentral gyrus, which implies that the pain-taker's financial situation modulated brain empathic response (Guo et al., 2012).

We can tell that the empathic responses are strongly modulated by external and internal factors. Even though a quite rich literature proves that empathy can be modulated, until now, very little is still known about the brain regions causing the modulation, but a number of frontal regions have been associated with this modulation (vmPFC, the dorsolateral PFC, the ACC, anterior insula, pars orbitalis and pars triangularis of the IFG; (Miller and Cohen, 2001;Critchley et al., 2002;Leiberg and Anders, 2006;Wager et al., 2008;Critchley, 2009;Engen and Singer, 2012).

In the literature, the common experimental setting is that the empathizer is an onlooker who has nothing to do with causing of the other's pain. In one of our studies we make the empathizer believe that he or she is involved in causing the pain-taker's pain. We found that the bigger the empathizer's responsibility in causing the pain-taker's suffering, the stronger the empathic brain response when the pain-taker observes this pain (Chapter 4). Another behavioural study shows that if the empathizer is informed that the pain-taker will receive monetary compensation for his/her pain, they will subjectively judge that the pain-taker experiences the pain as less unpleasant compared to when the pain-taker does not get monetary compensation. We are currently investigating the neural basis of this monetary compensation modulation of empathy for pain but results could not yet be included in this thesis.

Outline of Thesis

In Chapter 2, we present an EMG-fMRI study designed to investigate how our brains perceive active hand movements differently from passive hand movements. In other words, how our brains distinguish our own motor commands and external motor forces. In this study, we found that motor cortices exchange more information with BA2 during active movements compared to passive movements. This result suggests that we should interpret activation in BA2 as a somatosensory-motor coding rather than sensory coding alone. In Chapter 3, we present an fMRI-EEG study to find out if sVx in fMRI studies are a likely source of the modulation of the mu-rhythm found in EEG studies. We found that the mu suppression indexes the activity of brain regions that overlap with the MNS as localized using sVx, including BA2, IPL, and dPM, but may be not BA44. In Chapter 4, we studied how the social factor "responsibility in causing other's pain" modulates the empathic response for this pain. We found that when a participant is fully responsible for an observed pain, the vicarious signals detected in the anterior cingulate cortex, insula, amygdale and putamen are larger than if the participant shared responsibility or had none at all. We find that the insula was the entrance point onto the pain matrix of this modulation. Furthermore,

the right SMA seemed to be the brain area which processed the responsibility and modulated the insula. In Chapter 5, a preliminary behavioural study focused on how monetary compensation modulates empathy for pain. In this study we found that monetary compensation can reduce the unpleasantness the observers believe the pain-taker to feel during the painful experience. We also found that when the pain-taker got money for painless stimulation, the observer experienced more unpleasantness than when no money was paid for a painless stimulus. This increase of unpleasantness might be due to jealousy.

References Cited

Abbruzzese G, Ratto S, Favale E, Abbruzzese M (1981) Proprioceptive modulation of somatosensory evoked potentials during active or passive finger movements in man. J Neurol Neurosurg Psychiatry 44:942-949.

Agnew Z, Wise RJ (2008) Separate areas for mirror responses and agency within the parietal operculum. J Neurosci 28:12268-12273.

Agnew ZK, Bhakoo KK, Puri BK (2007) The human mirror system: a motor resonance theory of mind-reading. Brain Res Rev 54:286-293.

Apkarian AV, Darbar A, Krauss BR, Gelnar PA, Szeverenyi NM (1999) Differentiating cortical areas related to pain perception from stimulus identification: temporal analysis of fMRI activity. J Neurophysiol 81:2956-2963.

Arnstein D, Cui F, Keysers C, Maurits NM, Gazzola V (2011) mu-suppression during action observation and execution correlates with BOLD in dorsal premotor, inferior parietal, and SI cortices. J Neurosci 31:14243-14249.

Ball T, Schreiber A, Feige B, Wagner M, Lucking CH, Kristeva-Feige R (1999) The role of higher-order motor areas in voluntary movement as revealed by high-resolution EEG and fMRI. Neuroimage 10:682-694.

Banissy MJ, Ward J (2007) Mirror-touch synesthesia is linked with empathy. Nat Neurosci 10:815-816.

Baron-Cohen S, Wheelwright S (2004) The empathy quotient: an investigation of adults with Asperger syndrome or high functioning autism, and normal sex differences. J Autism Dev Disord 34:163-175.

Bernhardt BC, Singer T (2012) The neural basis of empathy. Annu Rev Neurosci 35:1-23.

Bird G, Silani G, Brindley R, White S, Frith U, Singer T (2010) Empathic brain responses in insula are modulated by levels of alexithymia but not autism. Brain 133:1515-1525.

Blair RJ (2005) Responding to the emotions of others: dissociating forms of empathy through the study of typical and psychiatric populations. Conscious Cogn 14:698-718.

Blakemore SJ, Bristow D, Bird G, Frith C, Ward J (2005) Somatosensory activations during the observation of touch and a case of vision-touch synaesthesia. Brain 128:1571-1583.

Blakemore SJ, Wolpert D, Frith C (2000) Why can't you tickle yourself? Neuroreport 11:R11-R16.

Blakemore SJ, Wolpert DM, Frith CD (1998) Central cancellation of self-produced tickle sensation. Nat Neurosci 1:635-640.

Caetano G, Jousmaki V, Hari R (2007) Actor's and observer's primary motor cortices stabilize similarly after seen or heard motor actions. Proc Natl Acad Sci U S A 104:9058-9062.

Casile A (2013) Mirror neurons (and beyond) in the macaque brain: an overview of 20 years of research. Neurosci Lett 540:3-14.

Caspers S, Zilles K, Laird AR, Eickhoff SB (2010) ALE meta-analysis of action observation and imitation in the human brain. Neuroimage 50:1148-1167.

Chen AC (2001) New perspectives in EEG/MEG brain mapping and PET/fMRI neuroimaging of human pain. Int J Psychophysiol 42:147-159.

Chen AC, Rappelsberger P, Filz O (1998) Topology of EEG coherence changes may reflect differential neural network activation in cold and pain perception. Brain Topogr 11:125-132.

Chen J (2009) Toward the brain matrix of pain. Neurosci Bull 25:234-236.

Chen W, Yuan TF (2008) Mirror neuron system as the joint from action to language. Neurosci Bull 24:259-264.

Cooper DL (2006) Broca's arrow: evolution, prediction, and language in the brain. Anat Rec B New Anat 289:9-24.

Corradi-Dell'Acqua C, Hofstetter C, Vuilleumier P (2011) Felt and seen pain evoke the same local patterns of cortical activity in insular and cingulate cortex. J Neurosci 31:17996-18006.

Critchley HD (2009) Psychophysiology of neural, cognitive and affective integration: fMRI and autonomic indicants. Int J Psychophysiol 73:88-94.

Critchley HD, Melmed RN, Featherstone E, Mathias CJ, Dolan RJ (2002) Volitional control of autonomic arousal: a functional magnetic resonance study. Neuroimage 16:909-919.

Davis MH (1983) Measuring individual differences in empathy: evidence for a multidimentsional approach. J Pers Soc Psychol 44:126.

de Vignemont F, Singer T (2006) The empathic brain: how, when and why? Trends Cogn Sci 10:435-441.

Decety J, Echols S, Correll J (2010) The blame game: the effect of responsibility and social stigma on empathy for pain. J Cogn Neurosci 22:985-997.

Derbyshire SW (2000) Exploring the pain "neuromatrix". Curr Rev Pain 4:467-477.

Derbyshire SW, Jones AK, Gyulai F, Clark S, Townsend D, Firestone LL (1997) Pain processing during three levels of noxious stimulation produces differential patterns of central activity. Pain 73:431-445.

di Pellegrino G, Fadiga L, Fogassi L, Gallese V, Rizzolatti G (1992) Understanding motor events: a neurophysiological study. Exp Brain Res 91:176-180.

Dinstein I, Hasson U, Rubin N, Heeger DJ (2007) Brain areas selective for both observed and executed movements. J Neurophysiol 98:1415-1427.

Ebisch SJ, Perrucci MG, Ferretti A, Del GC, Romani GL, Gallese V (2008) The sense of touch: embodied simulation in a visuotactile mirroring mechanism for observed animate or inanimate touch. J Cogn Neurosci 20:1611-1623.

Eisenberg N (2007) Empathy-related responding and prosocial behaviour. Novartis Found Symp 278:71-80.

Eisenberg N, Miller PA (1987) The relation of empathy to prosocial and related behaviors. Psychol Bull 101:91-119.

Engen HG, Singer T (2012) Empathy circuits. Curr Opin Neurobiol.

Fan Y, Duncan NW, de GM, Northoff G (2011) Is there a core neural network in empathy? An fMRI based quantitative meta-analysis. Neurosci Biobehav Rev 35:903-911.

Freund HJ (2002) fMRI studies of the sensory and motor areas involved in movement. Adv Exp Med Biol 508:389-395.

Gallese V (2003) The manifold nature of interpersonal relations: the quest for a common mechanism. Philos Trans R Soc Lond B Biol Sci 358:517-528.

Gallese V (2007) Before and below 'theory of mind': embodied simulation and the neural correlates of social cognition. Philos Trans R Soc Lond B Biol Sci 362:659-669.

Gallese V, Fadiga L, Fogassi L, Rizzolatti G (1996) Action recognition in the premotor cortex. Brain 119 (Pt 2):593-609.

Gallese V, Goldman A (1998) Mirror neurons and the simulation theory of mind-reading. Trends Cogn Sci 2:493-501.

Gallese V, Keysers C, Rizzolatti G (2004) A unifying view of the basis of social cognition. Trends Cogn Sci 8:396-403.

Gallese V, Sinigaglia C (2011) What is so special about embodied simulation? Trends Cogn Sci 15:512-519.

Gazzola V, Keysers C (2009) The observation and execution of actions share motor and somatosensory voxels in all tested subjects: single-subject analyses of unsmoothed fMRI data. Cereb Cortex 19:1239-1255.

Grezes J, Armony JL, Rowe J, Passingham RE (2003) Activations related to "mirror" and "canonical" neurones in the human brain: an fMRI study. Neuroimage 18:928-937.

Guo X, Zheng L, Zhang W, Zhu L, Li J, Wang Q, Dienes Z, Yang Z (2012) Empathic neural responses to others' pain depend on monetary reward. Soc Cogn Affect Neurosci 7:535-541.

Haggard P, Whitford B (2004) Supplementary motor area provides an efferent signal for sensory suppression. Brain Res Cogn Brain Res 19:52-58.

Hamzei F, Rijntjes M, Dettmers C, Glauche V, Weiller C, Buchel C (2003) The human action recognition system and its relationship to Broca's area: an fMRI study. Neuroimage 19:637-644.

Hein G, Lamm C, Brodbeck C, Singer T (2011) Skin conductance response to the pain of others predicts later costly helping. PLoS One 6:e22759.

Hein G, Silani G, Preuschoff K, Batson CD, Singer T (2010) Neural responses to ingroup and outgroup members' suffering predict individual differences in costly helping. Neuron 68:149-160.

Hein G, Singer T (2008) I feel how you feel but not always: the empathic brain and its modulation. Curr Opin Neurobiol 18:153-158.

Hoffman ML (1977) Empathy, its development and prosocial implications. Nebr Symp Motiv 25:169-217.

Hudson AJ (2000) Pain perception and response: central nervous system mechanisms. Can J Neurol Sci 27:2-16.

Iacoboni M, Mazziotta JC (2007) Mirror neuron system: basic findings and clinical applications. Ann Neurol 62:213-218.

Iacoboni M, Molnar-Szakacs I, Gallese V, Buccino G, Mazziotta JC, Rizzolatti G (2005) Grasping the intentions of others with one's own mirror neuron system. PLoS Biol 3:e79.

Iacoboni M, Woods RP, Brass M, Bekkering H, Mazziotta JC, Rizzolatti G (1999) Cortical mechanisms of human imitation. Science 286:2526-2528.

Iannetti GD, Mouraux A (2010) From the neuromatrix to the pain matrix (and back). Exp Brain Res 205:1-12.

Ishida H, Nakajima K, Inase M, Murata A (2010) Shared mapping of own and others' bodies in visuotactile bimodal area of monkey parietal cortex. J Cogn Neurosci 22:83-96.

Jabbi M, Bastiaansen J, Keysers C (2008) A common anterior insula representation of disgust observation, experience and imagination shows divergent functional connectivity pathways. PLoS One 3:e2939.

Jabbi M, Swart M, Keysers C (2007) Empathy for positive and negative emotions in the gustatory cortex. Neuroimage 34:1744-1753.

Jackson PL, Meltzoff AN, Decety J (2005) How do we perceive the pain of others? A window into the neural processes involved in empathy. Neuroimage 24:771-779.

Kapreli E, Athanasopoulos S, Papathanasiou M, Van HP, Strimpakos N, Gouliamos A, Peeters R, Sunaert S (2006) Lateralization of brain activity during lower limb joints movement. An fMRI study. Neuroimage 32:1709-1721.

Keysers C, Gazzola V (2007) Integrating simulation and theory of mind: from self to social cognition. Trends Cogn Sci 11:194-196.

Keysers C, Gazzola V (2009) Expanding the mirror: vicarious activity for actions, emotions, and sensations. Curr Opin Neurobiol 19:666-671.

Keysers C, Gazzola V (2010) Social neuroscience: mirror neurons recorded in humans. Curr Biol 20:R353-R354.

Keysers C, Kaas JH, Gazzola V (2010) Somatosensation in social perception. Nat Rev Neurosci 11:417-428.

Keysers C, Kohler E, Umilta MA, Nanetti L, Fogassi L, Gallese V (2003) Audiovisual mirror neurons and action recognition. Exp Brain Res 153:628-636.

Keysers C, Wicker B, Gazzola V, Anton JL, Fogassi L, Gallese V (2004) A touching sight: SII/PV activation during the observation and experience of touch. Neuron 42:335-346.

Kilner JM, Friston KJ, Frith CD (2007) Predictive coding: an account of the mirror neuron system. Cogn Process 8:159-166.

Knapp HP, Corina DP (2010) A human mirror neuron system for language: Perspectives from signed languages of the deaf. Brain Lang 112:36-43.

Kohler E, Keysers C, Umilta MA, Fogassi L, Gallese V, Rizzolatti G (2002) Hearing sounds, understanding actions: action representation in mirror neurons. Science 297:846-848.

Krach S, Cohrs JC, de Echeverria Loebell NC, Kircher T, Sommer J, Jansen A, Paulus FM (2011) Your flaws are my pain: linking empathy to vicarious embarrassment. PLoS One 6:e18675.

Lamm C, Batson CD, Decety J (2007a) The neural substrate of human empathy: effects of perspective-taking and cognitive appraisal. J Cogn Neurosci 19:42-58.

Lamm C, Decety J, Singer T (2011) Meta-analytic evidence for common and distinct neural networks associated with directly experienced pain and empathy for pain. Neuroimage 54:2492-2502.

Lamm C, Fischer MH, Decety J (2007b) Predicting the actions of others taps into one's own somatosensory representations--a functional MRI study. Neuropsychologia 45:2480-2491.

Lamm C, Nusbaum HC, Meltzoff AN, Decety J (2007c) What are you feeling? Using functional magnetic resonance imaging to assess the modulation of sensory and affective responses during empathy for pain. PLoS One 2:e1292.

Laurent B, Peyron R, Garcia LL, Mauguiere F (2000) [Positron emission tomography to study central pain integration]. Rev Neurol (Paris) 156:341-351.

Lee RG, White DG (1974) Modification of the human somatosensory evoked response during voluntary movement. Electroencephalogr Clin Neurophysiol 36:53-62.

Leiberg S, Anders S (2006) The multiple facets of empathy: a survey of theory and evidence. Prog Brain Res 156:419-440.

Mehrabian A (1997) Relations among personality scales of aggression,violence and empathy: validational evidence bearing on the risk of eruptive violence scale. Aggress Behav433-445.

Melzack R (2001) Pain and the neuromatrix in the brain. J Dent Educ 65:1378-1382.

Meyer ML, Masten CL, Ma Y, Wang C, Shi Z, Eisenberger NI, Han S (2012) Empathy for the social suffering of friends and strangers recruits distinct patterns of brain activation. Soc Cogn Affect Neurosci.

Miller EK, Cohen JD (2001) An integrative theory of prefrontal cortex function. Annu Rev Neurosci 24:167-202.

Mima T, Sadato N, Yazawa S, Hanakawa T, Fukuyama H, Yonekura Y, Shibasaki H (1999) Brain structures related to active and passive finger movements in man. Brain 122 (Pt 10):1989-1997.

Morrison I, Downing PE (2007) Organization of felt and seen pain responses in anterior cingulate cortex. Neuroimage 37:642-651.

Morrison I, Lloyd D, di PG, Roberts N (2004) Vicarious responses to pain in anterior cingulate cortex: is empathy a multisensory issue? Cogn Affect Behav Neurosci 4:270-278.

Morrison I, Tipper SP, Fenton-Adams WL, Bach P (2012) "Feeling" others' painful actions: The sensorimotor integration of pain and action information. Hum Brain Mapp.

Mouraux A, Diukova A, Lee MC, Wise RG, Iannetti GD (2011) A multisensory investigation of the functional significance of the "pain matrix". Neuroimage 54:2237-2249.

Mukamel R, Ekstrom AD, Kaplan J, Iacoboni M, Fried I (2010) Single-neuron responses in humans during execution and observation of actions. Curr Biol 20:750-756.

Muthukumaraswamy SD, Johnson BW (2004) Primary motor cortex activation during action observation revealed by wavelet analysis of the EEG. Clin Neurophysiol 115:1760-1766.

Muthukumaraswamy SD, Johnson BW, McNair NA (2004) Mu rhythm modulation during observation of an object-directed grasp. Brain Res Cogn Brain Res 19:195-201.

Newton JM, Sunderland A, Gowland PA (2005) fMRI signal decreases in ipsilateral primary motor cortex during unilateral hand movements are related to duration and side of movement. Neuroimage 24:1080-1087.

Oberman LM, Hubbard EM, McCleery JP, Altschuler EL, Ramachandran VS, Pineda JA (2005) EEG evidence for mirror neuron dysfunction in autism spectrum disorders. Brain Res Cogn Brain Res 24:190-198.

Oberman LM, Pineda JA, Ramachandran VS (2007) The human mirror neuron system: a link between action observation and social skills. Soc Cogn Affect Neurosci 2:62-66.

Oberman LM, Ramachandran VS, Pineda JA (2008) Modulation of mu suppression in children with autism spectrum disorders in response to familiar or unfamiliar stimuli: the mirror neuron hypothesis. Neuropsychologia 46:1558-1565.

Ohara S, Ikeda A, Kunieda T, Yazawa S, Baba K, Nagamine T, Taki W, Hashimoto N, Mihara T, Shibasaki H (2000) Movement-related change of electrocorticographic activity in human supplementary motor area proper. Brain 123 (Pt 6):1203-1215.

Perlovsky LI, Ilin R (2013) Mirror neurons, language, and embodied cognition. Neural Netw 41:15-22.

Perry A, Stein L, Bentin S (2011) Motor and attentional mechanisms involved in social interaction--evidence from mu and alpha EEG suppression. Neuroimage 58:895-904.

Pineda JA, Allison BZ, Vankov A (2000) The effects of self-movement, observation, and imagination on mu rhythms and readiness potentials (RP's): toward a brain-computer interface (BCI). IEEE Trans Rehabil Eng 8:219-222.

Preston SD, de Waal FB (2002) Empathy: Its ultimate and proximate bases. Behav Brain Sci 25:1-20.

Price DD (1999) Psychological mechanisms of pain and analgesia. pp 1-248. Seattle:IASP press.

Rizzolatti G, Craighero L (2004) The mirror-neuron system. Annu Rev Neurosci 27:169-192.

Rizzolatti G, Fabbri-Destro M, Cattaneo L (2009) Mirror neurons and their clinical relevance. Nat Clin Pract Neurol 5:24-34.

Rizzolatti G, Fadiga L, Fogassi L, Gallese V (1999) Resonance behaviors and mirror neurons. Arch Ital Biol 137:85-100.

Rizzolatti G, Fadiga L, Gallese V, Fogassi L (1996) Premotor cortex and the recognition of motor actions. Brain Res Cogn Brain Res 3:131-141.

Rizzolatti G, Sinigaglia C (2007) Mirror neurons and motor intentionality. Funct Neurol 22:205-210.

Salmelin R, Hamalainen M, Kajola M, Hari R (1995) Functional segregation of movement-related rhythmic activity in the human brain. Neuroimage 2:237-243.

Schnitzler A, Ploner M (2000) Neurophysiology and functional neuroanatomy of pain perception. J Clin Neurophysiol 17:592-603.

Singer T (2006) The neuronal basis and ontogeny of empathy and mind reading: review of literature and implications for future research. Neurosci Biobehav Rev 30:855-863.

Singer T, Lamm C (2009) The social neuroscience of empathy. Ann N Y Acad Sci 1156:81-96.

Singer T, Seymour B, O'Doherty J, Kaube H, Dolan RJ, Frith CD (2004) Empathy for pain involves the affective but not sensory components of pain. Science 303:1157-1162.

Singer T, Seymour B, O'Doherty JP, Stephan KE, Dolan RJ, Frith CD (2006) Empathic neural responses are modulated by the perceived fairness of others. Nature 439:466-469.

Southgate V, Johnson MH, Osborne T, Csibra G (2009) Predictive motor activation during action observation in human infants. Biol Lett 5:769-772.

Suzuki A (2010) [Insula and disgust]. Rinsho Shinkeigaku 50:1000-1002.

Tsakiris M, Haggard P (2003) Awareness of somatic events associated with a voluntary action. Exp Brain Res 149:439-446.

Wager TD, Davidson ML, Hughes BL, Lindquist MA, Ochsner KN (2008) Prefrontal-subcortical pathways mediating successful emotion regulation. Neuron 59:1037-1050.

Warreyn P, Ruysschaert L, Wiersema JR, Handl A, Pattyn G, Roeyers H (2013) Infants' mu suppression during the observation of real and mimicked goal-directed actions. Dev Sci 16:173-185.

Weiller C, Juptner M, Fellows S, Rijntjes M, Leonhardt G, Kiebel S, Muller S, Diener HC, Thilmann AF (1996) Brain representation of active and passive movements. Neuroimage 4:105-110.

Wicker B, Keysers C, Plailly J, Royet JP, Gallese V, Rizzolatti G (2003) Both of us disgusted in My insula: the common neural basis of seeing and feeling disgust. Neuron 40:655-664.

Wolpert DM (1997) Computational approaches to motor control. Trends Cogn Sci 1:209-216.

Functional Magnetic Resonance Imaging Connectivity Analyses Reveal Efference-Copy to Primary Somatosensory Area, BA2.

F Cui1, 2, D Arnstein1, RM Thomas2, NM Maurits3, C Keysers1,2, V Gazzola1,2,*

1: University of Groningen and University Medical Center Groningen, Department of Neuroscience, 9713AW Groningen, The Netherlands

2: Netherlands Institute for Neuroscience, an institute of the Royal Netherlands Academy for Arts and Sciences, 1105BA Amsterdam, The Netherlands

3: Department of Neurology, University Medical Center Groningen, University of Groningen, 9713 GZ Groningen, The Netherlands.

* **Corresponding author:** Valeria Gazzola, v.gazzola@nin.knaw.nl, Meibergdreef 47, 1105BA Amsterdam, The Netherlands

Abstract

Some theories of motor control suggest efference-copies of motor commands reach somatosensory cortices. Here we used functional magnetic resonance imaging to test these models. We varied the amount of efference-copy signal by making participants squeeze a soft material either actively or passively. We found electromyographical recordings, an efference-copy proxy, to predict activity in primary somatosensory regions, in particular BA 2. Partial correlation analyses confirmed that brain activity in cortical structures associated with motor control (premotor and supplementary motor cortices, the parietal area PF and the cerebellum) predicts brain activity in BA2 without being entirely mediated by activity in early somatosensory (BA3b) cortex. Our study therefore provides valuable empirical evidence for efference-copy models of motor control, and shows that signals in BA2 can indeed reflect an input from motor cortices and suggests that we should interpret activations in BA2 as evidence for somatosensory-motor rather than somatosensory coding alone.

Introduction

The blood oxygen level dependent (BOLD) signal in premotor (PM) and, as recently described, primary somatosensory cortices (SI, Brodmann Area (BA) 2 in particular), is increased while participants perform actions and while they witness similar actions performed by others(Caspers et al., 2010;Gazzola et al., 2006;Gazzola and Keysers, 2009a) suggesting a duality: witnessing others' actions triggers vicarious motor representations in PM and vicarious somatosensory representations in BA2(Keysers and Gazzola, 2009a;Keysers et al., 2010) This duality is prompted by reverse inference(Poldrack, 2006): because electro-stimulation of PM can lead to overt movements and that of BA2 to somatosensory percepts(Desmurget et al., 2009), activations in the former are thought to reflect motor, and in the latter somatosensory processes.

Contemporary theories of motor control however suggest intensive crosstalk between motor and somatosensory regions: each motor command sent to the body also reaches somatosensory cortices, as an efference-copy that forward internal models convert into expected sensory consequences(Blakemore et al., 1999;Wolpert and Flanagan, 2001;Wolpert and Ghahramani, 2000;Wolpert and Miall, 1996;Johansson and Flanagan, 2009) The supplementary motor area (SMA) is considered the most likely source of the efference-copy(Haggard and Whitford, 2004). The notion of efference-copy blurs the duality in the distinction between motor and somatosensory information and begs the question whether activations measured in BA2 in a variety of paradigms

necessarily always represent somatosensory information alone or, at least sometimes, also (efference copies of) motor commands. Only very few studies have investigated this question.

Christensen and colleagues (2007) blocked sensory afference from the leg and compared the difference between active and passive ankle movements while the participant was or was not under the influence of ischemia. As expected, ischemia reduced SI activation during passive ankle movements, but this was not the case during active movements, suggesting that an efference-copy of the motor signal can determine activation of SI if actual somatosensory afference from the leg is missing or reduced.

Whether an efference-copy can significantly influence BA2 activation in the presence of normal physiological afference to BA2 however remains controversial. Two studies found no SI difference between the active and passive execution of a movement(Blakemore et al., 1998;Weiller et al., 1996a) while one found smaller activation in SI during active compared to passive finger tapping(Agnew and Wise, 2008).

To provide further insights into this question, we compared participants' brain activity, measured with functional magnetic resonance image (fMRI) with their muscle activity, measured with electromyograhy (EMG) during active (ACT) and passive (PASS) squeezing (Fig. 1a and b). While during ACT trials participants gently squeezed bubble-wrap attached to the palm of the right hand, during PASS trials the experimenter pressed the subject's fingers around the bubble-wrap (see Methods for more details). Muscle activity was measured to quantify the intensity of the actual motor output and as a proxy of the motor command17 and hence efference-copy signal intensity. By comparing muscle activity with brain activation, we investigated if SI activation can reflect the magnitude of the motor efference. In addition, we used two connectivity analyses to localize the likely source of this efference-copy and distinguish it from somatosensory re-afferences.

Results

EMG

Figure 1c presents the average rectified (i.e. absolute value) electromyography (EMG) responses across subjects over a 10s interval centered on the onset of the instruction to squeeze. The clear peaks and valleys of the EMG indicate good within- and between-subject consistency in the timing of the four squeezes.

For each trial, the rectified EMG during baseline (i.e. -5s to -0.5 s relative to the onset of the task instruction) and experimental epochs (i.e. the 4s of ACT or PASS) were averaged separately and the former average subtracted from the latter to yield baseline-corrected estimates of the EMG activity for each experimental trial. The baseline-corrected estimates for ACT and PASS where then averaged across trials to yield a single value per subject and condition that were then compared using t-tests across participants. These values were greater than zero for both ACT (Mean = 77.18 μV; $t(17) = 6.88$, $p<10^{-7}$) and PASS (Mean = 32.04 μV; $t(17) = 3.25$, $p<0.002$), and the difference between ACT and PASS was highly significant ($t(17) = 5.5$, $p<10^{-4}$).

General Linear Models (GLM)

Two GLMs were then calculated for the fMRI data (Fig. 1d). In the first model a standard boxcar predictor was produced separately for ACT and PASS and convolved with the canonical hemodynamic response function (HRF). In the second model a single 'generic task' boxcar predictor was produced which contained both ACT and PASS blocks. In addition, a first-order parametric modulator was defined using the EMG (EMGpm). The value for a particular block was calculated as the average EMG during the 4 s block minus the average EMG during the preceding baseline (from -5 to -0.5 s of the appearance of the task instruction). The parametric modulator (EMGpm) was then demeaned and standardized, and both predictors (the generic task predictor, and the generic task predictor * the EMG) were convolved with the HRF.

Figure 1e-f show the fMRI results of comparing ACT versus PASS conditions and EMGpm versus zero. Both ACT>PASS and EMGpm>0 revealed widespread differential activations in areas typically associated with motor programming and execution including the cerebellum, primary motor cortex (M1), SMA, PM and the posterior parietal lobe, including area PF and the superior parietal lobule (Table 1).

Cluster size in number of voxels	Number of voxels in CytoArea	Hem	Cyto/anatomical area	% of CytoArea activated	x	y	z	T
ACT>PASS								
33901	2132	L	Area 6	48	N/A			N/A
	1978.1	R	Area 6	44.6	N/A			N/A
	1463.3	R	Cerebellar Lobule VI (Hem)	76.4	6	-68	-18	17.77
	1396	L	Cerebellar Lobule VI (Hem)	69.3	-32	-56	-30	11.61
					-28	-60	-30	11.26
					-14	-62	-22	10.7
					-12	-58	-18	10.31
	725	R	Cerebellar Lobule VIIa Crus I (Hem)	21.5	N/A			N/A
	608.4	L	Cerebellar Lobule VIIa Crus I (Hem)	19.2	N/A			N/A
	580.1	R	Cerebellar Lobule V	70.1	2	-56	-10	14.31
					12	-54	-22	10.93
	458.9	L	Cerebellar Lobule V	60.3	N/A			N/A
	446.8	L	Area 2	47.9	N/A			N/A
	409.5	R	Area 2	41.6	N/A			N/A
	375.7	R	Area 44	41.3	N/A			N/A
	368.7	R	hOC3v (V3v)	52.9	30	-84	-8	10.09
					34	-88	-8	9.48
	339.2	L	Cerebellar Lobules I-IV (Hem)	67.5	N/A			N/A
	N/A	R	Middle Cingulate Cortex	N/A	10	10	34	10.1
	N/A	L	hIPI, BA3a, BA4a, BA4p	N/A	N/A			N/A
	N/A	R	hIP2, BA44, SPL(7A and 7P)	N/A	N/A			N/A
	N/A	L/R	hIP3, BA3b, Insula, Putamen, Pallidum, Thalamus	N/A	N/A			N/A
440	316.4	L	SPL (7A)	19.1	-16	-68	54	6
					-14	-54	68	4.81
	52.3	L	SPL (7P)	9.6	-14	-68	58	5.65
	32	L	SPL (5L)	6	-14	-52	64	4.59
	N/A	L	Superior Parietal Lobule	N/A	-18	-66	58	5.74
					-18	-54	62	4.48
					-20	-56	48	3.99
	N/A	L	Precuneus	N/A	-16	-58	66	4.13
90	20.1	R	Cerebellar Lobule VIIIa (Hem)	2.8	24	-60	-50	6.8
	14.5	R	Cerebellar Lobule VIIIb (Hem)	2	N/A			N/A
	12	R	Cerebellar Lobule VIIa Crus II (Hem)	0.8	34	-62	-50	5.06

	4.8	R	Cerebellar Lobule VIIb (Hem)	0.7	N/A			N/A
57	N/A	R	Middle Frontal Gyrus	N/A	44	58	8	4.64
					46	56	4	4.54
					42	48	12	4.12
52	N/A	L	Middle Frontal Gyrus	N/A	-36	54	30	4.89
					-42	48	28	3.87
12	5.4	L	Hipp (CA)	0.7	-34	-26	-10	4.01
					-38	-24	-14	3.91
10	N/A	L	Middle Orbital Gyrus		-26	56	-14	4.33
	N/A				-22	58	-12	4.02
PASS>ACT								
1748	347	R	IPC (PGa)	36	60	-60	26	7.6
					62	-58	22	7.5
					56	-52	14	5.93
	321.1	R	IPC (PGp)	27.5	52	-68	38	5.93
	25.4	R	hOC5 (V5)	25.6	N/A			N/A
	N/A	R	Middle Temporal Gyrus	N/A	56	-44	10	6.72
					52	-56	10	5.87
					46	-58	8	5.6
					44	-48	18	5.44
					56	-38	2	4.96
					60	-38	2	4.93
1113	N/A	R/L	Precuneus	N/A	4	-54	26	6.34
	N/A				0	-56	26	6.24
	N/A	R	Middle Cingulate Cortex	N/A	4	-50	32	6.23
	N/A	L	Cuneus	N/A	-14	-58	26	4.3
1111	N/A	R	Medial Temporal Pole	N/A	40	16	-32	7.52
	N/A	R	Middle Temporal Gyrus	N/A	58	4	-26	7.5
					54	-2	-22	6.92
					60	0	-20	6.53
					64	-8	-18	6.33
					60	-4	-18	6.15
					50	-10	-24	6.09
	N/A	R	Medial Temporal Pole	N/A	48	8	-30	5.73
	N/A	R	Superior Temporal Gyrus	N/A	58	-8	-8	5.72
	N/A	R	Middle Temporal Gyrus	N/A	66	-18	-10	5.62
959	515.4	L	IPC (PGp)	47.5	-48	-76	32	5.56
					-44	-78	34	5.53
					-46	-80	26	5.37
					-52	-70	32	5.22
					-48	-62	24	4.92

					-40	-74	44	4.85
					-46	-62	28	4.7
	92.1	L	IPC (PGa)	11.9	-48	-56	24	4.5
					-42	-62	32	4.45
	N/A	L	Middle Temporal Gyrus	N/A	-50	-62	14	5.67
	N/A	L	Angular Gyrus	N/A	-44	-58	26	4.58
917	N/A	R/L	Mid Orbital Gyrus	N/A	8	52	-10	6.73
					-10	52	-8	6.18
					-8	42	-6	4.65
	N/A	L	Anterior Cingulate Cortex	N/A	-2	38	-8	4.45
	N/A	L	Mid Orbital Gyrus	N/A	-4	42	-12	4.37
	N/A	R/L	Anterior Cingulate Cortex	N/A	6	40	0	4.24
					8	42	2	4.16
					0	38	-4	4.14
					8	40	6	3.86
285	N/A	L	Middle Temporal Gyrus	N/A	-54	-36	0	5.27
					-64	-40	2	4.77
					-60	-40	0	4.65
					-60	-36	0	4.65
228	N/A	L	Middle Temporal Gyrus	N/A	-54	4	-24	6.79
					-50	8	-26	5.73
	N/A	L	Medial Temporal Pole	N/A	-44	14	-30	4.71
					-40	14	-30	4.6
					-48	6	-32	4.44
227	N/A	L	Middle Frontal Gyrus	N/A	-32	28	54	4.98
					-38	20	52	4.01
196	N/A	R/L	Superior Medial Gyrus	N/A	6	56	18	4.68
					10	60	24	4.49
					0	56	28	4.04
	N/A	R	Anterior Cingulate Cortex	N/A	8	54	10	3.77
93	N/A	L	Inferior Frontal Gyrus (p. Orbitalis)	N/A	-38	36	-10	6.55
93	52.1	R	Hipp (SUB)	10.1	N/A			N/A
	32.8	R	Hipp (CA)	4.1	26	-16	-20	7.33
	3.1	R	Hipp (FD)	3.7	N/A			N/A
	2.6	R	Hipp (EC)	0.4	N/A			N/A
50	21	L	IPC (PFcm)	5.6	-44	-34	16	4.53
	16.8	L	OP 1	2.8	-38	-32	18	4.68
	6.4	L	TE 1.1	3.8	N/A			N/A
	1.9	L	OP 2	1.6	N/A			N/A

30	N/A	R	Middle Orbital Gyrus	N/A	28	38	-12	3.98
	N/A	R	Inferior Frontal Gyrus (p. Orbitalis)	N/A	30	36	-14	3.92
21	N/A	R	Superior Frontal Gyrus	N/A	24	42	52	4.12
21	N/A	R	Superior Medial Gyrus	N/A	8	46	44	4.44
19	N/A	R	Superior Frontal Gyrus	N/A	28	56	8	4.11
					24	54	8	3.91
					22	58	2	3.84
	N/A		Middle Frontal Gyrus	N/A	26	56	2	3.77
16	16	L	Cerebellar Lobule VIIa Crus II (Hem)	1	-16	-86	-38	4.45
EMGpm > 0								
17151	1403.1	R	Cerebellar Lobule VI (Hem)	73	6	-64	-18	14.74
					34	-54	-30	8.52
					34	-50	-32	8.46
	1395.2	L	Cerebellar Lobule VI (Hem)	69	-28	-60	-30	11.55
					-32	-56	-30	10.72
					-6	-66	-16	10.61
					-24	-58	-26	10.37
					-16	-62	-22	8.65
	606.6	R	Cerebellar Lobule VIIa Crus I (Hem)	18	N\A			N/A
	587.6	L	Cerebellar Lobule VIIa Crus I (Hem)	18.5	N\A			N/A
	533.3	R	Cerebellar Lobule V	64.2	12	-54	-22	11.15
	429	L	Cerebellar Lobule V	56.2	N\A			N/A
	336.7	R	hOC3v (V3v)	48.2	N\A			N/A
	263.8	R	hOC4v (V4)	47.4	N\A			N/A
	232.9	R	Cerebellar Lobule VI (Vermis)	96.7	N\A			N/A
	224	L	Cerebellar Lobules I-IV (Hem)	44.4	N\A			N/A
	214.8	L	Cerebellar Lobule VI (Vermis)	99.5	N\A			N/A
	196.4	R	Area 18	11.8	N\A			N/A
	178.4	L	hOC3v (V3v)	26.4	N\A			N/A
	N/A	L	Pallidum	N/A	-24	-8	2	8.68
	N/A	L/R	Insula, Thalamus, Putamen	N/A	N\A			N/A
	N/A	R	Pallidum	N/A	N\A			N/A
11038	1995.3	L	Area 6 (SMA)	46.6	-24	-4	62	8.04
					-34	-10	50	7.78
					0	-2	60	7.65
					-32	-8	58	7.23
					-14	-2	56	7.14
	1857.5	R	Area 6	43.5	N/A			N/A
	461.9	L	Area 2	51.3	N/A			N/A

	421	R	Area 2	44.3	38	-34	44	7.42
	197.1	L	IPC (PFt)	49	N/A			N/A
	184.4	R	IPC (PFt)	42.1	N/A			N/A
	172.6	L	hIP1	37.5	-30	-46	40	8.34
	169.5	R	Area 1	20.4	54	-30	56	7.02
					52	-32	58	6.99
	138.9	L	IPC (PF)	14.1	N/A			N/A
	138.3	L	Area 4p	24.4	N/A			N/A
	121.5	L	hIP2	53.8	N/A			N/A
	121.4	L	hIP3	43.3	N/A			N/A
	114.6	L	Area 4a	9.9	N/A			N/A
	N/A	R	Middle Cingulate Cortex	N/A	12	4	44	8.22
					8	10	34	7.56
	N/A	R	hIP1,hIP2,hIP3, BA3b, BA4a, BA4p	N/A	N\A			N/A
	N/A	L	BA3a, BA3b	N/A	N\A			N/A
434	332.4	L	SPL (7A)	20.1	-16	-68	50	5.9
					-20	-64	58	5.61
					-16	-60	58	5.29
					-18	-54	58	4.63
	52.3	L	SPL (7P)	9.6	-14	-70	58	5.51
	12	L	SPL (5L)	2.2	N\A			N/A
427	150.5	R	SPL (7A)	13.9	26	-54	56	4.24
					26	-56	62	3.91
	75.1	R	SPL (7P)	11.2	14	-68	56	4.49
	39.9	R	SPL (7PC)	9.8	34	-54	62	4.81
	34.6	R	hIP3	11.3	N\A			N/A
178	144.9	L	Area 44	12.4	-56	10	14	4.94
					-52	6	22	4.86
	6.1	L	Area 6	0.1	-58	8	34	4.19
152	N/A	R	Middle Frontal Gyrus		40	50	28	5.63
111	N/A	R	Middle Frontal Gyrus	N/A	48	52	4	4.86
					44	58	8	4.43
					44	48	10	4.07
92	1.5	L	Area 44	0.1	N\A			N/A
		L	Temporal Pole	N/A	-58	12	-4	5.13
20	N/A	L	Middle Orbital Gyrus	N/A	-26	56	-14	4.9
					-22	56	-12	4.39
EMGpm < 0								
878	N/A	R	Medial Temporal Pole	N/A	40	16	-32	9.8
	N/A	R	Middle Temporal Gyrus	N/A	58	-2	-20	7.04
					62	-6	-20	6.62

					66	-18	-10	5.25
	N/A	R	Superior Temporal Gyrus	N/A	58	-8	-10	4.96
828	N/A	R	Precuneus	N/A	4	-54	26	5.62
	N/A	R	Middle Cingulate Cortex	N/A	4	-54	32	5.61
	N/A	L/R	Precuneus	N/A	0	-56	26	5.42
					14	-50	24	5.42
					6	-50	26	5.25
692	N/A	R/L	Mid Orbital Gyrus	N/A	6	56	-10	7.19
					-6	52	-8	5.36
					16	58	-4	3.97
	N/A	L	Anterior Cingulate Cortex	N/A	-2	38	-8	3.91
544	357.5	L	IPC (PGp)	32.9	-48	-76	32	5.4
					-46	-78	28	5.12
					-52	-72	30	5.12
					-54	-68	30	5.08
					-44	-78	34	5.07
					-56	-64	34	4.88
					-52	-64	24	4.54
					-48	-62	24	4.4
	63.9	L	IPC (PGa)	8.2	N\A			N/A
	N/A	L	Angular Gyrus	N/A	-48	-56	24	4.58
	N/A	L	Middle Temporal Gyrus	N/A	-46	-62	12	4.44
442	128.3	R	IPC (PGa)	13.3	62	-58	26	5.32
	123.9	R	IPC (PGp)	10.6	52	-68	38	4.44
					56	-68	26	4.19
					54	-70	30	3.92
	N/A	R	Angular Gyrus	N/A	62	-58	26	5.32
	N/A	R	Middle Temporal Gyrus	N/A	50	-58	8	4.4
					60	-38	2	4.15
	N/A	R	Superior Temporal Gyrus	N/A	54	-32	2	4.1
					54	-42	12	4.07
	N/A	R	Middle Occipital Gyrus	N/A	54	-72	26	4.05
	N/A	R	Middle Temporal Gyrus	N/A	52	-54	16	3.94
					48	-50	16	3.87
190	N/A	L/R	Superior Medial Gyrus	N/A	10	60	22	4.49
					2	58	24	4.15
					0	56	28	4.01
					-4	58	30	3.99
187	N/A	L	Middle Temporal Gyrus	N/A	-54	6	-24	5.23
					-50	8	-26	5.11
	N/A	L	Medial Temporal Pole	N/A	-44	14	-32	4.93

	N/A	L	Middle Temporal Gyrus	N/A	-56	8	-28	4.75
					-60	2	-24	4.57
63	N/A	L	Middle Frontal Gyrus	N/A	-30	22	44	4.22
					-30	26	48	3.93
					-32	20	48	3.72
45	27.6	L	Area 3b	4.3	-58	-8	32	4.46
					-56	-6	28	4.31
	9.3	L	Area 4p	1.6	N\A			N/A
	4.9	L	Area 3a	1	N\A			N/A
	3	L	Area 1	0.3	-62	-6	32	3.73
34	16.8	R	Area 3a	3.6	54	-6	22	4.51
	12.1	R	Area 3b	1.3	56	-6	28	4.31
	4.4	R	Area 4p	0.9	N\A			N/A
26	12.6		IPC (PFcm)	3.4	-44	-34	18	4.8
	11.4		OP 1	1.9	-40	-32	22	4.44
	1		TE 1.1	0.6	N\A			N/A
12	N/A	R	Superior Medial Gyrus	N/A	8	46	44	4.26
12	N/A	R	Superior Frontal Gyrus		24	54	8	4.32
PPI > 0								
3064	990	L	Area 6 (SMA)	23.1	-4	-22	50	9.88
					-6	-14	54	9.86
					-8	-4	56	7.89
					-2	14	48	7
					-2	0	54	6.68
					-6	12	44	6.67
	334.6	L	Area 2	37.2	-58	-22	40	8.21
					-34	-46	52	6.67
	334.5	R	Area 6	7.8	N\A			N/A
	181.6	L	Area 3b	28.3	N\A			N/A
	177.3	L	Area 1	19.2	-32	-46	56	7.07
	174	L	Area 4a	15	-58	-16	42	6.95
	97.3	L	Area 4p	17.1	N\A			N/A
	75.9	L	IPC (PFt)	18.9	N\A			N/A
	31.4	L	Area 3a	6.3	N\A			N/A
	N/A	L	Middle Cingulate Cortex	N/A	-8	-24	48	10.08
		L	SPL(7PC)	N/A	N\A			N/A
1671	603.9	R	Cerebellar Lobule VI (Hem)	32.7	22	-50	-22	10.62
					10	-62	-22	5.16
	170	R	hOC4v (V4)	31.8	N\A			N/A
	51.8	R	hOC5 (V5)	52.1	54	-68	0	6.99
	45	R	hOC3v (V3v)	6.7	N\A			N/A
	33.3	R	Cerebellar Lobule V	4.2	N\A			N/A

	22	R	Cerebellar Lobule VIIa Crus I (Hem)	0.7	N\A			N/A
	N/A	R	Fusiform Gyrus	N/A	32	-58	-14	7.42
					30	-66	-18	7.37
					34	-60	-18	7.27
					38	-54	-22	6.22
	N/A	R	Middle Temporal Gyrus	N/A	56	-70	2	7.17
					42	-66	2	6.75
	N/A	R	Inferior Temporal Gyrus	N/A	52	-68	-6	5.39
1327	389.1	L	Cerebellar Lobule VI (Hem)	20	-28	-64	-22	9.15
					-20	-70	-24	6.66
	147.3	L	Cerebellar Lobule VIIa Crus I (Hem)	4.8	-36	-60	-30	6.24
					-38	-58	-28	6.19
					-34	-78	-22	5.59
	81.5	L	hOC4v (V4)	11.7	N\A			N/A
	46	L	hOC5 (V5)	63.4	N\A			N/A
	15.8	L	hOC3v (V3v)	2.4	N\A			N/A
	N/A	L	Middle Temporal Gyrus	N/A	-44	-70	8	7.2
	N/A	L	Fusiform Gyrus	N/A	-32	-60	-16	7.18
	N/A	L	Cerebellum	N/A	-32	-72	-20	5.57
	N/A	L	Inferior Occipital Gyrus	N/A	-38	-72	-10	5.49
					-52	-72	-4	5.45
	N/A	L	Middle Occipital Gyrus	N/A	-50	-70	-2	5.32
646	214.6	R	Area 1	25.9	58	-12	38	8.09
					52	-18	50	6.75
	130.8	R	Area 3b	14.2	62	-14	28	4.84
	100.6	R	Area 2	10.6	46	-26	52	6.58
	49.4	R	IPC (PFt)	11.3	54	-26	46	4.18
	39.5	R	Area 6	0.9	N\A			N/A
	11.1	R	Area 4a	1	N\A			N/A
	6.9	R	IPC (PFop)	2.5	54	-20	36	8.69
	N/A	R	Precentral Gyrus	N/A	60	-10	48	5.76
					56	2	50	4.72
	N/A	R	Postcentral Gyrus	N/A	66	-12	38	5.63
	N/A	R	SupraMarginal Gyrus	N/A	68	-16	30	5.48
556	365	R	Area 44	41.6	62	14	26	7.5
					60	18	14	7.41
					56	10	16	7.26
					56	14	14	6.89
					54	14	2	5.38
	37.4	R	Area 45	3.5	N\A			N/A
	N/A	R	Rolandic Operculum	N/A	48	4	6	5.66
					50	6	4	5.46

	N/A	R	Temporal Pole	N/A	62	10	-2	4.85
					64	4	0	4.78
436	103.6	L	Area 44	8.9	-48	10	4	6.04
					-62	8	20	5.57
					-54	8	16	5.51
					-56	6	8	5.09
	N/A	L	Superior Temporal Gyrus	N/A	-52	6	-4	6.42
403	220.8	L	OP 1	37.1	-52	-32	24	7.35
					-58	-18	16	7.2
	95.9	L	IPC (PFcm)	25.5	-48	-32	20	7.92
	49.6	L	IPC (PFop)	17.5	N\A			N/A
	7.1	L	IPC (PF)	0.7	N\A			N/A
	5.3	L	OP 4	0.9	N\A			N/A
	N/A	L	Superior Temporal Gyrus	N/A	-54	-40	20	4.66
					-50	-44	16	4.39
					-54	-44	14	4.21
361	138.3	R	IPC (PF)	15.6	64	-36	12	10.05
	57.6	R	OP 1	11.3	66	-20	14	5.26
					50	-22	18	4.49
					52	-26	18	4.17
	33.9	R	IPC (PFcm)	10.7	N\A			N/A
204	N/A	L	Thalamus	N/A	-8	-22	4	7.02
143	31.9	L	Amyg (SF)	17	-24	-2	-10	6.11
	3.8	L	Amyg (LB)	1.2	N\A			N/A
	2.1	L	Amyg (CM)	4	N\A			N/A
	N/A	L	Putamen	N/A	-22	8	-4	5.57
	N/A	L	Amygdala	N/A	-16	0	-14	4.96
85	N/A	L	Putamen	N/A	-22	8	10	5.66
					-22	-4	12	5.11
81	N/A	R	Putamen	N/A	24	10	-4	6.53
					28	6	8	5.02
47	N/A	R	Insula	N/A	30	22	10	5.29
					34	24	14	5.01
44	N/A	R	Thalamus	N/A	6	-24	-2	5.43
					10	-20	0	5.15
18	17.9	L	Area 6	0.4	-52	-4	44	4.58
15	N/A	R	Middle Cingulate Cortex	N/A	10	20	30	4.48
14	4.5	L	Area 18	0.3	-8	-62	-2	4.37
	1.3	L	Cerebellar Lobule VI (Hem)	0.1	N\A			N/A
	0.3	L	Cerebellar Lobule VI (Vermis)	0.1	N\A			N/A
	N/A	L	Cerebellar Vermis	N/A	-4	-70	-6	4.61

12	5.4	R	Hipp (SUB)	1	16	-40	-4	4.91
	N/A	R	Lingual Gyrus	N/A	12	-42	-2	5.21
11	1.6	L	Area 17	0.1	N\A			N/A
	0.4	L	Area 18	0	N\A			N/A
	0.1	L	hOC4v (V4)	0	N\A			N/A
	N/A	L	Lingual Gyrus	N/A	-24	-62	-6	4.73

Table1: Clusters of activity resulting from the contrasts ACT>PASS, PASS>ACT, EMGpm>0, EMGpm<0, and the PPI analysis. From left to right we first list the cluster size in number of voxels. Then if the cluster encompasses cytoarchitectonically mapped brain regions (CytoArea, as by the Anatomy toolbox), the number of voxels activated within that CytoArea; hemisphere; name of CytoArea and the percentage of that CytoArea activated within this cluster. If the cluster extends beyond CytoAreas, the macroanatomical name are indicated instead, but the number of voxels within the CytoArea and the % activated are then not available (N/A). The final two columns apply if a local maximum falls within the Cyto- or anatomical area, in which case we mention the MNI coordinates (in mm) and the T value of the maximum. Note that if an area encompasses less than 1% of the cluster, the anatomy toolbox does not provide the Number of voxels or % of CytoArea activated, but we still list these clusters here for completeness because they encompass more than our threshold of 10 voxels.

Most relevant for the present report, SI was activated in both of these contrasts, in particular its BA2 sub-region. In the EMGpm>0 analysis, both the left and the right BA2 showed significant modulation, with a larger proportion of the left BA2 (51.3%; contra-lateral to the squeezing hand) being modulated than the right BA2 (44.3%; ipsilateral to the squeezing hand).

The inverse contrasts ACT<PASS and EMGpm<0 mainly recruited areas along the superior temporal sulcus, parietal operculum and cingulate cortex. In line with our results, reduction of tactile responses in these areas have been previously described in humans14 (anterior cingulate cortex and parietal operculum) and monkeys18 (superior temporal sulcus) while participants were actively generating the tactile stimulus. In the interest of our focus on BA2, the results in PASS<ACT and EMGpm<0 will not be further discussed.

As expected given that the EMG was higher in ACT than PASS, the comparisons between ACT and PASS and EMGpm versus zero showed very similar activations. Conceptually, if the EMG is taken as a proxy for motor efference, and thus efference-copy, EMGpm>0 is the most direct localization of the efference-copy effect, can capture variance even within conditions, and will thus be used instead of ACT>PASS throughout the remainder of the paper.

Psycho-Physiological Interaction (PPI)

Increased activation of BA2 during blocks with higher EMG activity could be due to increased re-afference (i.e. more somatosensory input from the active hand) or efference-copy (more input from motor programming regions). If signals from motor regions contribute to the heightened BA2 activity during blocks with greater muscle activity, then the correlation between BA2 and motor regions should be higher on blocks with high muscle activity (i.e., active blocks) than on blocks with low muscle activity (i.e., passive blocks), when little efference-copy signals should be sent. Therefore, we performed a PPI interaction analysis with BA2 as the seed region and EMG as the interacting physiological signal to find areas where the connection with BA2 increases on blocks with high muscle activity.

The results are presented in Figure 1g and Table 1. Supporting the influence of motor signals on SI, we found a large cluster with peaks in the SMA, which shows higher connectivity with SI during trials with more EMG, and

hence, motor command generation 13. A number of other regions associated with motor control also showed increased connectivity: PM, PF, M1, and cerebellum, in accord with the results found using ischemia(Christensen et al., 2007). However, there was also a peak in bilateral BA3b, which suggests an alternative explanation of why BA2 activity is heightened in blocks with high EMG. Proprioceptive and tactile feedback was similar but not identical during ACT and PASS blocks, so it is possible that heightened BA2 activity on blocks with high EMG could be due to the differences in somatosensory re-afference from BA3b to BA2 through what we will call the 'body-loop'.

No voxels surviving FDR correction were found for the inverse, negative correlation (the first 16 voxels cluster within the gray matter appears at punc<0.002, qFDR>0.99, in the left hippocampus at MNI -30 -32 -12).

Partial Correlations

To explore whether the modulation of BA2 by regions involved in motor programming could simply be due to re-afference through the body-loop, we calculated partial correlations between activity in BA2 and the candidate motor control regions (SMA, PM, M1, PF and cerebellum). These partial correlations were obtained, in different analyses, after removing the variance shared (i) with the generic task time course (after HRF convolution), to remove variance due to the timing of the squeezing task; or (ii) the generic task and BA3b time courses, to exclude variance that could be associated with re-afference through BA3b. Figure 2 illustrates the rationale behind removing the generic task time-course (after HRF convolution), and calculating partial correlations over the entire (residual) time course of a run. If a ROI responds similarly to ACT and PASS trials, regressing out the generic task time course will generate an essentially flat residual, with only noise left. If the ROI responds differently to ACT and PASS trials, regressing out the generic task will preserve the variance between ACT and PASS trials in the residuals. Performing a correlation between the residuals across ROIs then specifically looks at whether variance in responses between ACT and PASS trials in one ROI predicts variance in the other, as would be expected if efference-copy signals are transmitted along that path. However, the entire time-course of each ROI flows into the analysis, so that spontaneous (resting-state-like) fluctuations in one region would also remain in the residual time-course, and its transmission along the path would also benefit the analysis.

Correlations that only partial out the task (Fig. 1h, black bars) confirm the significant link between BA2 and all the motor control regions as well as BA3b. Removing the variance shared with BA3b (gray bars) reduces the correlation with M1 to non-significance (p>0.8 after bonferroni correction, b.c., for 5 ROI), suggesting that the association between M1 and BA2 could be entirely mediated by the body-loop, i.e. by BA3b. For PF, cerebellum, SMA and PM, the correlation with BA2 is reduced (matched-sample t-test, all p<0.001 after b.c. for 5 ROI) but remains significant (all p<0.003 after b.c. for 5 ROIs). This suggests that these regions are linked to BA2 both through the body-loop and through an efference-copy. Finally, because PF shows a particularly high partial correlation with BA2 after removing BA3b variance, and because PF is a key anatomical hub linking frontal motor regions with BA2(Pons TP and Kaas JH, 1986;Rozzi et al., 2006) we explored if PF mediates the effect of SMA, PM and cerebellum on BA2, by additionally removing variance shared with PF (i.e., a partial correlation calculated after removing the variance shared with the generic task, BA3b and PF time courses; white bars). Doing so significantly reduced the partial correlations for all the ROIs (for SMA, PM and cerebellum, p<0.001; for M1, p<0.03 after b.c. for 4 ROIs), and all partial correlations were no longer significantly above zero (all p>0.2 even without b.c. for 4 ROIs), confirming a likely mediation by PF.

Inverse covariance method

For a more comprehensive path analysis, we used the inverse covariance method, that identifies which nodes have direct connections by exploring the significance of the partial correlation between these regions after removing variance shared with any other ROIs or the task (see methods). This analysis revealed two pathways

through which BA2 is connected with motor structures: one through BA3b (Fig. 1i, gray lines) and one through PF (black lines).

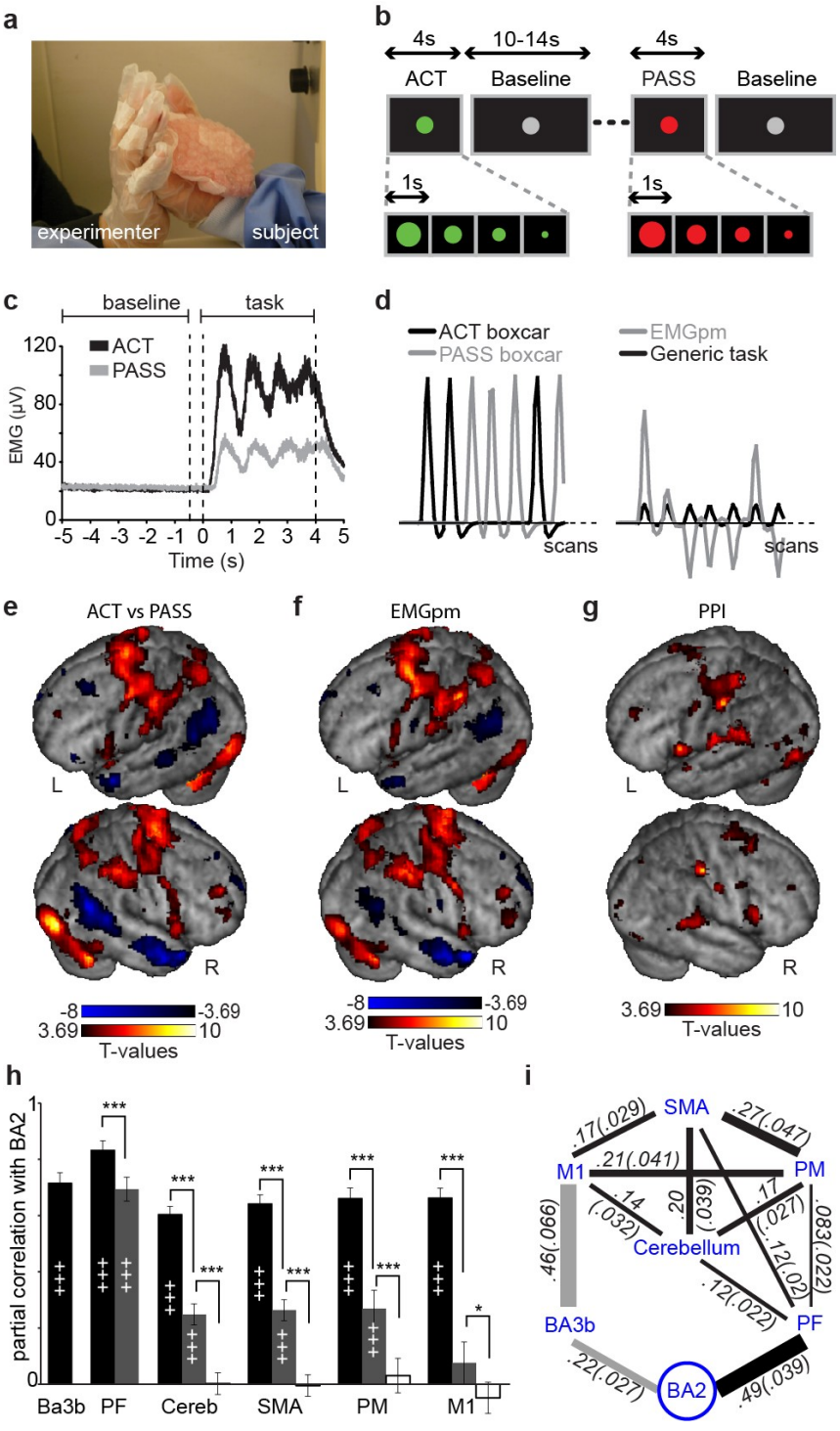

Figure1. (a) A photo of the experimental set-up. (b) Schematic diagram of the experimental design. (c) Comparison of the standard boxcar approach (left graph) to the data-driven EMG approach (right graph) to modeling the fMRI data of a representative subject. In the standard approach, a boxcar predictor models ACT blocks and another PASS blocks. In the EMG approach, a boxcar predictor models the effects of a nonspecific, generic task (i.e. a single predictor models both the ACT and PASS blocks); and the standardized and mean-corrected EMG is included as a first-order parametric modulator (EMGpm) of the generic task predictor. (d) Grand-average EMG responses during ACT and PASS conditions. Time 0 marks the onset of the 4 s blocks. (e) fMRI results of the comparison between the ACT and PASS conditions. (f) fMRI results of EMGpm versus

baseline. (g) PPI results. (h) Partial correlation between BA2 and the key ROIs revealed by the PPI analysis as a function of the variance that has been removed (task only, black bars; task and BA3b, gray bars; task and BA3b and PF, white bars). ***: one tailed paired t-test p<0.001 Bonferroni-corrected for 5 ROIs (task only vs. task and BA3b removed) or 4 ROIs (task and BA3b vs. task, BA3b and PF). *: same at p<0.05. +++: one-tailed t-test against zero, p<0.001, Bonferroni-corrected for 6 ROIs (task only), 5 ROIs (task and BA3b) or 4 ROIs (task and BA3b and PF). (i) ICOV analysis revealing the pattern of direct connectivity between the selected ROIs. Connection strength (visually presented as line thickness), as average partial correlation value (± standard deviation), is indicated on each significant partial correlation. Connections between the nodes represent all the significant partial correlations (at p<0.05, bonferroni corrected for 21 possible pair-wise correlations, two-tailed t-test). Connections in grey are likely to represent re-afference through the body loop, those in black neural connections that could carry efference-copy signals.

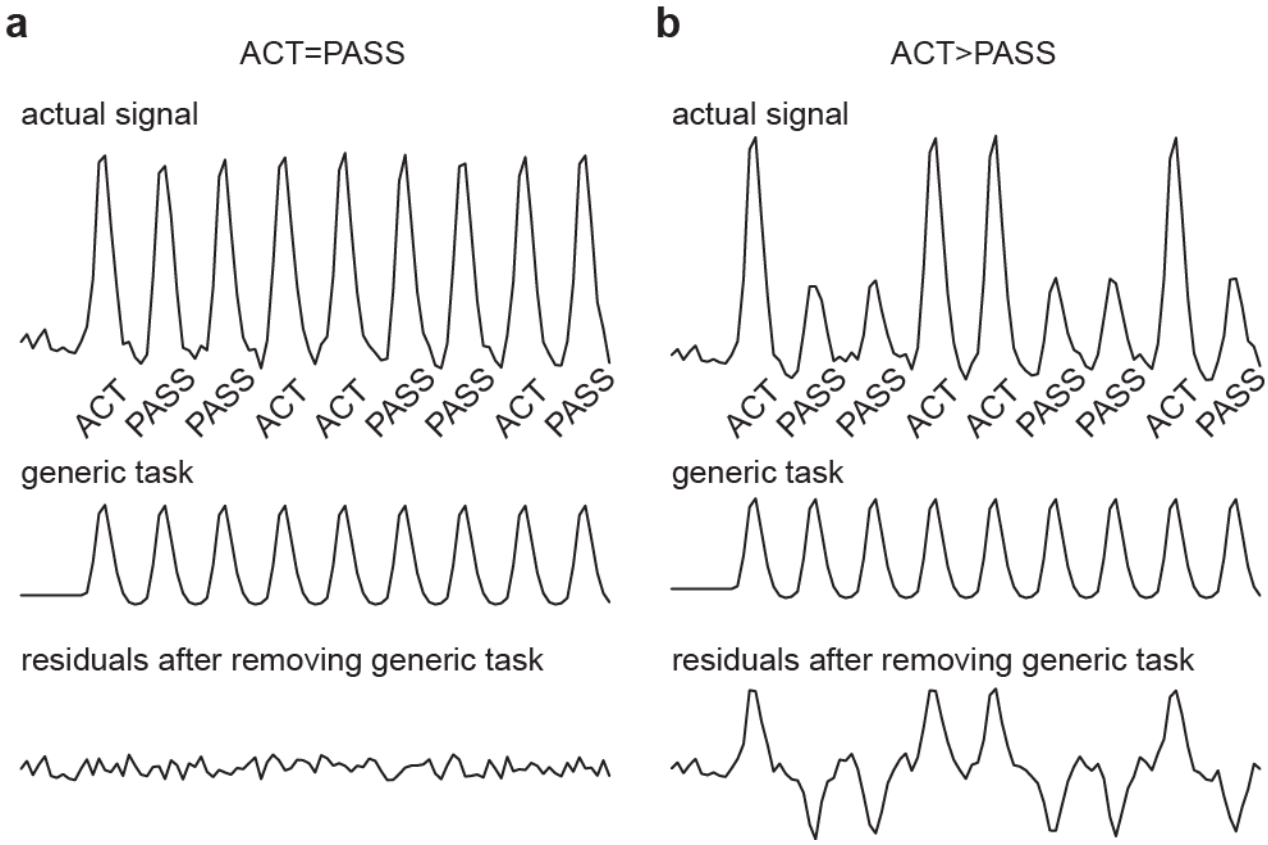

Figure 2: Illustration of the Partial Correlation Logic. (A) If a ROI has an actual BOLD response similar during ACT and PASS blocks, regressing out the time course of the generic task (after HRF convolution) leaves only noise in the residuals. (B) If a ROI responds differently to ACT and PASS, regressing out the same generic task retains the variance between conditions in the residual time-course. These residuals can then serve to track how differences between ACT and PASS are transmitted from ROI to ROI. The time-courses in this figure are not actual data, but simulated data to caricature the concept.

Discussion

In our study, we challenge the validity of reverse inferences, suggesting that activations in BA2 exclusively reflect somatosensory processes, by investigating whether BA2 activation can instead also reflect motor commands (e.g. efference-copies), as suggested by modern theories of motor control (Blakemore et al., 1999;Wolpert and Flanagan, 2001;Wolpert and Ghahramani, 2000;Wolpert and Miall, 1996;Johansson and Flanagan, 2009;Kawato, 1999). We varied the efference-copy signal by making participants squeeze a soft material in their hand either actively or passively. We measured the EMG activity in the participants' lower arm to quantify the amount of motor efference. We then used the magnitude of this measure on a given trial as a proxy for the magnitude of the efference-copy.

By correlating the EMG with the BOLD signals throughout the brain we show that in addition to early somatosensory regions (BA3b) and regions involved in motor programming (SMA, PM, M1, cerebellum and PF), BA2 activity was also positively correlated with the EMG signal. This correlation is compatible with the efference-copy account: BA2 activity is higher on high EMG trials because higher activity in motor regions, SMA in particular(Haggard and Whitford, 2004), would lead to higher efference-copy signals to BA2 through the known anatomical connections between the motor structures and BA2(Pons TP and Kaas JH, 1986), in particular through area PF(Rozzi et al., 2006). The presence of a similar correlation between EMG and BA3b is however compatible with an alternative body-loop account: despite our efforts to equate tactile sensations across conditions, the high EMG (active) trials might still have induced stronger tactile sensations that then activated BA2 more strongly via BA3b(Pons TP and Kaas JH, 1986).

A PPI analysis revealed that the connectivity with BA2 is augmented as a function of EMG with both somatosensory (BA3b) and motor control regions (SMA, PM, PM, M1, cerebellum and PF). This analysis is therefore again equally consistent with a body-loop (mediated by Ba3b) and efference-copy account of the BA2 modulation.

To establish whether some of the correlation in brain activity between BA2 and the motor control regions reflects an efference-copy, we removed any variance shared with BA3b using the most robust connectivity analyses available: partial correlations(Smith et al., 2011). Results indicated that although part of the association between the activity in these motor control structures and BA2 seems indeed to be mediated by BA3b, for all regions except M1, another significant part is not. This shared variance between BA2 and the motor control regions, not mediated by BA3b, is exactly what efference-copy theories would predict, and excludes the possibility that tactile differences between the conditions could have been the only driving force behind the differential BA2 activity. A mathematically similar analysis, the inverse covariance method, corroborated this conclusion: BA2 is linked to motor control structures along two complementary paths that map onto the notion of a body-loop and an efference-copy. The body-loop corresponds to a path where motor control structures feed onto M1, which feeds onto BA3b and finally BA2. Because no direct anatomical connections exist between M1 and BA3b(Jones et al., 1978), this M1->BA3b pathway probably reflects M1 triggering body motion that changed tactile input to BA3b. The other pathway involves the motor control structures feeding onto PF then BA2. This pathway is in agreement with the main anatomical connections between frontal structures and BA2(Pons TP and Kaas JH, 1986;Rozzi et al., 2006), and is therefore likely to reflect connections conveying an efference-copy.

While BA1 is known to play a critical role in relaying information from BA3b to BA2, this region is spatially so close to BA2 and BA3b, that its signal would have been highly correlated with that of the regions we already model. In the interest of the balance between accuracy and complexity BA1 was therefore not modeled.

Voluntary action is thought to originate in the frontal lobe, and the efference-copy could derive from premotor, supplementary motor and/or primary motor regions. Although most of the previous experiments are compatible with many of these routes, Haggard and colleagues identified SMA as a strong candidate13. Our own data indicates that SMA and/or PM, but not M1, are likely frontal source of the efference-copy to the somatosensory cortex, and suggest that PF is the main hub through which this efference-copy is sent to BA2. The cerebellum also seems to mediate part of that information in agreement with many theories(Kawato, 1999;Wolpert and Flanagan, 2001;Gazzola and Keysers, 2009a).

Two families of methods currently exist to explore connectivity in fMRI data(Smith et al., 2011). Undirected methods explore which brain regions are connected (directly or indirectly) using (partial) correlations, and simulations indicate these methods to be accurate and reliable(Smith et al., 2011). Directed methods additionally

attempt to derive the direction of information flow across regions but often lead to erroneous directions, and are thus less reliable(Smith et al., 2011;Schippers et al., 2011). Also in our case, undirected, correlation based analyses lead to a stable patterns of connectivity while our attempts to use directional methods (Dynamic Causal Modelling(Friston et al., 2003a)) lead to less stable results. In particular, the connection pattern, complexity or number of ROIs included in the model comparison altered depending on whether the winning directed model explained BA2 activation differences in terms of efferenc-copy alone, a direct input to BA2 or as a combination of efference-copy and re-afference (see Supplementary Method S1, and Supplementary Fig. S1 and S2). Accordingly, we decided not to present or interpret the results of the directed analysis measures any further. With this caveat in mind, that frontal motor regions send the efference-copy to PF and then onwards to BA2 is one of the interpretations of the data. Alternatively PF might be the origin of the 'decision' to move, sending information to frontal motor regions to generate an overt movement and to BA2 as somatosensory predictions. Attributing a seminal role to the parietal lobe in the generation of visually instructed action is compatible with findings that electro-stimulation of the posterior parietal lobe can generate a volition to act(Desmurget et al., 2009). Electroencephalographic investigations might in the future provide data with higher temporal resolution to further disentangle these alternatives.

Generally, our data however dovetail well with those of the study of Weber and colleagues(Weber et al., 2011), who recorded BA2 neurons in monkeys that showed changes in activity preceding active movements, of London and colleagues(London and Miller, 2013) who recorded neurons within SI (in particular BA2) that only discharged during passive and others only during active movements; and of Christensen and colleagues(Christensen et al., 2007), who, by depriving the brain of the afferent input to SI, provided evidence for the presence of an efference-copy signal to BA2. By maintaining normal somatosensory afference in our experiment, but keeping it relatively constant across active and passive trials with very different levels of efference-copy signal, we provide evidence that even in the context of normal physiological afference, EMG-correlated neural signals from the SMA and/or PM have a significant predictive power on BA2 activation levels.

That early studies failed to find a difference in BA2 activity when comparing active and passive conditions could be due to a lack of power since they included only 6 participants(Weiller et al., 1996a;Blakemore et al., 1998). That one study measured a reduction in BA2 activation in active compared to passive finger-tapping(Agnew and Wise, 2008) is however compatible with the idea that an efference-copy modulates BA2 activation but raises the question of when such an efference-copy augments and when it decreases BA2 activation.

In conclusion, our study suggests that the BOLD signal in BA2 can, under certain circumstances, reflect an input from motor control structures (SMA, PM, the cerebellum or PF in particular). This provides neural evidence for the recent view that efference-copy signals and internal models are part of the neural architecture of motor control (Blakemore et al., 1999;Johansson and Flanagan, 2009;Wolpert and Flanagan, 2001;Wolpert and Ghahramani, 2000;Wolpert and Miall, 1996;(Kawato, 1999). It additionally invites us to interpret activations in SI more carefully. That BOLD activation in BA2 can be significantly explained, in the sense of partial correlations, by signals from these motor control regions that scale with motor efference and that cannot be explained by BA3b activity, favors interpreting our effect in BA2 as at least partially motor rather than purely somatosensory. Theoretical models suggest that an internal model transforms the motor efference-copy into predicted somatosensory consequences(Caspers et al., 2010;Gazzola et al., 2006;Gazzola and Keysers, 2009a;Keysers and Gazzola, 2009a;Keysers et al., 2010). This interpretation would warrant calling the modulation of BA2 we measured somatosensory-motor rather than strictly motor. Accordingly, together with the data of Christensen et al(Christensen et al., 2007), London et al.(London and Miller, 2013) and Weber et al.(Weber et al., 2011) and the modern visions of sensorimotor control Blakemore et al., 1999;Johansson and Flanagan, 2009;Wolpert and

Flanagan, 2001;Wolpert and Ghahramani, 2000;Wolpert and Miall, 1996;(Kawato, 1999), our experiment suggests that we should interpret activations in BA2 in fMRI experiments as evidence for somatosensory-motor coding. Interpreting BA2 activations as evidence for somatosensory as opposed to, and qualitatively distinct from, motor coding, on the other hand, seems no longer appropriate.

Method

Nineteen right-handed subjects (11 male, 21.6 years ± 4.5 s.e.m.) with no history of neurological disorders participated in the experiment. One was excluded from all analyses due to electromyography recording problems, and one from the connectivity (incl. partial correlation) analyses because a stronger EMG response during passive compared to active blocks suggested poor understanding of task instructions. The research was approved by the Medical Ethical Committee of the University Medical Center Groningen (NL) and all subjects provided informed consent.

Participants and the experimenter wore a thin latex glove on their right hand (Fig. 1a). On the palm side of the subject's glove, a bubble wrap was attached as object to squeeze. During PASS, participants were shown a sequence of four 1s red circles of decreasing size (Fig. 1b). At the onset of each circle, author CF squeezed the bubble wrap, by acting upon the subject's right hand fingers. During ACT, the circles were green instead of red, and the participant gently squeezed the bubble wrap. Because subject's and experimenter's gloves were glued together, during ACT the experimenter could follow, with her fingers, the subject's movements, introducing a light pressure (i.e. an afference signal) similar to the one in PASS. Prior to scanning, (i) participants and author CF rehearsed to make the squeezing force and range of motion as similar as possible in both conditions to ensure that somatosensory feedback would be closely matched, and (ii) participants were trained, by EMG biofeedback, to keep the EMG as small as possible during PASS. The 20 ACT and 20 PASS blocks were presented in a pseudo-randomized order. A random duration (10-14 s) centered gray circle separated the blocks.

Surface EMG monitored muscle activity from the flexor digitorum superficialis (FDS) muscle. A bipolar recording was made from two electrodes, placed longitudinally with respect to the muscle fibers above the FDS on the skin, close to the more superficially positioned flexor carpi radialis muscle, using the BrainAmp MR plus system (Brain Products GmbH, Munich, Germany). The electrode locations were determined by observing and palpating muscle contractions, using maximum voluntary contractions (as measured by the EMG) towards the specific pulling direction of the FDS. A reference electrode was placed on the right wrist, at the processus styloideus. All data were recorded at 5 kHz using the Brain Vision Recorder 1.03 software (Brain Products, Munich, Germany). BrainVison Analyzer 1.05 was used to correct the EMG data for MRI artifacts using the standard averaging and subtraction method. A 10 Hz high-pass filter was applied to remove movement artifacts (van Rootselaar AF et al., 2007). The data were then rectified and down sampled to 250 Hz.

Functional MRI images (EPIs) were acquired, with a Philips Intera 3T Quasar whole body scanner, using a a T2-weighted echo-planar sequence (39 interleaved, 3.5 mm axial slices, no gap; TR=2000 ms; TE=30 ms; flip angle = 80°; FOV = 224x224 mm; 64x64 matrix of 3.5 mm isotropic voxels), and were followed by a whole brain T1-weighted anatomical image (1x1x1mm), parallel to the bicommissural plane. All EPIs were slice-time corrected and realigned to the subject's mean EPI. The normalization parameters from the segmentation of the mean-co-registered T1 images were then applied to all EPIs. Data were smoothed with a 9mm isotropic FWHM Gaussian kernel (SPM8; http:www.fil.ion.ucl.ac.uk/ spm/software/ spm8).

An MR-compatible 32-channel BrainAmp system (Brain Products, Munich, Germany) was used to record EEG simultaneously for purposes not discussed in this paper 29. For most subjects, there was a drop in BOLD signal intensity over the left parietal lobe, likely an artifact caused by the EEG cables. SPM8 therefore considered these

voxels out of the brain. The procedure described in Arnstein et al. (2011) was used to allow SPM8 to accurately identify the boundaries of the parietal lobe. Additionally, regression analyses found no significant relationship between the amount of attenuation within regions of interest in a participant and the connectivity measures derived from those regions in that participant (see Supplementary Method S3).

In both GLMs blocks in which the task was performed incorrectly were modeled separately with a boxcar predictor of no interest and then convolved with the HRF. To account for head movements we included 24 parameters (three translations, three rotations, their first temporal derivative, their quadratic, and these head motion parameters shifted forward by 1TR), as covariates of no interest, not convolved with the HRF.

Activity in left BA2, defined using the Anatomy Toolbox 1.7 maps (Eickhoff SB et al., 2005; http://www.fz-juelich.de/ime/spm_anatomy_toolbox) for SPM8, was the physiological predictor for the PPI analysis. At first level, for each subject, we visualized EMGpm>0 at punc<0.001, and extracted the first eigenvariate from a 6 mm sphere, centered on the individual's absolute maximum within the left BA2 masked results. The EMGpm of each participant's original GLM was the psychological variable. The SPM8 PPI function then determined the interaction term. We used the psycho-physiological option because the EMG measurement, like a psychological variable, does not lag behind the underlying neural process. The physio-physiological option, terminologically more appropriate, would instead have de-convolved the EMGpm signal. A new GLM was then created for each participant using these three predictors. The parameter estimates for the interaction term were brought to second level analysis, comparing it against zero using a t-test. Only 14 out of the 17 subjects had a maximum within left BA2 at punc<0.001. For the PPI analysis, we therefore only show group results coming from them. A similar analysis, reducing the thresholds for the ROI definition to include all 17 participants led to virtually identical results (see Supplementary Methods S2 and Fig. S3).

All analyses were initially thresholded at punc<0.001 (k>10) at the second, group level. To control the overall false discovery rate, we only report results that also survive a voxelwise qFDR<0.05.

Based on the PPI results, for the partial correlation analyses, we defined (Anatomy Toolbox) seven anatomical ROIs: BA2, BA3b, PF, cerebellum, SMA, PM and M1. All, but SMA, only included the left hemisphere. BA2 and BA3b maps were directly selected from the toolbox; PF included the PF, PFt, PFop, PFm, PFcm; and M1 the BA4a and 4p. Based on visual inspection of the averaged anatomy of our group, and on the Harvard-Oxford cortical atlas (http:// www. cma.mgh.harvard.edu/ fsl_atlas.html), to obtain the SMA, we intersected (Marsbar, http://marsbar.sourceforge.net) left and right BA6 maps with a box containing all voxels along y and z, but only from -17 to +17 along x. For left PM, we combined BA6 and 44 and used all x<-17. Cerebellum included lobule 5 and 6, which contain the main cerebellar hand representation and are connected with motor, parietal and somatosensory hand representations in the cortex(Ramnani, 2012). For each ROI and participant, we extracted the first eigen-time-course from all voxels for which EMGpm>0 at punc<0.05. Only 14 participants contained at least 5 significant voxels in all ROIs, and the analysis was restricted to them. The mean partial correlation values for the 14 participants in the three correlation analyses were assessed at second level using a one tailed t-test against zero. All significant t-test results were also significant when using non-parametric tests (Wilcoxon-Signe Rank or Mann-Whitney U).

To identify which ROIs are directly connected, we explored the significance of the partial correlation between these regions after removing variance shared with any other ROI or the task. Assuming that the matrix of plausible connections between the ROIs is sparse, the inverse covariance method ("glasso" implementation in the R Statistical package) leverages the fact that a full set of partial correlations can be computed using the inverse of the covariance matrix(Marrelec et al., 2006) and then constrains the sum of the absolute coefficients of

the individual regressors of the partial correlation matrix to be less than a given constant tuning parameter λ. This Lasso shrinkage method(Banerjee O et al., 2006;Friedman et al., 2008) sets many of the entries in the partial correlation matrix to zero as a function of λ. Note that λ=0 corresponds to a full partial correlation and successively incrementing λ sets many of the partial correlation values to zero, while resulting in different fitting errors for the model. We present the results corresponding to λ=0.01 and the results remain robust against slight variations of this value.

References Cited

Agnew, Z., and R. J. Wise, 2008, Separate areas for mirror responses and agency within the parietal operculum: J.Neurosci., v. 28, no. 47, p. 12268-12273.

Banerjee O, El Ghaoui L, d'Aspremont A, Natsoulis G. Convex optimization techniques for fitting sparse Gaussian graphical models. Proceedings of the 23rd international conference on Machine learning. 2006.
Ref Type: Conference Proceeding

Blakemore, S. J., C. D. Frith, and D. M. Wolpert, 1999, Spatio-temporal prediction modulates the perception of self-produced stimuli: J.Cogn Neurosci., v. 11, no. 5, p. 551-559.

Blakemore, S. J., D. M. Wolpert, and C. D. Frith, 1998, Central cancellation of self-produced tickle sensation: Nat.Neurosci., v. 1, no. 7, p. 635-640.

Caspers, S., K. Zilles, A. R. Laird, and S. B. Eickhoff, 2010, ALE meta-analysis of action observation and imitation in the human brain: Neuroimage, v. 50, no. 3, p. 1148-1167.

Christensen, M. S., J. Lundbye-Jensen, S. S. Geertsen, T. H. Petersen, O. B. Paulson, and J. B. Nielsen, 2007, Premotor cortex modulates somatosensory cortex during voluntary movements without proprioceptive feedback: Nat.Neurosci., v. 10, no. 4, p. 417-419.

Desmurget, M., K. T. Reilly, N. Richard, A. Szathmari, C. Mottolese, and A. Sirigu, 2009, Movement intention after parietal cortex stimulation in humans: Science, v. 324, no. 5928, p. 811-813.

Friedman, J., T. Hastie, and R. Tibshirani, 2008, Sparse inverse covariance estimation with the graphical lasso: Biostatistics., v. 9, no. 3, p. 432-441.

Friston, K. J., L. Harrison, and W. Penny, 2003, Dynamic causal modelling: Neuroimage, v. 19, no. 4, p. 1273-1302.

Gazzola, V., L. Aziz-Zadeh, and C. Keysers, 2006, Empathy and the somatotopic auditory mirror system in humans: Curr.Biol., v. 16, no. 18, p. 1824-1829.

Gazzola, V., and C. Keysers, 2009, The observation and execution of actions share motor and somatosensory voxels in all tested subjects: single-subject analyses of unsmoothed fMRI data: Cereb.Cortex, v. 19, no. 6, p. 1239-1255.

Haggard, P., and B. Whitford, 2004, Supplementary motor area provides an efferent signal for sensory suppression: Brain Res.Cogn Brain Res., v. 19, no. 1, p. 52-58.

Johansson, R. S., and J. R. Flanagan, 2009, Coding and use of tactile signals from the fingertips in object manipulation tasks: Nat.Rev.Neurosci., v. 10, no. 5, p. 345-359.

Jones, E. G., J. D. Coulter, and S. H. Hendry, 1978, Intracortical connectivity of architectonic fields in the somatic sensory, motor and parietal cortex of monkeys: J Comp Neurol, v. 181, no. 2, p. 291-347.

Kawato, M., 1999, Internal models for motor control and trajectory planning: Curr.Opin.Neurobiol., v. 9, no. 6, p. 718-727.

Keysers, C., and V. Gazzola, 2009, Expanding the mirror: vicarious activity for actions, emotions, and sensations: Curr.Opin.Neurobiol., v. 19, no. 6, p. 666-671.

Keysers, C., J. H. Kaas, and V. Gazzola, 2010, Somatosensation in social perception: Nat.Rev.Neurosci., v. 11, no. 6, p. 417-428.

London, B. M., and L. E. Miller, 2013, Responses of somatosensory area 2 neurons to actively and passively generated limb movements: J Neurophysiol., v. 109, no. 6, p. 1505-1513.

Marrelec, G., A. Krainik, H. Duffau, M. Pelegrini-Issac, S. Lehericy, J. Doyon, and H. Benali, 2006, Partial correlation for functional brain interactivity investigation in functional MRI: Neuroimage, v. 32, no. 1, p. 228-237.

Poldrack, R. A., 2006, Can cognitive processes be inferred from neuroimaging data?: Trends Cogn Sci., v. 10, no. 2, p. 59-63.

Pons TP, and Kaas JH, 1986, Corticocortical connections of area 2 of somatosensory cortex in macaque monkeys: a correlative anatomical and electrophysiological study: J Comp Neurol, v. 248, no. 3, p. 313-335.

Ramnani, N., 2012, Frontal lobe and posterior parietal contributions to the cortico-cerebellar system: Cerebellum., v. 11, no. 2, p. 366-383.

Rozzi, S., R. Calzavara, A. Belmalih, E. Borra, G. G. Gregoriou, M. Matelli, and G. Luppino, 2006, Cortical connections of the inferior parietal cortical convexity of the macaque monkey: Cereb.Cortex, v. 16, no. 10, p. 1389-1417.

Schippers, M. B., R. Renken, and C. Keysers, 2011, The effect of intra- and inter-subject variability of hemodynamic responses on group level Granger causality analyses: Neuroimage, v. 57, no. 1, p. 22-36.

Smith, S. M., K. L. Miller, G. Salimi-Khorshidi, M. Webster, C. F. Beckmann, T. E. Nichols, J. D. Ramsey, and M. W. Woolrich, 2011, Network modelling methods for FMRI: Neuroimage, v. 54, no. 2, p. 875-891.

Weber, D. J., B. M. London, J. A. Hokanson, C. A. Ayers, R. A. Gaunt, R. R. Torres, B. Zaaimi, and L. E. Miller, 2011, Limb-state information encoded by peripheral and central somatosensory neurons: implications for an afferent interface: IEEE Trans.Neural Syst.Rehabil.Eng, v. 19, no. 5, p. 501-513.

Weiller, C., M. Juptner, S. Fellows, M. Rijntjes, G. Leonhardt, S. Kiebel, S. Muller, H. C. Diener, and A. F. Thilmann, 1996, Brain representation of active and passive movements: Neuroimage, v. 4, no. 2, p. 105-110.

Wolpert, D. M., and J. R. Flanagan, 2001, Motor prediction: Curr.Biol., v. 11, no. 18, p. R729-R732.

Wolpert, D. M., and Z. Ghahramani, 2000, Computational principles of movement neuroscience: Nat.Neurosci., v. 3 Suppl, p. 1212-1217.

Wolpert, D. M., and R. C. Miall, 1996, Forward Models for Physiological Motor Control: Neural Netw., v. 9, no. 8, p. 1265-1279.

Acknowledgments: The work was supported by a Marie Curie Excellence Grant of the European Commission and a VIDI grant of the Dutch science foundation to CK (N.W.O.), a VENI grant of N.W.O. to VG, Fulbright scholarship to DA and the China Scholarship Council for State Scholarship Fund to FC.

Current affiliation for author D.A.: Department of Cognitive Neurology, Hertie Institute for Clinical Brain Research, University of Tübingen, 72076 Tübingen, Germany

Author Contribution: The first two, and the last three authors contributed equally to this work. F.C. and D.A. collected the data with the help and supervision of N.M.M and V.G., and performed the analyses and discussed the results with the help and supervision of C.K., N.M.M., V.G. (all parts) and R.M.T. (partial correlations and inverse covariance analyses). C.K. and V.G. conceived the study with suggestion from N.M.M., F.C. and D.A. All authors discussed the results and implications and commented on the manuscript, who was initially written by D.A. and F.C., then edited by C.K. and V.G., with extensive comments from N.M.M.

Supplementary Materials

Supplementary Method S1: Dynamic causal modeling (DCM)

Directed methods such as the DCMS1 attempt to derive the direction of information flow across regions. A limitation of DCM is the astronomic number of possible models to account for the connectivity pathways in even a limited number of regions of interest. Indeed, even with just five regions of interest, the number of possible connections between them and the possible task effects are in the order of many millionsS2, orders of magnitude more than the number of data points acquired in typical fMRI experiments, making a systematic comparison impossible. Picking out a small number of models based on a priori hypotheses on the other hand becomes so arbitrary and subjective that it no longer satisfies the criteria for objectivity and reproducibility so important to science. In addition, simulations have shown that methods like DCM or Granger Causality, that aim to detect the direction of information flow in the brain, often detect directions of information that are opposite to the ones actually in the dataS3, . We nevertheless tried to run two DCM analyses, with different numbers of regions of interests that were suggested by the PPI results, to disentangle whether differences between conditions depend on efference-copies from motor regions or re-afference from somatosensory cortices.

Based on the idea proposed by Haggard and WhitfordS5 that the most likely source of the efference copy to somatosensory areas is the SMA, the first set of models only included the SMA, BA3b and BA2 regions of interest. The anatomical areas were again chosen from the cytoarchitectonic information provided by the Anatomy Toolbox 1.7 for SPM8, and again, due to the unilaterality of our task, which was only performed with the right hand, for BA2 and BA3b we only considered the left hemisphere. Subdividing SMA in right and left hemispheres is less justifiable since SMA covers the medial wall. Hence, as for the PPI analysis presented in the main text, SMA, was defined by including only the medial region ($-17 \leqslant x \leqslant 17$) of BA6. The eigen-vectors needed to run the DCM analysis were calculated at the first level by looking at the EMGpm>0 results with a threshold of punc<0.05. This threshold was chosen to guarantee enough subjects in the analysis. Fourteen out of the seventeen subjects had significant voxels within the selected ROIs and they were therefore included in the final

analysis. After defining candidate models, we used random effect Bayesian model selection implemented in SPM8 to identify the model with the highest evidence in the applied Bayesian framework. The investigated models and the results of this DCM analysis are shown in Supplementary Figure S1. Results indicate that the efference-copy only model, in which the effect of EMG is introduced by the SMA is the most likely model. Models including an effect of EMG into BA3b, as would be the case if the somatosensory differences between high- and low-EMG trials were reaching BA2 through BA3b, are less likely.

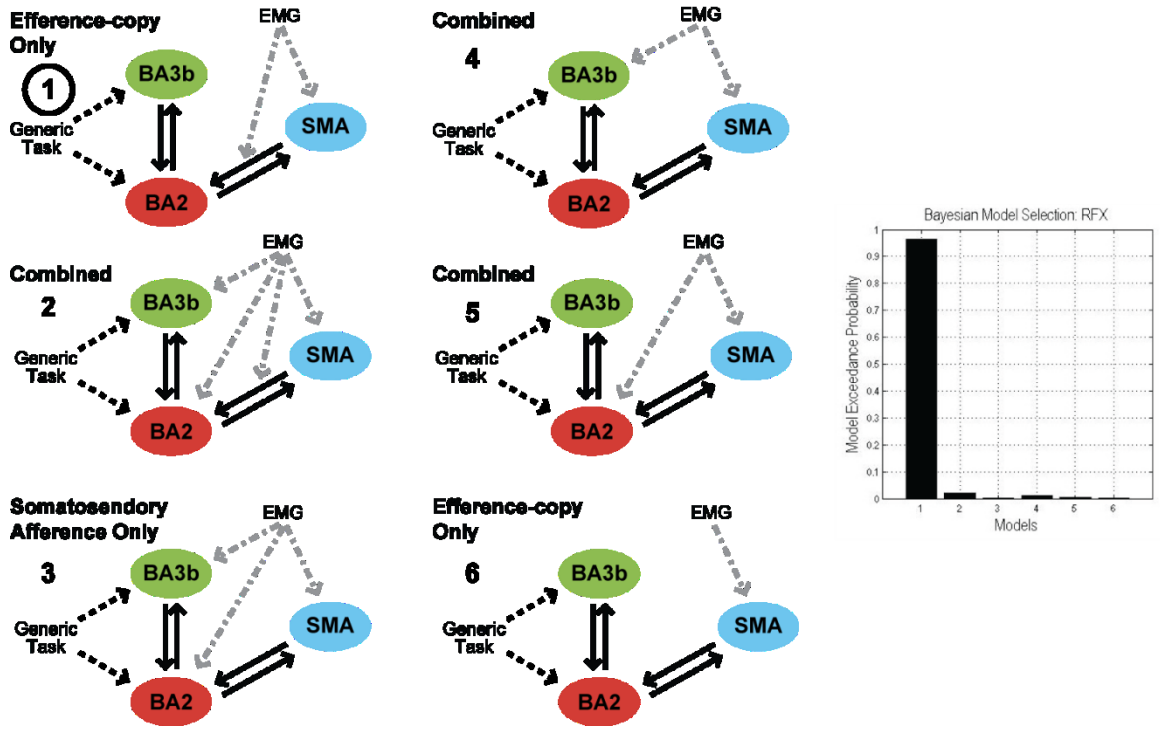

Supplementary Figure S1: Graphical illustration of the six models compared in DCM, with RFX Bayesian model comparison results in the graph on the right. The numbers in the top left of each graph correspond to those in the x-axis of the chart.

In the second DCM analysis we included other possible sources of the efference-copy signal, in particular the premotor and the primary motor cortices. As Supplementary Figure S2 illustrates, adding additional nodes tips the balance towards mixed models (similar to the results of our inverse covariance matrix analysis in the main paper). The winning model (model 9) is indeed one in which BA2 is influenced by a task dependent modulation from both BA3b and the motor regions. The next-best model however, is of much lower complexity (making the comparison difficult), and includes a direct effect of EMG on BA2 that is difficult to interpret. This result raises many questions, about the role complexity plays in the Bayesian comparison, and about whether variants of the models would winS2, making DCM ill suited for our purpose. We therefore do not explore DCM further for this data-set.

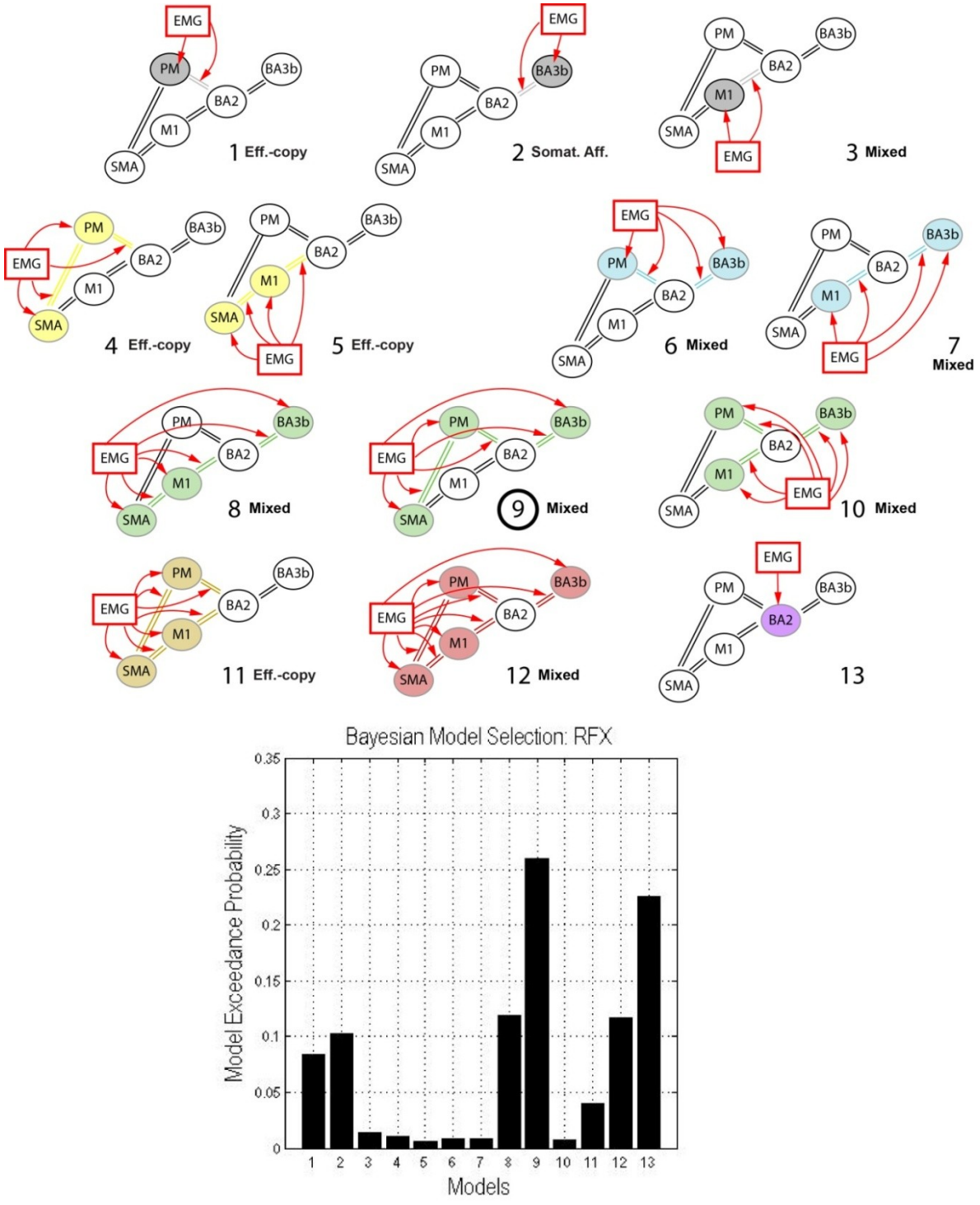

Supplementary Figure S2: Graphical illustration of the models including M1 and PM compared in the DCM analysis, with RFX Bayesian model comparison results in the graph on the right. The numbers in the right underside of each graph correspond to those in the x-axis of the chart. Note that the generic task is always included as modulator of both BA3b and BA2, as in the previous analysis.

For the main paper, we therefore felt that an approach that can accommodate all relevant ROIs, and that can explore the whole search space of possible connections and task effects in a principled and exhaustive manner would be preferable to an arguably arbitrary a priori selection of models. Because Lohmann et al.S2, essentially point out that DCM cannot do that, and because Smith et al.S4 came to the conclusion that methods based on

partial correlation are the most robust methods to explore connectivity from fMRI data, we opted to use partial correlations as our main tool in the main manuscript. Reasuringly, partial correlations confirmed the tentative conclusion of our DCM analyses, namely that an input to BA2 from motor structures is significant, and cannot be reduced to re-afference from BA3b alone.

Supplementary method S2: PPI analysis including all 17 subjects

To be able to include the data (i.e. eigen-vector) from all our participants, and therefore have results that, although most likely influenced by noise, are more representative of the group, we re-run the PPI analysis by lowering the single subjects threshold of the EMGpm>0 single subject results used to identify the local maxima within our left BA2 region of interest. For the 4 subjects at which there were no voxels left at punc<0.001 we therefore used punc<0.5. The results of the second level of the analysis, run in the same way presented in the current manuscript, are presented in Supplemental Figure 1 and Table1. Both analyses gave very similar results (both at p<0.001 also surviving pFDR<0.05)

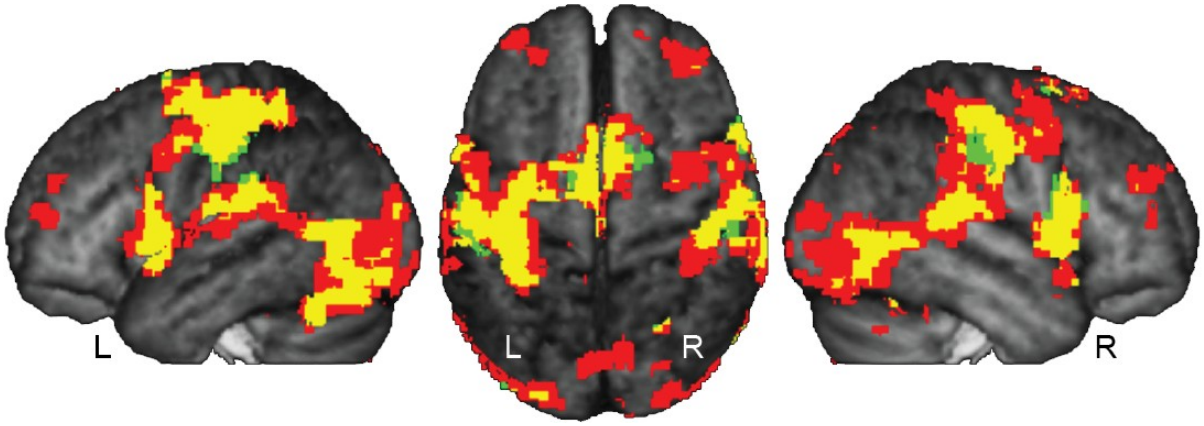

Supplemental Figure S3. PPIs group results. *Green color:* second level PPI results currently presented in the manuscript (T<4.02 at p_{unc}<0.001, all survive q_{fdr} <0.05). The eigen-vectors were extracted from a 6mm sphere centered on the local maxima within the anatomical BA2 ROI. Eigen-vectors were extracted at the single subject level at p_{unc} <0.001 for 14 out of 17 subjects. *Red color:* second level PPI results for the entire group of 17 subjects (T>3.69, p_{unc} <0.001, all voxels also survive q_{fdr}<0.05). As for green, the eigen-vectors were extracted from a 6mm sphere centered on the local maxima within the anatomical BA2 ROI. Eigen-vectors were extracted at single subject level within that region from all voxels where a subject showed a correlation with EMG, at p_{unc}<0.001 threshold for 14 out of 17 subjects, and at p_{unc}<0.5 for the remaining 4. *Yellow color:* overlap between Red and Green.

Supplementary method S3: Influence of the EEG artifact on the partial correlation analyses

As mentioned in the method section, during the whole experimental session, subjects wore an EEG cap. This is because the data presented here were collected together with the data presented in Arnstein et al. 2010S6, for which the EEG was required. Unexpectedly, the bundle of cables connecting the EEG cap to the amplifier, which was often pressed close to the subject's scalp by the MRI head coil, was the likely source of the drop in BOLD signal intensity over the left parietal lobe observed in most subjects. These reduced EPI signals lead SPM8 to consider these voxels out of the brain. To solve this problem: (a) all subjects' smoothed and normalized mean EPIs were averaged into a grand mean EPI; (b) this grand mean EPI was divided by each subject's mean EPI; (c) we then multiplied, for each subject separately, all the smoothed EPIs by the subject's correction map obtained in point (b) (see Supplementary Fig. 1 from Arnstein et al. (2011) for more details, http://www.herseninstituut.knaw.nl/Portals/0/ Department/ keysers/ Arnstein%20SupplementaryFigures.pdf). This procedure allowed SPM8 to accurately identify the boundaries of the left parietal lobe for all subjects. While this

procedure does not bias the significance of the univariate approach of the General Linear Model that examines changes over time, because the same correction factor was applied to all EPI images of the same participant, it might affect the connectivity analyses run on the data presented in the current manuscript. Because we explore efference-copy signals using partial correlations between BA2 and five motor control ROIs after removing the effect of task and BA3b, if dropout would bias these connectivity measures, we would expect a correlation across participants: the amount of dropout in a participant should predict the value of the connectivity measure between the ROIs in that participant. We thus explored whether individual differences in signal drop-out in BA2 predict individual differences in the partial correlation between BA2 and any of the motor control ROIs (SMA, PM, M1, Cerebellum and PF). We found that in none of these cases, the correlation between the dropout in BA2 (quantified as the average correction index within the BA2 ROI) and the connectivity measure (partial correlation BA2 and motor control ROI after taking out the effect of task and BA3b) was significant. The five correlations ranged from $r=.33$ to $r=.18$, with p values ranging from $p=0.25$ to $p=0.51$. Also, no significant correlations were found, when using the dropout in a motor control ROI to predict the partial correlation between that region and BA2. This suggests that our connectivity analyses were not systematically biased by dropout over BA2 or any of the motor control ROIs. There was also no linear relationship between the variance (over time) of the ROI time course in BA2 (after correction) and the average drop-out in that ROI ($p>0.83$).

Mu-suppression during action observation and execution correlates with BOLD in dorsal premotor, inferior parietal and SI cortices.

Dan Arnsteina, Fang Cuia,b, Christian Keysersb,a, Natasha M. Mauritsc, Valeria Gazzolaa,b

a: Department of Neuroscience, University Medical Center Groningen, University of Groningen

b: Netherlands Institute for Neuroscience, Royal Netherlands Academy for Arts and Sciences, Amsterdam

c: Department of Neurology, University Medical Center Groningen, University of Groningen

The first two, and the last three authors contributed equally.

Corresponding author: Valeria Gazzolab,a, v.gazzola@nin.knaw.nl, Meibergdreef 47, 1105BA Amsterdam

Acknowledgments: The work was supported by a Marie Curie Excellence Grant of the European Commission and a VIDI grant of the Dutch science foundation to CK (N.W.O.), a VENI grant of N.W.O. to VG, Fulbright scholarship to DA and the China Scholarship Council for State Scholarship Fund to FC. We also thank Alessandro Rigon, Paolo Toffanin, Nikola Valchev and Idil Kokal for their help in preparing the experiment.

Abstract

The discovery of mirror neurons in the monkey, that fire during both the execution and the observation of the same action, sparked great interest in studying the human equivalent. For over a decade, both functional magnetic resonance imaging (fMRI) and electroencephalography (EEG) have been used to quantify activity in the human mirror neuron system (MNS) - yet, little is still known about how fMRI and EEG measures of the MNS relate to each other. To test the frequent assumption that regions of the MNS as evidenced by fMRI are the origin of the suppression of the EEG μ-rhythm during both action execution and observation, we recorded EEG and BOLD-fMRI signals simultaneously while participants observed and executed actions. We found that the suppression of the μ-rhythm in EEG covaried with BOLD activity in typical MNS regions (IPL, dPM and BA2) during both action observation and execution. In contrast, in BA44, only non-overlapping voxels correlated with μ-suppression during observation and execution. These findings provide direct support for the notion that μ-suppression is a valid indicator of MNS activity in BA2, IPL and dPM, but argues against the idea that mirror neurons in BA44 are the prime source of μ-suppression. These results shed light on the neural basis of μ-suppression and provide a basis for integrating more closely the flourishing but often separate literatures on the MNS using fMRI and EEG.

Introduction

The discovery of mirror neurons (Gallese et al., 1996; Umilta et al., 2001; Kohler et al., 2002) has sparked great interest in measuring the activity of the mirror neuron system (MNS) in humans (Keysers, 2009) and psychiatric patients in particular (Iacoboni and Dapretto, 2006; Rizzolatti et al., 2009). Two methods are dominant: functional magnetic resonance imaging (fMRI) and electroencephalography (EEG). Although they are assumed to both measure activity in the same MNS, little is known about how these measures of the MNS relate to each other.

fMRI typically maps the MNS as voxels active when a participant executes and perceives similar actions (Grezes et al., 2003; Dinstein et al., 2007; Gazzola and Keysers, 2009; Turella et al., 2009) – so called shared voxels (sVx;

(Gazzola and Keysers, 2009)). Regions involved in hand-action execution are localized using relatively complex movements (reaching and manipulating an object). EEG typically quantifies MNS activity using the modulations of a ~10Hz rhythm (lower μ) recorded over the sensorimotor cortex. Mu is measured while participants observe hand actions (Gastaut, 1952; Pineda et al., 2000; Oberman et al., 2005; Pineda, 2005; Southgate et al., 2009), and while repeatedly executing the same action (Pineda et al., 2000; Oberman et al., 2005; Raymaekers et al., 2009), e.g. closing and opening a hand. Mu power is reduced during both action observation and execution. Mu is most powerful in the primary somatosensory cortex (SI; (Salmelin et al., 1995; Ohara et al., 2000; Caetano et al., 2007)), however we lack evidence for the assumption that regions of the MNS, the ventral premotor cortex in particular (Pineda, 2005), are responsible for μ-modulation and that fMRI and μ-suppression experiments measure the functioning of the same MNS . Elegant MEG experiments also investigated a ~20Hz μ-component which rebounds after action observation and execution (Hari et al., 1998), but because optimal designs to study 10Hz and 20Hz components differ, we focus here on the most studied, 10Hz component, and will use μ as shorthand for that component alone.

Hence, we simultaneously measured EEG and fMRI while participants observed and executed hand actions. If fMRI and μ-suppression EEG both record the activity of the same underlying MNS, on a trial-by-trial basis, the μ-power should be negatively correlated with the BOLD signal during both observation and execution of actions, mainly in regions typically associated with the human MNS. These include Brodmann Area (BA) 44 and the IPL, and other regions that have been associated with the MNS more recently (Keysers and Gazzola, 2009), including the supplementary motor area (SMA(Mukamel et al.; Gazzola and Keysers, 2009)), the dorsal premotor cortex (Cisek and Kalaska, 2004; Gazzola and Keysers, 2009) and BA2 (Gazzola and Keysers, 2009; Keysers et al., 2010).

Methods

Participants

Nineteen subjects (11 male, average age 21.6 years, range: 18-28 y.) participated in the experiment. Prescreening excluded subjects with a history of neurological disorders, impaired vision after correction, or who were left-handed. The research was approved by the Medical Ethical Commission of the University Medical Center Groningen (NL) and all subjects provided informed consent.

Experimental Task

The experiment consisted of three sessions, one of observation and two of execution.

(1) *Observation session (OBS)*. Participants viewed one of three types of movies (Figure 1A): a right hand entering from the right side of the screen to manipulate an object on a table (e.g. watering a plant or cracking nuts; Manipulate_OBS); a right hand entering the screen and moving continuously without interacting with the objects on the table (Move_OBS); or a right hand resting on the table close to the object (Static_OBS). The hand and the object in the Static_OBS condition were positioned not to imply a goal directed action. To enable a correlation analysis between μ-power and BOLD, we chose these three conditions to vary in how strongly they activate the MNS, with Manipulate_OBS, Move_OBS and Static_OBS expected to activate the MNS strongly, mildly and weakly.

The duration of the movies, either 2 or 3 seconds, was chosen based on the optimal time needed to manipulate the object. The two control conditions were then matched for duration. To avoid habituation, each movie was shown only once in the experiment, and each object was used exactly for one movie of each condition. Additionally, 4 different actors played in the movies (balanced across conditions) to vary the hand and kinematics

across movies. The background was kept constant and consisted of a table covered with a blue tablecloth in front of a wall covered by a grayish fabric.

Each condition was presented in a block design. Each block lasted 7s and included a random set of two 2-second stimuli and one 3-second stimulus of the same condition. Blocks were presented in a pseudo-randomized order (no more than 2 consecutive repetitions of the same condition were allowed) that differed for each subject. There were 13 blocks (i.e. repetitions) for each condition separated by a random 10-14s interval in which a gray and blue rectangle, that resembled the colors of the table and the wall, were presented together with a skin-colored fixation cross in the middle. This baseline was chosen to limit the "surprise transition effect" between the baseline and the beginning of each block.

Movies were recorded using a digital video camera (Sony DSR-PDX10P) and elaborated using AdobePremiere (www.adobe.com) and Windows MovieMaker (www.microsoft.com).

(2) *Manipulate vs. Eye Execution session (Manipulate_EXE vs Eye_EXE)*. In the scanner, a T-shaped plastic table was placed over the waist of the participant. A coffee cup was placed at the end closest to the participant, a wine glass was placed on the right end, and a bowl and spoon were placed at the intersection (Figure 1A). Subjects had to watch a screen on which a circle appeared on the bottom, right, or intersection of a diagram of the table. If the circle was green, participants had to manipulate the corresponding object on the real table with their hand (Manipulate_EXE) by grasping the cup and bringing it toward their mouth, grasping the wine glass and swirling it, or grasping the spoon and manipulating it as if to ladle soup. The circle would shrink, and subjects were instructed to perform the action until the circle disappeared. Every block consisted of all three actions in a random order, with the circles timed to make two of the actions last 3 seconds and one lasting 4 seconds. Participants were prevented from seeing themselves perform the actions, and were trained in the task outside the scanner and again in the scanner immediately before the beginning of the session. If the circle was red (Eye_EXE), participants had to move their eye gaze to the location of the circle on the screen instead of moving their hands. Except for the color of the circles, the visual stimuli and their timing were matched in the Eye_EXE and Manipulate_EXE conditions. Block order was pseudo-randomized (no more than 2 consecutive trials of the same condition) both within and between subjects. Participants completed 13 blocks for each condition. Blocks were separated by a random 10-14s interval showing a diagram of the table with a small gray circle in the middle as fixation point. During this time, participants were requested to rest their hand in a comfortable position close to the table and to avoid contact with the objects.

These two motor conditions were chosen to resemble those typically used in fMRI experiments (12-17).

(3) *Squeeze Execution session (Squeeze_EXE).* Throughout the session, participants wore a glove on the right hand, with bubble-wrap packing material attached to the palm (Figure 1A). During each of the 20 blocks, participants were shown a sequence of four green circles of decreasing size, each lasting 1s. At the onset of each green circle, participants were instructed to squeeze the material gently between the fingers and palm, leading to 4 squeezes in each block. Blocks were separated by a random 10-14s interval with a gray circle in the middle of the screen. Participants were prevented from seeing themselves perform the actions, and were trained in the task outside the scanner and again in the scanner immediately before the beginning of the session. This run was performed to resemble the motor task of typical EEG experiments (23, 27, 30).

The observation session was always completed before the execution sessions to avoid motor priming. The experimental tasks were designed to induce modulations in μ power as well as the BOLD signal in the MNS. All

stimuli were delivered using Presentation (www.neuro-bs.com), and projected with an LCD projector on a semi-opaque screen placed at the head end of the bore and seen through a mirror placed on the head coil.

Data Acquisition

fMRI: Philips Intera 3T Quaser whole-body scanner equipped with a circular sense head coil. We used a T2*-weighted echo-planar sequence with 39 interleaved 3.5 mm thick axial slices with no gap for functional imaging (TR=2000 ms, TE=30 ms, flip angle = 80°, FOV = 224 mm x224 mm, 64x64 matrix of 3.5 mm isotropic voxels). The slice acquisition frequency (19.5 Hz) was selected to minimize noise in the μ frequency band (8-13 Hz). At the end of the functional scanning, a T1-weighted anatomical image (1x1x1mm), parallel to the bicommissural plane and covering the whole brain, was acquired.

EEG: MR-compatible 32-channel BrainAmp system (Brain Products, Munich, Germany). The 29 scalp electrodes were set-up according to the international 10-20 system. One additional channel was dedicated to EOG and two channels to EKG. The reference electrode was positioned at FCz (between Fz and Cz). The impedances of all channels were maintained below 20 kΩ. All data were recorded using the Brain Vision Recorder 1.03 software (Brain Products, Munich, Germany) with a sampling frequency of 5 kHz.

Data Processing

fMRI. fMRI data were preprocessed using SPM8 (www.fil.ion.ucl.ac.uk). All echo planar images (EPIs) were slice-time corrected and realigned to the subject's mean EPI. T1 images were then co-registered to the mean EPI, segmented, and the gray matter was used to estimate the normalization parameters which were then applied to all EPIs. Normalized EPIs were smoothed with a 9 mm isotropic FWHM Gaussian kernel.

For most subjects, there was a drop in BOLD signal intensity over the left parietal lobe, likely an artifact caused by the cables connecting the EEG electrodes to the amplifier, which were often pressed close to the subject's scalp by the MRI head coil. These reduced EPI signals lead SPM8 to consider these voxels out of the brain. To solve this problem: (a) all 19 subjects' smoothed mean EPIs were averaged into a grand mean EPI; (b) this grand mean EPI was divided by each subject's smoothed mean EPI; (c) we then multiplied, for each subject separately, all the smoothed EPIs by the subject's correction map obtained in point (b).This procedure allowed SPM8 to accurately identify the boundaries of the left parietal lobe for all subjects. Because the same correction factor was applied to all EPI images of the same participant, this procedure does not bias the General Linear Model that examines changes over time.

EEG. BrainVison Analyzer 1.05 software (Brain products, Munich, Germany) was used for off-line correction of MRI scanner artifacts and pulse artifacts as described elsewhere (Allen et al., 1998; Allen et al., 2000). The data were then filtered with a 40 Hz low-pass filter (slope = 24 dB/octave). In EEGlab , an independent component analysis (ICA) was performed using the TDsep (Ziehe et al., 2000) algorithm (http://sccn.ucsd.edu/eeglab/) and components visually identified as ocular artifacts or residual MRI artifacts were removed.

According to the literature, EEG mu-suppression is clearest in the contralateral hemisphere (Harmon-Jones, 2006; Perry & Bentin, 2009). Since our subjects used the right hand in the Manipulate_EXE and only observed right hands in the Manipulate_OBS condition, we mainly focus on mu-power recorded from C3. The data from C3 were therefore convolved with a 10-Hz Morlet wavelet (Morlet parameter = 5) in BrainVision Analyzer to obtain a time course of μ-power throughout the experiment.

To minimize the impact of remaining artifacts, μ-power values differing more than two standard deviations from the mean were rejected and replaced using a linear interpolation based on the previous and subsequent power values. Approximately 2.5% of the data was replaced using this method.

Additionally, we observed that when scanner and/or pulse artifacts survived the correction procedures, the correction failed on all sites, not just C3. Therefore, we computed correlations between alpha power at C3 and every other site for each block and baseline, and when the average correlation was greater than 0.8, the block or baseline was labeled as contaminated. Visual inspection suggested that 0.8 was an effective threshold for eliminating blocks with residual artifacts (61/874) while sparing clean blocks. In the combined EEG/fMRI analyses described below, bad baselines (56/874) were excluded from the calculation of average baseline power, and bad blocks were modeled separately with a boxcar predictor of no interest.

Data Analyses

fMRI task effect and sVx identification

At the first, subject level, a general linear model (GLM) was applied to the fMRI data, separately for each session. Each condition within each session was modeled by using a standard boxcar function convolved with the hemodynamic response function (HRF). Six additional predictors of no interest were entered in the GLM to account for translations and rotations of the head. For all analyses, the highpass filter was chosen such that the period was equal to the maximum time between repetitions of a condition plus 15 seconds (to account for hemodynamic delays) plus 10 percent. Blocks labeled as bad (due to high intercorrelations between EEG sites or poor performance of the task) were modeled separately with a boxcar predictor of no interest. Data was then analyzed at the second level using t-tests on the parameter estimates for each subject obtained at the first level.

Shared voxels (sVx; i.e. voxels activated during both action execution and observation) were defined at the second level as in (Gazzola and Keysers, 2009) using the conjunction of contrast Manipulate_EXE>Eye_EXE ($p<0.001$), Manipulate_OBS>Move_OBS ($p<0.01$) and Manipulate_OBS>Static_OBS ($p<0.01$). For Manipulate_OBS>Move_OBS and Manipulate_OBS>Static_OBS, an uncorrected $p<.01$ ($k>10$) threshold was used because the conjunction of the two contrasts has a false positive rate of between .01 and .0001, approximating a $p<.001$ threshold (Gazzola and Keysers, 2009).

Given the difference in motor task used by typical fMRI and EEG experiments, we also examined the impact of using Squeeze_EXE instead of Manipulate_EXE to define the sVx by correlating the second-level t maps of Squeeze_EXE and Manipulate_Exe and by overlapping the significantly activated voxels.

EEG only analyses

Before running the combined EEG-fMRI recordings, we investigated whether the more complex task commonly used in fMRI experiments would also produce measurable μ-suppression. With this aim we conducted a pilot EEG experiment outside the scanner in which 13 student participants (none of which participated in the main study) performed the Manipulate_EXE and Eye_EXE task. Figure 1B shows that, compared to average baseline power, Manipulate_EXE did produce μ-suppression, and more so than Eye_EXE.

Unfortunately, during the combined EEG-fMRI recordings, the EEG data corresponding to the Manipulate_EXE condition were contaminated by large artifacts that could not be corrected because their shape varied from trial to trial. Since these artifacts were frequent only in this condition, we suspect that the arm movements required for this task caused head movements, and therefore EEG sensor movements, that, although small (<1.7mm based on MRI realignment parameters), caused irregular magnetic induction artifacts that could not be removed. In the

main analyses we therefore only analyzed the Squeeze_EXE and Eye_EXE conditions which didn't show this type of artifact.

For the observation, Squeeze_EXE, Eye_EXE conditions collected during the EEG-fMRI recordings and for the Manipulate_EXE and Eye_EXE in the pilot study, the μ-power was averaged during the relevant blocks and expressed as a percent power change relative to the average power during the baseline of each run. The baseline power was calculated based on the epoch 7s to 1s before a block would start rather than over the full inter-block interval. This choice of baseline allows at least 3s for the μ-rebound to occur without affecting the baseline estimate, and we chose to terminate the baseline 1 sec before the block onset because a 10-Hz wavelet defined with a Morlet parameter of 5 extends close to 1 second in either direction.

Combined EEG/fMRI analyses

(1) Observation: to focus our analysis on the differences in μ power between the three conditions (Manipulate_OBS, Move_OBS and Static_OBS) rather than the differences between the task and the baseline (which extensive low-level visual activations could account for), we removed the BOLD variance which was common to all the conditions. Specifically, we defined a GLM at the first, subject level that contained a single boxcar predictor containing all periods of visual stimulation and an orthogonalized C3 -power predictor. The C3 μ-predictor was set to zero during baselines and to the actual instantaneous μ-power minus the average baseline power during Manipulate_OBS, Move_OBS, and Static_OBS blocks, then orthogonalized with respect to the visual boxcar task predictor. The μ-predictor and boxcar visual predictor were then convolved with the HRF, and the convolved μ-predictor was subsampled at 0.5Hz (at the time of acquisition of the reference slice of each fMRI volume) and standardized to zero mean and unit variance.

When building the μ-predictors, the baseline power was calculated as described in the EEG only analyses section..

(2) Squeeze_EXE: for the combined EEG/fMRI analysis of Squeeze_EXE, a GLM was applied with C3 μ-power as a predictor. The μ-predictor was set to the actual μ-power minus the average baseline power (calculated between 7 and 1 sec pre-block) during Squeeze_EXE condition and to zero at all other times. The predictor was then convolved with the HRF, subsampled and standardized.

Unless otherwise specified, all results are presented at a threshold of $p<0.001$ uncorrected and all clusters also survive to FDR-corrected $p<.05$ ($k>10$).

Results

EEG

During observation, μ-suppression was significant at C3 while observing actors manipulate objects and actors move their hands but not while viewing static images of the hands and objects (Figure 1B). A three-condition ANOVA revealed a significant effect of condition ($F(2,36)=3.6$, $p<0.05$), and posthoc testing (LSD) showed this was due to Manipulate_OBS eliciting greater μ-suppression than Static_OBS.

Relative to average baseline power, there was also significant μ-suppression at C3 while participants squeezed an object (bubble foil, Squeeze_EXE; $t=-4.680$, $p<0.001$), replicating the finding of typical EEG μ-suppression studies. This μ-suppression also exceeded that during Eye_EXE ($t=-4.820$, $p<0.001$, Figure 1B), suggesting that μ-suppresion during Squeeze_EXE was not due to unspecific visual or executive processes.

fMRI

In line with our previous fMRI experiments (Gazzola et al., 2006; Gazzola et al., 2007; Gazzola and Keysers, 2009), we localize the MNS by mapping shared voxels (sVx), i.e. voxels with BOLD activity larger while participants reach for and manipulate objects than while performing eye movements (Manipulate_EXE-Eye_EXE, $p<0.001$) AND larger while viewing actors manipulate objects than both while viewing them move their hand without manipulating an object and while viewing a still image of the hand and object (Manipulate_OBS-Move_OBS, $p<0.01$ & Manipulate_OBS-Static_OBS, $p<0.01$). The locations of the sVx are consistent with past findings (Grezes et al., 2003; Gazzola et al., 2006; Dinstein et al., 2007; Filimon et al., 2007; Gazzola et al., 2007; Gazzola and Keysers, 2009; Turella et al., 2009; Caspers et al., 2010) and include BA2, BA44, dPM, the SMA, IPL and SPL (see Figure 1C).

To compare the motor properties of the MNS defined in typical fMRI and EEG experiments, we compared the pattern of BOLD activation induced by Manipulate_EXE and Squeeze_EXE. Computing a spatial correlation between the t-maps obtained at the second level of analysis of the BOLD signal for Squeeze_EXE and Manipulate_EXE revealed a high correlation ($r=0.83$) and Squeeze_EXE activated a network of brain regions very similar to, although slightly smaller than, Manipulate_EXE (Figure 1D).

Combined EEG/fMRI

Figure 1E-F shows the voxels in which the BOLD signal was negatively correlated with μ-power (i.e. higher BOLD activity in trials with higher μ-suppression) while participants observed (Figure 1E) or executed (Squeeze_EXE, Figure 1F) actions. In accordance with our predictions, during observation μ-suppression co-varied with BOLD signal in regions typically associated with the MNS: BA2, BA44, dPM, the SMA, and IPL. The same was true during action execution. Furthermore, many of the voxels that correlated with μ-suppression during Squeeze_EXE also correlated with μ-suppression during observation (Figure 1G, in blue). This was true in left BA2, left dPM, bilateral IPL and right SPL. However, voxels in BA44 correlating with μ-suppression were different during action observation and action execution.

Furthermore, we found that all four clusters showing a correlation between BOLD signal and μ-suppression overlapped with sVx (Figure 1G in pink and Table 1). This was true although the motor component of sVx was defined using Manipulate_EXE-Eye_EXE while the correlates of motor μ-suppression were localized using Squeeze_EXE.

Cluster size (voxels)	MIN coordinates x,y,z (mm)	T	Hem	Region	Cytoarchitectionic Area
	-50 -30 45	4.65	L	Postcentral Gyrus	Area 2
	-60 -20 32	4.61	L	SupraMarginal Gyrus	IPC (PFt)
	-54 -28 43	4.46	L	Inferior Parietal Lobule	IPC (PFt)
	-62 -22 36	4.42	L	SupraMarginal Gyrus	IPC (PFt)
130	54 -24 34	4.87	R	SupraMarginal Gyrus	IPC (PFt)
127	38 -46 58	6.61	R	Superior Parietal Lobule	SPL (7PC)
25	-36 -14 62	5.57	L	Precentral Gyrus	Area 6

Table 1. Overlap between the MNS based on EEG and fMRI criteria.

Voxels with sVx properties and BOLD signal significantly negatively correlated with μ-power during action observation and execution (pink clusters of Figure 1G). "T" refers to the peak correlation between μ-power and BOLD signal during OBS,

"Region" to a macroanatomical description of the location of the peak, “Cytoarchitectonic Area” to the label the anatomy toolbox associates to the peak (if available).

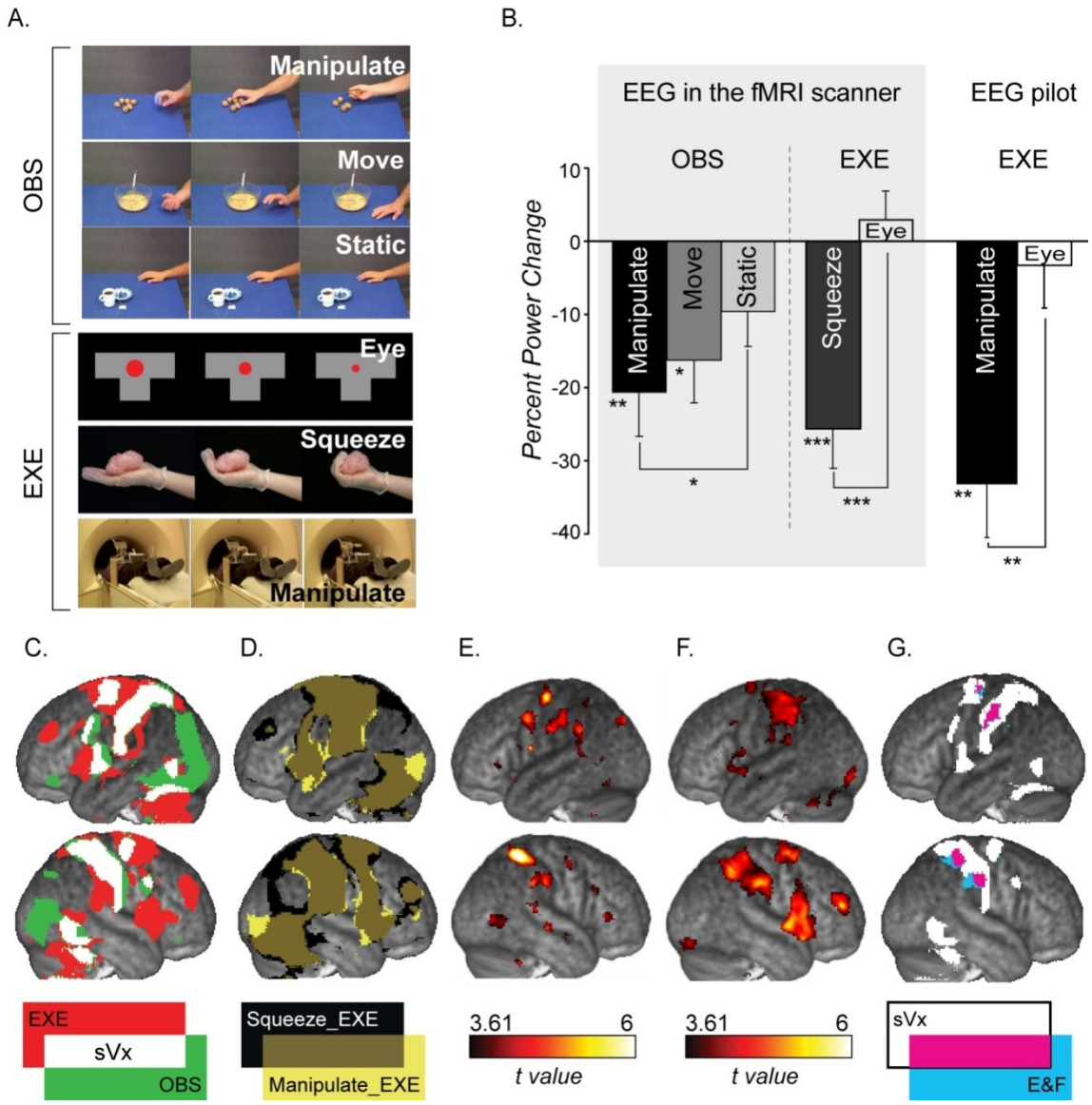

Figure1. (A) Snapshots from the different experimental conditions. (B) Percent μ-power change relative to average baseline power in C3 while participants observed or performed actions within the scanner environment and while participants performed the Manipulate_EXE condition in the pilot experiment. * p<0.05; ** p<0.01; ***p<0.001; t-tests against zero (=baseline) when over a bar or matched-sample t-test when over square brackets. (C) Shared Voxels (sVx) fMRI localizer, i.e. voxels activated during action execution (Manipulate_EXE-Eye_EXE, punc<0.001, red), during action observation (Manipulate_OBS-Move_OBS, punc<0.01 & Manipulate_OBS-Static_OBS, punc<0.01, green) or both (white, sVx). (D) Comparison of voxels significantly activated during Squeeze_EXE (black) and Manipulate_EXE (yellow) (E) Voxels with μ-power correlating negatively with BOLD signal during OBS (punc<0.001, all clusters survive pFDR<0.05). (F) Same for Squeeze_EXE. (G) sVx (white as in C), voxels correlating with μ-power suppression during observation and execution (i.e. overlap of e&f, blue), and their overlap (pink).

Discussion

It has been assumed (i) that the MNS in general, and BA44 and the IPL in particular, are responsible for modulating μ-power during action execution and observation (Oberman et al., 2005; Pineda, 2005) and (ii) that experiments using fMRI and μ-suppression to study the function of the MNS in clinical populations, autism

spectrum disorders in particular, study the integrity of the same system (Iacoboni and Dapretto, 2006). Here we tested these assumptions by simultaneously recording EEG and fMRI of our participants during both action execution and observation.

Correlating μ-suppression with the BOLD signal revealed that, in a number of brain regions, BOLD activity covaried with μ-suppression in the EEG during the squeezing of a bubble foil and the same was true during the observation of stimuli varying in how strongly they should activate the MNS (static images, hand movements, and hand-object manipulations). In both cases, these regions almost exclusively included regions that have been associated with the MNS in the literature: BA44, IPL, dPM and BA2 (Kohler et al., 2002; Grezes et al., 2003; Keysers et al., 2003; Cisek and Kalaska, 2004; Raos et al., 2004; Gazzola et al., 2006; Iacoboni and Dapretto, 2006; Dinstein et al., 2007; Filimon et al., 2007; Gazzola et al., 2007; Rozzi et al., 2008; Evangeliou et al., 2009; Gazzola and Keysers, 2009; Keysers, 2009; Keysers and Gazzola, 2009; Kilner et al., 2009; Turella et al., 2009; Caspers et al., 2010; Keysers et al., 2010; Rizzolatti and Sinigaglia, 2010). Overlapping these two separate analyses revealed that three of these regions, IPL, dPM and BA2, contained voxels of which the BOLD signal correlated with the amount of μ-suppression measured in the EEG during both the observation conditions and while participants squeezed the bubble foil. Importantly, these clusters of voxels with BOLD signal correlating with μ-suppression during both execution and observation also overlapped with the mirror neuron system of our participants defined as typical fMRI experiments would.

The IPL has always been considered one of the two core regions of the MNS: mirror neurons have been recorded in this region in the monkey (Rozzi et al., 2008) and human fMRI experiments have consistently shown that this region is active during both action observation and execution (Grezes et al., 2003; Gazzola et al., 2006; Filimon et al., 2007; Gazzola et al., 2007; Gazzola and Keysers, 2009; Turella et al., 2009; Caspers et al., 2010).

The dPM has been less intensively investigated in the monkey for the presence of mirror neurons, but it contains mirror-like neurons active both while moving a cursor on a screen and while witnessing the cursor being moved by another individual (Cisek and Kalaska, 2004). In humans, the dPM is also very consistently activated both during action observation and execution (Grezes et al., 2003; Gazzola et al., 2006; Filimon et al., 2007; Gazzola et al., 2007; Gazzola and Keysers, 2009; Turella et al., 2009; Caspers et al., 2010), and is therefore increasingly incorporated into models of the MNS (Keysers and Gazzola, 2009).

BA2 finally has not been investigated at all for the presence of mirror neurons using single cell recordings in monkeys, but 14C-deoxyglucose studies have shown that this region has enhanced metabolism during action observation and execution (Raos et al., 2004; Evangeliou et al., 2009). In humans this region is consistently activated both during the observation and the perception (observation and listening) of hand actions (Grezes et al., 2003; Gazzola et al., 2006; Dinstein et al., 2007; Filimon et al., 2007; Gazzola et al., 2007; Gazzola and Keysers, 2009; Turella et al., 2009; Caspers et al., 2010). The pattern of activity in this region provides information about which of two actions is being performed during both action perception and execution (Etzel et al., 2008) and voxels with coordinates in BA2 show repetition suppression both during action observation and execution (Dinstein et al., 2007). Because this region represents the highest level of proprioceptive processing in SI and receives input from regions containing mirror neurons in the monkey, it has been proposed that BA2 activity during action observation may represent a somatosensory simulation of what observed movements would feel like, and this somatosensory simulation is thought to integrate and supplement the motor simulation performed in premotor regions (Keysers et al., 2010). Interestingly, BA2 not only seems to have mirror properties – it is also part of the sensorimotor strip in which μ-power is strongest (Salmelin and Hari, 1994; Salmelin et al.,

1995; Ohara et al., 2000; Caetano et al., 2007), and might therefore be particularly suited for modulating μ-power during action observation and execution.

Interestingly, the fourth region, BA44, which has often been considered the most likely source of μ-suppression during action observation (Pineda, 2005) contained voxels that predicted μ-suppression during observation trials and other voxels that predicted μ-suppression during action execution trials, but none that predicted both, arguing against the idea that mirror neurons in this region would be the prime source of modulation of μ-power.

A caveat of our correlational approach is that although a brain region causing μ-suppression would be expected to have a BOLD signal that correlates with μ-suppression during action observation and execution, if a number of regions show such correlation, it might be that only one directly causes μ-suppression while the others show such correlation by virtue of their functional connectivity or shared input with that region. In our case, this would suggest that some, but maybe not all, of the regions including the BA2, IPL, SPL or dPM cause μ-suppression during action observation and execution but that BA44 is less likely to do so. Repeating the experiment with a high density EEG system might help localize the origin of μ -suppression. Additionally, fMRI is currently acquired at a rate of a slice every ~50ms. This generates artifacts with a basic frequency of 20Hz, making it difficult to study μ -suppression in the beta range (~20Hz, Hari et al., 1998). As faster acquisition methods develop, the frequency of these artifacts will increase, and the beta range will become amenable to an analysis similar to the one we have performed for the alpha range.

Additionally, the overlap between sVx and voxels correlating with μ-suppression provides evidence that fMRI experiments identifying brain regions involved both during action observation and action execution (sVx) and EEG experiments measuring μ-suppression indeed quantify the activity of overlapping neural substrates. This was true despite defining the regions correlating with μ-suppression using the Squeeze_EXE condition in line with previous EEG experiments while defining the sVx using a different and more complex condition, Manipulate_EXE, in line with previous fMRI experiments. This overlap provides an empirical basis for combining evidence from EEG and fMRI experiments to study the integrity of the MNS in clinical populations, autism in particular (Iacoboni and Dapretto, 2006) and is in accord with a larger body of less direct evidence that has shown that the BOLD signal in fMRI studies and the μ-power in EEG studies have similar properties. Both μ-suppression and fMRI signals show a somatotopic organization that allows discriminating actions performed by different effectors (Pfurtscheller et al., 1997; Gazzola et al., 2006; Etzel et al., 2008). Both respond more to goal-directed transitive actions than meaningless intransitive actions (Buccino et al., 2001; Muthukumaraswamy et al., 2004). Both show higher signals when the observer has expertise in the particular action (Calvo-Merino et al., 2005; Orgs et al., 2008). Finally, both show predictive signals prior to an action that can be anticipated (Caetano et al., 2007; Southgate et al., 2009; Thioux et al., 2009).

In summary, with mirror neurons first discovered in the ventral premotor cortex (Gallese et al., 1996; Umilta et al., 2001; Kohler et al., 2002; Keysers et al., 2003), many assumed that μ-suppression quantifies activity in mirror neurons in general and in BA44 in particular (Pineda, 2005). Our results support the idea that μ-suppression measures activity of regions associated with the MNS, but they argue against the notion that μ-suppression primarily measures mirror activity in BA44: BOLD activity in BA2, the IPL and the dPM robustly and significantly correlated with μ-suppression during action observation and execution but that in BA44 did not. Additionally, our data suggest that although EEG and fMRI tasks have used somewhat different motor tasks in the past to test activity in the MNS, they have actually measured activity in overlapping neural substrates. We therefore hope that our findings provide a basis for integrating more closely the burgeoning but often separate literatures on the MNS using fMRI and EEG. By suggesting that μ-suppression may correlate more with BA2, IPL and dPM, than BA44

activity, we hope that our results will shed further light on the sometimes apparently contrasting findings in the study of patients with impairments of social cognition (Oberman et al., 2005; Dinstein et al., 2010).

References Cited

Allen PJ, Josephs O, Turner R (2000) A method for removing imaging artifact from continuous EEG recorded during functional MRI. Neuroimage 12:230-239.

Allen PJ, Polizzi G, Krakow K, Fish DR, Lemieux L (1998) Identification of EEG events in the MR scanner: the problem of pulse artifact and a method for its subtraction. Neuroimage 8:229-239.

Buccino G, Binkofski F, Fink GR, Fadiga L, Fogassi L, Gallese V, Seitz RJ, Zilles K, Rizzolatti G, Freund HJ (2001) Action observation activates premotor and parietal areas in a somatotopic manner: an fMRI study. Eur J Neurosci 13:400-404.

Caetano G, Jousmaki V, Hari R (2007) Actor's and observer's primary motor cortices stabilize similarly after seen or heard motor actions. Proc Natl Acad Sci U S A 104:9058-9062.

Calvo-Merino B, Glaser DE, Grezes J, Passingham RE, Haggard P (2005) Action observation and acquired motor skills: an FMRI study with expert dancers. Cereb Cortex 15:1243-1249.

Caspers S, Zilles K, Laird AR, Eickhoff SB (2010) ALE meta-analysis of action observation and imitation in the human brain. Neuroimage 50:1148-1167.

Cisek P, Kalaska JF (2004) Neural correlates of mental rehearsal in dorsal premotor cortex. Nature 431:993-996.

Dinstein I, Hasson U, Rubin N, Heeger DJ (2007) Brain areas selective for both observed and executed movements. J Neurophysiol 98:1415-1427.

Dinstein I, Thomas C, Humphreys K, Minshew N, Behrmann M, Heeger DJ (2010) Normal movement selectivity in autism. Neuron 66:461-469.

Etzel JA, Gazzola V, Keysers C (2008) Testing simulation theory with cross-modal multivariate classification of fMRI data. PLoS One 3:e3690.

Evangeliou MN, Raos V, Galletti C, Savaki HE (2009) Functional imaging of the parietal cortex during action execution and observation. Cereb Cortex 19:624-639.

Filimon F, Nelson JD, Hagler DJ, Sereno MI (2007) Human cortical representations for reaching: mirror neurons for execution, observation, and imagery. Neuroimage 37:1315-1328.

Gallese V, Fadiga L, Fogassi L, Rizzolatti G (1996) Action recognition in the premotor cortex. Brain 119 (Pt 2):593-609.

Gastaut H (1952) Etude électrocorticographique de la réactivité des rythmes rolandiques. Rev Neurol 87:176-182.

Gazzola V, Keysers C (2009) The observation and execution of actions share motor and somatosensory voxels in all tested subjects: single-subject analyses of unsmoothed fMRI data. Cereb Cortex 19:1239-1255.

Gazzola V, Aziz-Zadeh L, Keysers C (2006) Empathy and the somatotopic auditory mirror system in humans. Curr Biol 16:1824-1829.

Gazzola V, Rizzolatti G, Wicker B, Keysers C (2007) The anthropomorphic brain: the mirror neuron system responds to human and robotic actions. Neuroimage 35:1674-1684.

Grezes J, Armony JL, Rowe J, Passingham RE (2003) Activations related to "mirror" and "canonical" neurones in the human brain: an fMRI study. Neuroimage 18:928-937.

Hari R, Forss N, Avikainen S, Kirveskari E, Salenius S, Rizzolatti G (1998) Activation of human primary motor cortex during action observation: a neuromagnetic study. Proc Natl Acad Sci U S A 95:15061-15065.

Harmon-Jones E (2006) Unilateral right-hand contractions cause contralateral alpha power suppression and approach motivational affective experience. Psychophysiology 43:598-603.

Iacoboni M, Dapretto M (2006) The mirror neuron system and the consequences of its dysfunction. Nat Rev Neurosci 7:942-951.

Keysers C (2009) Mirror neurons. Curr Biol 19:R971-973.

Keysers C, Gazzola V (2009) Expanding the mirror: vicarious activity for actions, emotions, and sensations. Curr Opin Neurobiol 19:666-671.

Keysers C, Kaas JH, Gazzola V (2010) Somatosensation in social perception. Nat Rev Neurosci 11:417-428.

Keysers C, Kohler E, Umilta MA, Nanetti L, Fogassi L, Gallese V (2003) Audiovisual mirror neurons and action recognition. Exp Brain Res 153:628-636.

Kilner JM, Neal A, Weiskopf N, Friston KJ, Frith CD (2009) Evidence of mirror neurons in human inferior frontal gyrus. J Neurosci 29:10153-10159.

Kohler E, Keysers C, Umilta MA, Fogassi L, Gallese V, Rizzolatti G (2002) Hearing sounds, understanding actions: action representation in mirror neurons. Science 297:846-848.

Mukamel R, Ekstrom AD, Kaplan J, Iacoboni M, Fried I Single-Neuron Responses in Humans during Execution and Observation of Actions. Curr Biol.

Muthukumaraswamy SD, Johnson BW, McNair NA (2004) Mu rhythm modulation during observation of an object-directed grasp. Brain Res Cogn Brain Res 19:195-201.

Oberman LM, Hubbard EM, McCleery JP, Altschuler EL, Ramachandran VS, Pineda JA (2005) EEG evidence for mirror neuron dysfunction in autism spectrum disorders. Brain Res Cogn Brain Res 24:190-198.

Ohara S, Ikeda A, Kunieda T, Yazawa S, Baba K, Nagamine T, Taki W, Hashimoto N, Mihara T, Shibasaki H (2000) Movement-related change of electrocorticographic activity in human supplementary motor area proper. Brain 123 (Pt 6):1203-1215.

Orgs G, Dombrowski JH, Heil M, Jansen-Osmann P (2008) Expertise in dance modulates alpha/beta event-related desynchronization during action observation. Eur J Neurosci 27:3380-3384.

Perry A, Bentin S, (2009) Mirror activity in the human brain while observing hand movements: a comparison between EEG desynchronization in the mu-range and previous fMRI results. Brain Res 1282:126-132.

Pfurtscheller G, Neuper C, Andrew C, Edlinger G (1997) Foot and hand area mu rhythms. Int J Psychophysiol 26:121-135.

Pineda JA (2005) The functional significance of mu rhythms: translating "seeing" and "hearing" into "doing". Brain Res Brain Res Rev 50:57-68.

Pineda JA, Allison BZ, Vankov A (2000) The effects of self-movement, observation, and imagination on mu rhythms and readiness potentials (RP's): toward a brain-computer interface (BCI). IEEE Trans Rehabil Eng 8:219-222.

Raos V, Evangeliou MN, Savaki HE (2004) Observation of action: grasping with the mind's hand. Neuroimage 23:193-201.

Raymaekers R, Wiersema JR, Roeyers H (2009) EEG study of the mirror neuron system in children with high functioning autism. Brain Res 1304:113-121.

Rizzolatti G, Sinigaglia C (2010) The functional role of the parieto-frontal mirror circuit: interpretations and misinterpretations. Nat Rev Neurosci 11:264-274.

Rizzolatti G, Fabbri-Destro M, Cattaneo L (2009) Mirror neurons and their clinical relevance. Nat Clin Pract Neurol 5:24-34.

Rozzi S, Ferrari PF, Bonini L, Rizzolatti G, Fogassi L (2008) Functional organization of inferior parietal lobule convexity in the macaque monkey: electrophysiological characterization of motor, sensory and mirror responses and their correlation with cytoarchitectonic areas. Eur J Neurosci 28:1569-1588.

Salmelin R, Hari R (1994) Spatiotemporal characteristics of sensorimotor neuromagnetic rhythms related to thumb movement. Neuroscience 60:537-550.

Salmelin R, Hamalainen M, Kajola M, Hari R (1995) Functional segregation of movement-related rhythmic activity in the human brain. Neuroimage 2:237-243.

Southgate V, Johnson MH, Osborne T, Csibra G (2009) Predictive motor activation during action observation in human infants. Biol Lett 5:769-772.

Thioux M, Greven I, Gazzola V, Keysers C (2009) Assessing Hand Actions with the Mirror Neuron System. In: 15th annual meeting of the Organization for Human Brain Mapping. San Francisco, CA.

Turella L, Erb M, Grodd W, Castiello U (2009) Visual features of an observed agent do not modulate human brain activity during action observation. Neuroimage 46:844-853.

Umilta MA, Kohler E, Gallese V, Fogassi L, Fadiga L, Keysers C, Rizzolatti G (2001) I know what you are doing. a neurophysiological study. Neuron 31:155-165.

Ziehe A, Muller KR, Nolte G, Mackert BM, Curio G (2000) Artifact reduction in magnetoneurography based on time-delayed second-order correlations. IEEE Trans Biomed Eng 47:75-87.

Supplementary Materials

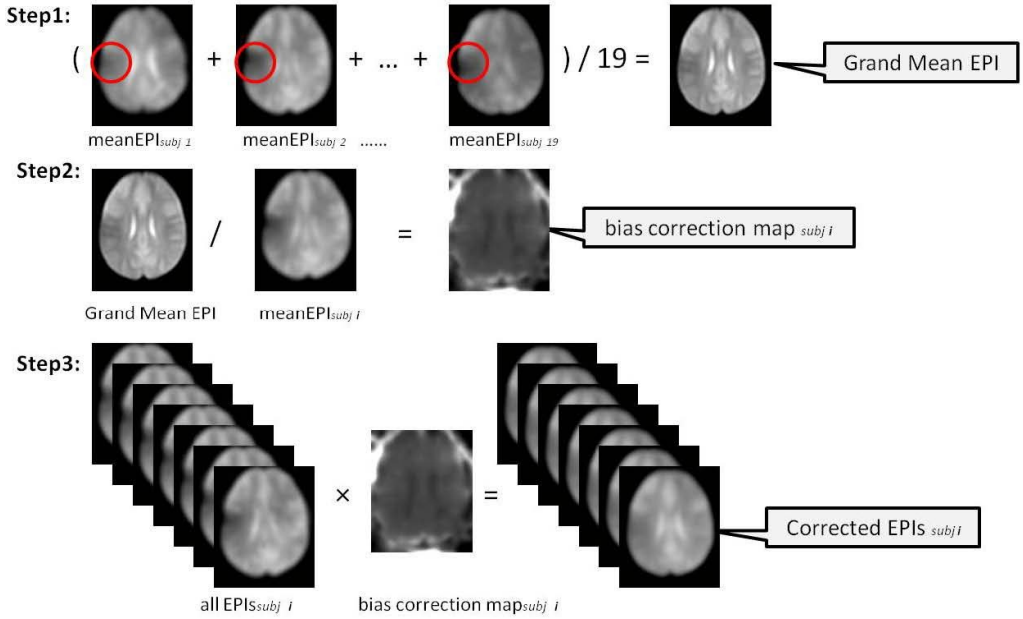

Supplementary Figure 1. Bias correction of the functional volumes. Red circles on the slices presented in Step1 of the figure show the location of the drop of signal (slice with the strongest drop of signal shown for three subjects). The location of the signal drop corresponds to that of the cables connecting the EEG cap to the amplifier. The signal was so low within these voxels that SPM8 considered them "out of the brain". We therefore corrected the images to normalize the mean EPI signal as shown in steps 1-3. Step 1: we created a grand mean EPI by averaging the 19 mean EPIs created during the realignment procedure. Step 2: we divided this grand mean by each of the 19 mean EPIs (voxel by voxel) to obtain what we called the bias correction map. Step 3: for each subject, we multiplied each single EPI volume by the bias correction map for that subject to obtain corrected EPIs. This transformation is similar to a grand mean normalization and, because it multiplies the EPI time series with a scalar, this normalization does not alter the temporal structure of the EPIs time series that is the foundation for the general linear model we used to analyze the data and its correlation with μ -power.

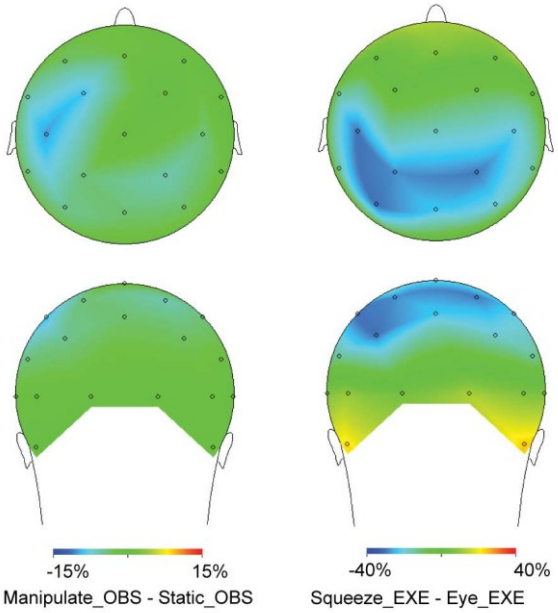

Supplementary Figure 2. Scalp topography of μ-power. Left: scalp topography of the difference in μ - power between the Manipluate_OBS and Static_OBS condition. Right: same for Squeeze_EXE - Eye_EXE. Colors code the degree of event-related desynchronization and synchronization. Note that the suppression of μ -power peaks in the rolandic area of the brain and is stronger in the left (C3) than right (C4) peri-rolandic electrode. This is congruent with the fact that actors in the movies and our subjects only used their right hands.

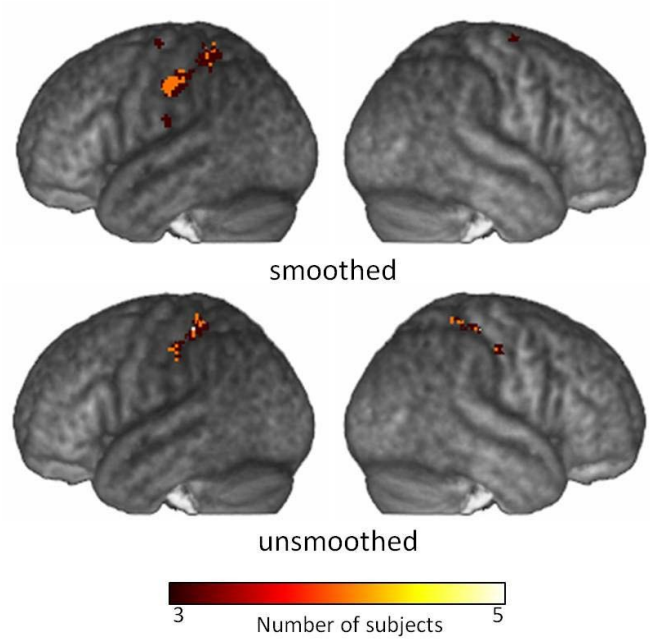

Supplementary Figure 3: Consistency maps. In accordance with the methods used in Gazzola & Keysers, 2009, for this figure, the data of each subject is analyzed separately, and maps show the number of participants for which a voxel shows evidence for (a) being part of the MNS and (b) has a BOLD signal correlated with μ-power during both observation and execution. At the single subject level, we therefore calculated a logical 'AND' function between five inequalities relative to the t-values the GLM associates with the following regressions or contrasts: r(μ-suppression, OBS)>3.61 & r(μ-suppression, EXE)>3.61 & (Manipulate_OBS-Move_OBS>2.55) & (Manipulate_OBS-Static_OBS>2.55) & (Manipulate_EXE-Eye_EXE>3.61). T>3.61 corresponds to p<0.001 and T>2.55 to p<0.01. For consistency with Gazzola & Keysers 2009, the visual response is tested using the conjunction of two contrasts at p<0.01, while all other components are tested at p<0.001. The upper renders

show the results of using smoothed single subject data, lower renders using unsmoothed data. Only voxels where at least 3 subjects showed the property are reported. This threshold was chosen to protect against family-wise error at $p<0.05$. We estimated the family-wise error using the cumulative binomial distribution with 19 repetitions and a ''success'' (i.e., false positive) probability of 0.001 (the threshold for each element of the conjunction of observation and execution). The results were then Bonferroni corrected for the number of voxels in the search volume (44294). In particular the threshold of at least three subjects was calculated in Mathematica (Wolfram Research) by solving for x the inequality 0.05>(1 - CDF[BinomialDistribution[19, 0.001], x-1])*44294).

Cluster size (voxels)	MIN coordinates (x,y,z) mm			N	Hem	Region	Cytoarchitectonic Area
Clusters resulting from smoothed single subjects data							
150	-48	-26	48	4	L	Postcentral Gyrus	Area 2
	-52	-24	48	3	L	Postcentral Gyrus	Area 1
107	-36	-42	64	4	L	Postcentral Gyrus	Area 1
13	30	-4	70	3	R	Superior Frontal Gyrus	Area 6
12	-28	-12	66	3	L	Precentral Gyrus	Area 6
12	-56	-18	22	3	L	Postcentral Gyrus	OP 1
Clusters resulting from unsmoothed single subjects data							
36	-38	-38	64	4	L	Postcentral Gyrus	Area 2
	-40	-42	62	3	L	Postcentral Gyrus	Area 2
26	-54	-26	46	4	L	Postcentral Gyrus	Area 2
18	-44	-36	56	5	L	Postcentral Gyrus	Area 2
	-50	-32	52	3	L	Postcentral Gyrus	Area 2
15	54	-28	56	5	R	Postcentral Gyrus	Area 1
	48	-30	58	3	R	Postcentral Gyrus	Area 1
12	56	-18	44	4	R	Postcentral Gyrus	Area 1
	58	-14	46	3	R	Postcentral Gyrus	Area 1
10	40	-44	62	4	R	Postcentral Gyrus	Area 1

Supplementary Table 1: Consistency maps. Tabulation of the results of the single subject analyses shown in Supplementary Figure 3. Convention as in Table 1, except that instead of looking at T values, the table examines the 'N'-value. N refers to the number of subjects for which, in a given voxel, the voxel is both (a) part of the MNS and (b) has a BOLD correlated with μ-power during both observation and execution.

Responsibility Increases Vicarious Activations to the Pain of Others.

Fang Cui1,2, Abdelrahman Abdelgabar1, Christian Keysers1,2 and Valeria Gazzola2,1*

1: Social Brain Lab, Netherlands Institute for Neuroscience, Royal Netherlands Academy for Arts and Sciences, 1105BA Amsterdam, The Netherlands

2: Department of Neuroscience, University Medical Center Groningen, University of Groningen, Groningen, The Netherlands

* To whom correspondence should be addressed: v.gazzola@nin.knaw.nl

Abstract

An agent's responsibility for someone else's harm weighs heavily in moral assessments. Here we examine whether our responsibility for another's harm influences a neural proxy of empathy. Participants played a franker task with a confederate. Whenever either erred, the confederate was seen to receive a painful shock. Using functional magnetic resonance imaging, we found regions of the functionally localized pain matrix of the participants (the anterior insula in particular) were activated most strongly when seeing the confederate receive a shock when only the participant had erred (and hence had full responsibility). When both or only the confederate had erred (i.e. participant's shared or no responsibility), significantly weaker vicarious pain-matrix activations were measured. The supplementary motor area played a key role in transforming performance feedback into this modulation of vicarious activation.

Introduction

Imagine you are the driver of a car involved in a car accident, and the accident happened because (a) the driver of the other car, (b) you or (c) both of you were writing a text message on a mobile phone while driving. You are unharmed, but you see the other drivers face covered in blood. Wouldn't you feel more distress in (b) than in (a) and (c)?

Empathy, the capacity to share another's emotion, is thought to be essential for moral development, to cause moral emotions like guilt and thereby to discourage behavior that harms others (Eisenberg, 2000;Hoffman, 2000). For an act to be morally wrong, it is however essential, that a moral agent's action is responsible for the harm of a moral patient (i.e. victim) (Blair, 1995;Meffert et al., 2013;Gray and Wegner, 2012). This raises the question of whether and how empathy, so seminal to morality, is modulated by responsibility, and from a neuroscience perspective, whether and how brain regions associated with empathy are modulated by responsibility for observed pain.

Painful stimuli elicit activity in a network of cortical areas named "pain matrix" (Mouraux et al., 2011;Iannetti and Mouraux, 2010;Apkarian et al., 2005;Apkarian et al., 1999). Some of these areas become vicariously activated when witnessing the pain of others, in particular the insula and rostral cingulate cortex (Koban et al., 2013;Corradi-Dell'Acqua et al., 2011;Lamm et al., 2011;Jackson et al., 2006). Some factors influencing the intensity of these vicarious activations have been studied(de Vignemont and Singer, 2006): vicarious pain activations are stronger when attention is directed to the pain(Gu and Han, 2007), when stimuli are more realistic(Gu and Han, 2007), when the observer is socially closer to the pain-taker(Cheng et al., 2010), considers the pain-taker fair(Singer et al., 2006a), belongs to the same group or race(Azevedo et al., 2012;Hein et al., 2010) and these modulations can be fast and implicit.

Although vicarious activations are thought to be seminal for morality, and responsibility is determining morality, whether and how responsibility for an observed pain modulates vicarious pain activations remains poorly understood. This is because vicarious pain activations have been studied in situations in which the participant witnesses pain he did not cause. We hypothesized, that if vicarious activations and empathy serve to guide our moral actions by punishing our actions when they harm others, vicarious activations should be strongest for pain we caused and weakest for pain we did not cause. We further hypothesize, based on the diffusion of responsibility literature, that if the cause of the pain is shared amongst multiple agents, vicarious activations should also be reduced(Darley and Latane, 1968).

To test these hypotheses, we performed an fMRI experiment. At the beginning of the experiment, experimenter AR introduced the participant to author FC (Chinese female) whom he described as another participant. The participant and FC then drew lots that were manipulated so that the participant was always assigned to the fMRI scanning. In the scanner, each of the 140 trials (4 runs of 35 trials each) started by displaying a central target letter flanked by distractors and the participant had to press the button corresponding to the central letter. This first epoch is called Flanker-epoch (Figure 1a). The participant was lead to believe that FC would have seen, simultaneously but in another room, the same display and performed the same task. Directly after the Flanker-epoch, the participant and FC were informed about the performance of both players (Feedback-epoch). If both performed the task correctly (NoPain condition), the participant believed FC would receive a weak, painless electroshock on her right hand. If any erred (i.e. only the participant, both, or only FC) a stronger, painful shock would be delivered to FC. Based on the performance of the two players, this generated trials in which the participant would have full responsibility for FC's pain (FullResp, see Table 1), trials in which the two players would share the responsibility (SharedResp) and trials in which the participant had no responsibility (NoResp). The participant was further lead to believe that he/she would then, after a random blank interval, see in real time (through a CCTV) FC receive the electroshock, be it painful or painless, depending on their joint performance. A 5 to 8 seconds blank screen separated consecutive trials. In reality, FC was not performing the task or receiving shocks during the experiment. Instead, a computer adjusted the presentation time of the flanker task, and hence its difficulty and simulated correct or incorrect performance of FC to ensure a minimum number of trials for each condition (Table 1, last column). The movies were prerecorded to ensure that all participants viewed the same movies (Supplementary information: Movie 1 and 2). FC only received shocks during movie recording.

Participant's response	FC's response	Condition name	Electrical stimulation	% of trials (average ± s.e.m.)
Right	Right	NoPain	Not painful	32.4+0.82
Wrong	Right	FullResp	Painful	18.6+0.71
Wrong	Wrong	SharedResp	Painful	17.8+0.69
Right	Wrong	NoResp	Painful	31.2+0.71

Table1. Experimental design and conditions. From left to right: participant's and author FC's flanker task performance; condition name from participant's responsibility point of view; type of electric stimulation given to FC during video-recording for each condition; average number of trials for each condition included in the analysis. Note that a GLM comparing two conditions is valid even if the two conditions have different numbers of trials, and our main contrast (FullResp-SharedResp) is performed at the second level, across conditions with similar numbers of trials at the first level.

To localize regions involved in the painfulness of the participant's own nociceptive experiences, after the main experiment, the participant went through another fMRI scanning session (Pain-localizer) in which painful and non-painful electroshocks were delivered to the participant's right hand in the scanner.

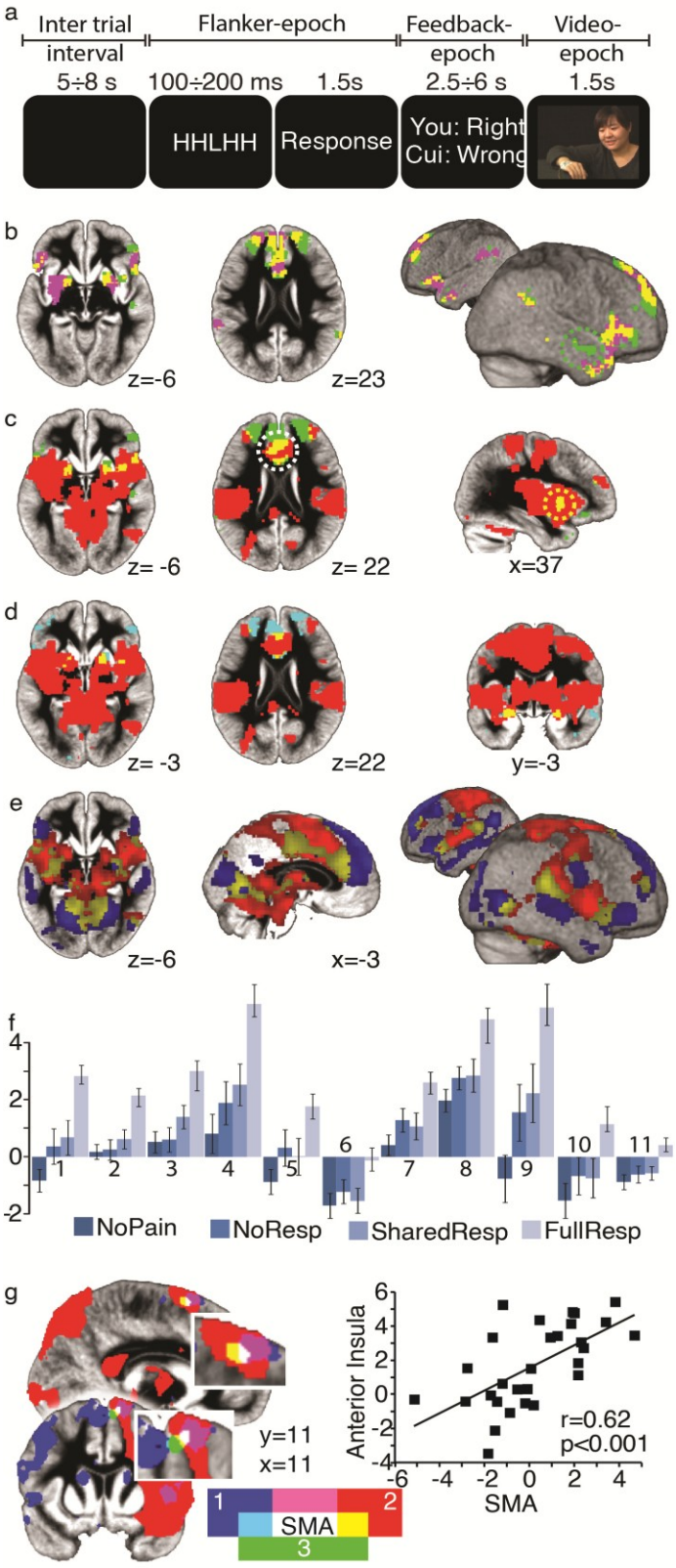

Figure1: Experimental Task and Results Trial structure for the main responsibility task, with a screenshot taken from one of the painful videos (See also Movie1 and 2). (b-e) Purple: VideoFullResp-VideoNoResp. Green: VideoFullResp-VideoSharedResp. Red: Pain-localizer. Cyan: (VideoFullResp-VideoSharedResp)-(FeedbackFullResp-FeedbackSharedResp).Blue: (VideoFullResp +VideoSharedResp +VideoNoResp) - 3VideoNoPain. Yellow: overlap between the other two colors shown in the same render. All the images shown from b to e were thresholded at punc<0.001, k>10 and

survived qFDR<0.05. In panel e the colors are shaded to indicate the strength of the BOLD signal, in terms of t-values. The gradient goes from t=3.13 to t=7. (f) Signal extracted from the 11 ROIS in c, also listed in Table 5. (g) Blue: regions associated with Reappraisal (z>2, Blue, Buhle et al., 2012). Red: anatomical connectivity with the AI ROI (n>2, Red, Cerliani et al., 2012). Green: FeedbackFullResp-FeedbackSharedResp (p<0.001). Graph: regression between the signal for the contrast VideoFullResp-VideoSharedResp from the SMA ROI (white) and the AI ROI (the AI ROI is outlined in panel c using a dotted yellow circle on the sagittal slice, see also Table 5).

Results

Behavioral Results

Average performance at the flanker task was 62.8% correct, with no significant difference between males and females, or Chinese and Caucasian (t-tests, all p>0.2). We had at least 17 repetitions of each of the four conditions in all participants (Table 1).

After telling the participants the truth about the experimental design, they were asked: “Do you think the experimental setup was realistic enough to believe it (1=strongly disagree 7=strongly agree)?” in a feedback questionnaire. The average rating was 6.2 ±0.7 (s.d) and none of the 30 included participants even somewhat disagreed with the statement, demonstrating the credibility of our design. Two of the initial 33 participants had voiced doubts about the experiments before debriefing, and were excluded from the analysis. They were the only participants that selected “somewhat disagree”.

Our experimental design was motivated by the assumption that people would feel varying degrees of responsibility based on who erred, with full-responsibility > shared > no-responsibility in terms of perceived responsibility for the participant. However, we had not directly asked the participants if that was true. Accordingly, we tried to contact all participants again to ask them “Please rate how responsible you felt for the pain of the other in each condition, on a scale from 1=not responsible at all to 9=extremely responsible”. Only eighteen of the participants could be contacted (the other students had changed their email address and phone number since). These 18 reported having felt most responsible for the pain in the FullResp (mean ± s.e., 7.5 ± 0.06) condition, less responsible in the SharedResp condition (3.5 ± 0.06) and felt close to no responsibility in the NoResp condition (1.3 ± 0.02), with all pair-wise differences significant (t-test, p<0.001). This validates the names given to the different conditions.

The Effect of Responsibility on Brain Activation

We used a within-subject ANOVA with 8 variables to explore the effect of responsibility on brain activation. This included the parameter estimates of the four conditions during the Video-epoch (VideoNoPain, VideoFullResp, VideoSharedResp, VideoNoResp), and four conditions during the Feedback-epoch (FeedbackNoPain, FeedbackFullResp, FeedbackSharedResp, FeedbackNoResp). The contrast VideoFullResp - VideoNoResp revealed stronger activations in conditions in which the witnessed pain was entirely due to the participant's mistake than those that were entirely due to author FC’s mistake. Regions showing this difference (punc<0.001, k>10, T>3.13; also qFDR<0.05) included regions involved in empathy (ACC, AI), in emotional processing (amygdala, striatum), in cognition and reappraisal (right superior frontal) and regions involved in the observation of biological motion (middle temporal cortex and inferior frontal gyrys) (Table 2, Figure 1b, purple). The reverse contrast revealed no activations (at qFDR <0.05). To explore whether simply sharing responsibility for the pain would suffice to reduce the response to witnessing the pain, we contrasted VideoFullResp – VideoSharedResp.

Cluster Size (voxels)	Peak MIN coordinates (mm)	Peak T-values	Hem	Peak anatomical location

3573	0	44	12	5.08	L	Anterior Cingulate Cortex
	18	56	30	4.86	R	Superior Frontal Gyrus
	-12	42	46	4.58	L	Superior Frontal Gyrus
	8	36	54	4.51	R	Superior Medial Gyrus
	-20	52	26	4.48	L	Middle Frontal Gyrus
2011	-26	-6	-14	6.30	L	Amygdala
	-52	2	-28	4.57	L	Middle Temporal Gyrus
	-44	30	-12	4.28	L	Inferior Frontal Gyrus (p. Orbitalis)
	-46	18	-14	4.23	L	Temporal Pole
	-24	8	-8	4.15	L	Putamen
1565	22	-4	-14	5.55	R	Amygdala
	26	10	-18	5.34	R	Olfactory cortex
	22	8	-4	4.76	R	Putamen
	50	32	0	4.51	R	Inferior Frontal Gyrus (p. Triangularis)
	48	0	-32	4.32	R	Inferior Temporal Gyrus
	42	20	-28	4.16	R	Temporal Pole
212	4	-12	32	3.80	R	Middle Cingulate Cortex
	-2	-10	34	3.76	L	Middle Cingulate Cortex
122	16	10	16	4.04	R	Caudate Nucleus
	12	-12	12	3.69	R	Thalamus
106	-58	-36	26	3.86	L	SupraMarginal Gyrus
38	30	-20	4	3.86	R	Putamen
	34	-18	4	3.64	R	Insula Lobe

Table2. VideoFullResp-VideoNoResp (p_{unc}<0.001, k>10, survived q_{FDR}<0.05)

This revealed a similar circuit (Table 3, Figure 1b,c, green) that overlapped (yellow in Figure 1b) with VideoFullResp – VideoNoResp and included again the ACC, AI, amygdala, striatum, higher level visual areas of the temporal lobe and more cognitive regions including temporal pole and the superior frontal gyrus, (punc<0.001, k>10, T>3.42; also qFDR<0.05). Again, the reverse contrast revealed no activations (at qFDR <0.05). The contrast VideoFullResp – VideoSharedResp is methodologically 'cleaner', because the participant's performance was identical (incorrect) in both cases, and differences in activation can thus not be related to the participant's self-error-monitoring, which is known to activate regions similar to those of pain experience (Carter et al., 1998;Ullsperger and von Cramon, 2003;Taylor et al., 2007). Accordingly, we will focus on this contrast for further analyses. Finally, to explore if there is a further decrease in the response to seeing the painful videos if the participant had no rather than shared responsibility, we computed the VideoSharedResp - VideoNoResp contrast, but this revealed no significant differences at qFDR <0.05, nor did the reverse contrast, in line with the similarity between the contrasts of these respective conditions and VideoFullResp.

Cluster Size (voxels)	**Peak MIN coordinates (mm)**			**Peak T-Values**	**Hem**	**Peak anatomical location**
2831	18	56	34	5.55	R	Superior Frontal Gyrus
	4	36	24	4.73	R	Anterior Cingulate Cortex

	10	58	16	4.62	R	Superior Medial Gyrus
	-8	28	20	4.5	L	Anterior Cingulate Cortex
	-8	52	24	4.44	L	Superior Medial Gyrus
	-24	46	18	4.43	L	Middle Frontal Gyrus
511	18	8	-6	5.04	R	Putamen
	28	10	-14	3.98	R	Olfactory cortex
	20	-4	-14	3.73	R	Hippocampus
	28	10	-24	3.56	R	ParaHippocampal Gyrus
241	-24	-8	-12	4.39	L	Amygdala
	-42	2	-20	3.86	L	Temporal Pole
	-18	6	-8	3.75	L	Putamen
193	48	40	-4	3.96	R	Inferior Frontal Gyrus (p. Orbitalis)
	50	32	2	3.76	R	Inferior Frontal Gyrus (p. Triangularis)
	46	40	-8	3.7	R	Inferior Frontal Gyrus (p. Orbitalis)
156	10	36	54	4.3	R	Superior Medial Gyrus
	14	24	58	3.46	R	SMA
114	38	8	0	4.37	R	Insula lobe
	38	10	-6	4.06	R	Insula lobe
	54	20	-4	3.89	R	Inferior Frontal Gyrus (p. Orbitalis)
	58	20	2	3.61	R	Inferior Frontal Gyrus (p.Triangularis)
83	58	2	-16	3.96	R	Medial Temporal Pole
	54	-10	-12	3.55	R	Superior Temporal Gyrus
69	-40	42	-12	3.66	L	Inferior Frontal Gyrus (p. Orbitalis)
49	-50	24	-4	3.52	L	Inferior Frontal Gyrus (p. Orbitalis)
	-50	16	-10	3.29	L	Temporal Pole
42	62	-46	26	3.53	R	SupraMarginal Gyrus
35	46	22	-28	4.08	R	Temporal Pole
30	-46	12	-36	3.94	L	Medial Temporal Pole
16	-26	-4	12	4.28	L	Putamen

Table 3. VideoFullResp-VideoSharedResp (p_{unc}<0.001, k>10, survived q_{FDR}<0.05)

Consistent with the literature, our Pain-localizer activated areas associated with the pain matrix, including the bilateral cingulate cortex, bilateral insula, sensorimotor strip (Brodman Area, BA, 2, 3b, 4a), striatum, premotor cortex (BA6, and inferior frontal gyrus), inferior parietal cortex, and cerebellum (all punc<0.001, k>10, T>3.42; also qFDR<0.05, Table 4, Figure 1c,d,e red).

Cluster Size (Voxels)	Peak MIN coordinates (mm)			Peak T-Values	Hem	Peak anatomical location
56552*	40	-2	-2	9.54	R	Right Insula lobe
	4	-6	42	9.52	R	Middle Cingulate Cortex
	-38	-18	14	9.25	L	Left Insula lobe

	8	-6	8	8.6	R	Thalamus
	-4	-4	36	8.59	L	Middle Cingulate Cortex
	-18	6	-2	8.57	L	Pallidum
	-6	-6	52	8.48	L	SMA
218	-34	36	31	4.27	L	Middle Frontal Gyrus
161	38	52	18	4.93	R	Middle Frontal Gyrus

*** details of Cluster 1**

number of Voxels	**% of Cluster**	**% of Cluster Activated**	**Hem**	**Cytoarchitectonic area**
3142.6	5.8	71.2	L	Area 6
2935.5	5.2	64.5	R	Area 6
996.8	1.8	42.2	R	Area 17
941.8	1.7	49.2	R	Lobule VI (Hem)
861.9	1.5	68.1	L	Area 4a
736.6	1.3	36.6	L	Lobule VI (Hem)
701.3	1.2	84.9	R	Lobule V
679.3	1.2	73.3	L	Area 2
616.7	1.1	94.5	L	Th-Prefrontal
583.4	1	76.7	L	Lobule V
568.1	1	48.1	R	Area 4a
558	1	91.6	L	OP 1
556.2	1	30.6	L	SPL (7A)
538	1	23.6	L	Area 17
532.5	0.9	91.8	R	Th-Prefrontal
526.7	0.9	53.6	R	Area 2
489.9	0.9	93.3	R	OP 1
480.3	0.8	82.3	L	Area 4p
467	0.8	71.2	L	Area 3b
458.4	0.8	48.7	R	Area 3b
443.1	0.8	46.5	L	Area 1
415	0.7	75.7	L	Area 3a
386.2	0.7	23.4	R	Area 18
360.5	0.6	39.2	R	IPC (PF)
359.8	0.6	71.7	L	Lobules I-IV (Hem)
355	0.6	67.4	R	Lobules I-IV (Hem)
351.1	0.6	68.7	R	OP 4
345.7	0.6	55.8	L	OP 4
343.1	0.6	57.7	R	Th-Temporal
338.3	0.6	85.1	L	IPC (PFcm)
334.6	0.6	36.5	R	Area 44

330.7	0.6	88.9	L	SPL (5M)
318.9	0.6	91.8	R	Th-Parietal
314.8	0.6	59	L	SPL (5L)
313.3	0.6	54.8	L	Th-Temporal
302.7	0.5	67.4	R	SPL (5M)
276.4	0.5	56.7	R	Area 4p
269.8	0.5	82.1	L	Th-Parietal
247	0.4	75.3	R	IPC (PFcm)
246.1	0.4	48.6	R	Area 3a
244.8	0.4	14.5	L	Area 18
235.9	0.4	23.4	L	IPC (PF)
233.2	0.4	82.5	L	OP 3
222.3	0.4	84.2	R	OP 3
218.3	0.4	75	L	IPC (PFop)
208.5	0.4	74.9	R	IPC (PFop)
189.5	0.3	76.5	R	TE 1.0
186.4	0.3	28.2	R	SPL (5L)
183.8	0.3	21.4	R	Area 1
183.2	0.3	44.1	L	IPC (PFt)
182.3	0.3	89.4	L	TE 1.0
179.6	0.3	84.5	R	SPL (5Ci)
178.6	0.3	97.4	L	TE 1.1
176.9	0.3	32.8	R	Hipp (SUB)
173.9	0.3	33	L	Hipp (SUB)
170.8	0.3	100	L	Insula (Ig2)
163.3	0.3	36.4	R	IPC (PFt)
149.1	0.3	99.7	R	Insula (Ig2)
142.8	0.3	90.8	R	OP 2
135.7	0.2	76.5	R	TE 1.1
127.8	0.2	98.8	L	SPL (5Ci)
125.4	0.2	99.6	L	Th-Premotor
123	0.2	66.6	R	Amyg (SF)
117.7	0.2	100	L	OP 2
109	0.2	15.7	R	hOC3v (V3v)
105.8	0.2	87.8	L	Insula (Id1)
103.7	0.2	96.3	L	TE 1.2
101.9	0.2	71.7	R	Th-Premotor
101.5	0.2	99.4	R	TE 1.2
94.9	0.2	22.9	R	SPL (7PC)
90.3	0.2	19.7	L	TE 3
85.9	0.2	64.6	R	Insula (Id1)
83.8	0.1	95.2	R	Th-Somatosensory

80.8	0.1	9.5	R	Hipp (CA)
69.4	0.1	28.9	R	Lobule VI (Vermis)
67.4	0.1	100	L	Insula (Ig1)
65.8	0.1	8.2	L	Hipp (CA)
65.2	0.1	30.2	L	Lobule VI (Vermis)
59.7	0.1	4.9	L	Area 44
59	0.1	98.1	R	Insula (Ig1)
58.2	0.1	29.3	L	Amyg (SF)
57.8	0.1	29.8	L	SPL (7PC)
52.1	0.1	97.3	L	Th-Motor
47.3	0.1	4.2	R	Area 45
47.1	0.1	8.4	L	SPL (7P)
44	0.1	13.7	L	Amyg (LB)

Table 4. Pain-localizer (p_{unc}<0.001, k>10, survived q_{FDR}<0.05). The first part of the table lists the clusters and local maxima (peaks) of the pain localizer. Because the first cluster encompasses a large number of brain region, we detail the cytoarchitectonic brain regions it encompasses using the Anatomy Toolbox for SPM in the second half of the table.

Because an overlap between self- and other-emotions is considered a defining feature of the neural proxy of empathy (Wicker et al., 2003;Singer et al., 2004a;Keysers et al., 2004;Gazzola and Keysers, 2009b), to explore which of the regions with BOLD signals modulated by responsibility during the Video-epoch might be interpreted as a proxy of empathy, we inclusively masked the activation areas resulting from the contrast VideoFullResp - VideoSharedResp, with those from the Pain-localizer. We found a set of regions that overlapped with pain experience, and a set that did not. The former (Table 5; Figure 1c, yellow) includes the ACC, right AI, bilateral putamen, left amygdala, right and left inferior frontal gyrus and SMA. These regions are of particular relevance when it comes to empathy.

Cluster Size	**Peak MIN coordinates (mm)**	**Peak T-values**	**Hem**	**Anatomical Region**	**ROI**	**Chinese VS. Caucasians**		**Correlation with Interdependent Scores**	
						T-Value	**p-Value**	**r**	**p-Value**
383	4 36 24	4.73	R	Anterior Cingulate Cortex	1	0.114	0.91	0.066	0.729
	-8 28 20	4.5	L	Anterior Cingulate Cortex					
367	18 8 -6	5.04	R	Putamen	2	2.875	0.008**	0.467	0.009**
	38 8 -2	4.5	R	Insula Lobe					
	30 16 -12	3.99	R	Insula Lobe					
	28 10 -14	3.98	R	Olfactory cortex					
	20 -4 -14	3.73	R	Hippocampus					
142	-24 -4 -14	4.37	L	Amygdala	3	1.591	0.123	0.286	0.126

	-18	6	-8	3.74	L	Putamen					
76	54	20	-4	3.89	R	Inferior Frontal Gyrus (p. Orbitalis)	4	-0.58	0.566	0.363	0.049*
	58	20	2	3.61	R	Inferior Frontal Gyrus (p. Triangularis)		2.623	0.014*	-0.064	0.738
25	-30	46	20	3.74	L	Middle Frontal Gyrus	5				
20	-40	2	-20	3.83	L	Temporal Pole	6	0.397	0.694	0.455	0.011*
16	30	52	22	3.53	R	Middle Frontal Gyrus	7	0.341	0.736	-0.101	0.594
16	-50	20	-6	3.41	L	Inferior Frontal Gyrus (p. Orbitalis)	8	2.138	0.04*	0.429	0.618
12	14	24	58	3.46	R	SMA	9	-0.398	0.693	0.042	0.752
12	32	42	22	3.47	R	Middle Frontal Gyrus	10	-2.781	0.009**	-0.014	0.652
10	-24	-4	12	4.09	L	Putamen	11	-2.141	0.041*	0.021	0.468

Table 5. Overlap between VideoFullResp-VideoSharedResp and the Pain-localizer. Some voxels showing an effect of responsibility (VideoFullResp-VideoSharedResp) overlap with the Pain-localizer (and could thus relate to empathy) while others do not (and should thus not be interpreted as related to empathy). Accordingly, we thresholded the responsibility effect and the Pain-localizer individually at punc<0.001, k>10 (all also survived qFDR<0.05). Here, we list those voxels significant in both constrats (overlap) while Table 6 lists those significant in the responsibility but not the Pain-localizer. The T values listed are from VideoFullResp-VideoSharedResp. Column 'ROI' related to the numbering of the ROIs in Fig. 2f. From each of these ROIs/clusters, the mean signal was used to calculate parameter estimates used for further analyses. The columns labeled "Chinese VS. Caucasians" list the t and p values of a test comparing the parameter estimates within that cluster for VideoFullResp-VideoSharedResp (as obtained using Marsbar from the average signal of all the voxels within the cluster for each participant) across the two subgroups. Note that these are post-hoc tests following an ANOVA, and are therefore not corrected for multiple comparisons. The columns labeled "Correlation with Interdependent Scores" list the correlation values between the same parameter estimates and the score from Interdependence subscale of the Independent and Interdependent Self-Construal's Questionnaire (**: p<0.01; *: p<0.05, uncorrected for multiple comparison)

A number of clusters however clearly fell outside of the pain localizer, including high-level visual regions of the temporal lobe around the STS and the dorsolateral prefrontal cortex (Table 6; Figure 1c, green).

Cluster Size (voxels)	Peak MIN coordinates (mm)			Peak T-values	Hem	Peak anatomical location
193	48	40	-4	3.96	R	Inferior Frontal Gyrus (p. Orbitalis)

	48	36	-2	3.92	R	Inferior Frontal Gyrus (p. Triangularis)
	50	32	2	3.76	R	Inferior Frontal Gyrus (p. Triangularis)
144	10	36	54	4.3	R	Superior Medial Gyrus
	14	24	60	3.22	R	Superior Frontal Gyrus
84	58	2	-16	3.96	R	Medial Temporal Pole
	54	-10	-12	3.55	R	Superior Temporal Gyrus
	58	-6	-14	3.38	R	Middle Temporal Gyrus
70	-40	42	-12	3.66	L	Inferior Frontal Gyrus (p. Orbitalis)
43	62	-46	26	3.53	R	SupraMarginal Gyrus
	62	-52	26	3.47	R	Angular Gyrus
36	58	22	8	3.4	R	Inferior Frontal Gyrus (p. Triangularis)
35	46	22	-28	4.08	R	Temporal Pole
	50	20	-28	3.86	R	Medial Temporal Pole
30	-46	12	-36	3.94	L	Medial Temporal Pole
24	42	0	-36	4.54	R	Inferior Temporal Gyrus
	42	8	-40	3.59	R	Medial Temporal Pole
13	14	12	16	3.69	R	Caudate Nucleus
13	48	-20	-6	3.52	R	Superior Temporal Gyrus
11	-46	-2	-32	3.66	L	Inferior Temporal Gyrus

Table 6. VideoFullResp-VideoSharedResp *not* overlapping with Pain-localizer (p_{unc}<0.001, k>10, survived q_{FDR}<0.05). Both the responsibility effect and Pain-localizer were individually thresholded at punc<0.001, k>10, and survived qFDR<0.05. Only voxels significant in VideoFullResp-VideoSharedResp but not in the pain localizer are listed.

Next, we explored if characteristics of our participants influenced the modulation of vicarious activations by responsibility. We extracted the VideoFullResp - VideoSharedResp contrast from all 11 clusters common to VideoFullResp - VideoSharedResp and the Pain-localizer (yellow clusters in Figure 1c; Table 5), and compared parameter estimates extracted from these clusters with individual characteristics of the participants. First we performed a 2 Genders (Male vs Female) x 2 Races (Chinese vs. Caucasian) x 11 ROIs (Table 5) within-subject ANOVA. This revealed no main effects (all p>0.2), and all interactions including Gender were non-significant (all p>0.48), but there was a significant Race x ROI interaction (p<0.01). We then tested the Race effect separately in each of the 11 ROIs, and found the most significant Race effects in the right AI/putamen, middle frontal gyri and left putamen (Table 5, penultimate column). In addition, we reasoned that people vary along an individualist-collectivist dimension that can be assessed by questionnaires, with a sense of responsibility for others more pronounced in collectivist values. The modulation by responsibility we observed might thus be strongest in those that consider themselves most collectivist/interdependent. We asked our participants to fill out the interdependence questionnaire (Theodore M.Singelis, 1994) (example items: 'my happiness depends on the happiness of those around me', 'if my brother or sister fails, I feel responsible'). We found that in 3 of the ROIs (ACC, Insula and STS/MTG), the correlation between VideoFullResp-VideoSharedResp and the Interdependence Score was significant, and the strongest correlation was again with the right AI/putamen (Table 5, last column).

Additional Analyses

We performed a number of control analysis to further explore whether the contrast VideoFullResp - VideoSharedResp truly captures a modulation of the neural proxy of empathy by responsibility.

First, VideoFullResp and VideoSharedResp trials also differ based on the performance of the confederate FC (correct in FullResp but incorrectly in SharedResp). It has been shown that the errors and successes of others can vicariously activate regions encoding errors and successes in the self (Mathalon et al., 2003;Shane et al., 2008;Heldmann et al., 2008;Monfardini E et al., 2013). If differences during the Video-epoch were to reflect a spill-over from the vicarious processing of the success of another in the Feedback-epoch, we would expect the FullResp - SharedResp difference to be largest during the Feedback-epoch. If VideoFullResp - VideoSharedResp however reflects a true modulation of vicarious activations by responsibility, we would expect the difference to be larger during the Video-epoch when empathy is triggered by the movie. An interaction analysis (VideoFullResp - VideoSharedResp) > (FeedbackFullResp - FeedbackSharedResp) confirms that the AI and ACC showed a larger modulation during the Video-epoch compared to the Feedback-epoch (cyan in Figure 1d; Table 7), and that this overlaps with the Pain-localizer (yellow in Figure 1d).

Cluster Size (voxels)	Peak MIN coordinates (mm)			Peak T-values	Hem	Peak anatomical location
823	-22	46	16	4.2	L	Middle Frontal Gyrus
	-14	32	56	4.19	L	Superior Frontal Gyrus
	2	44	16	3.78	R	Anterior Cingulate Cortex
	0	44	22	3.72	R	Superior Medial Gyrus
737	14	54	36	5.17	R	Superior Frontal Gyrus
	10	36	54	4.58	R	Superior Medial Gyrus
	26	60	22	3.99	R	Middle Frontal Gyrus
251	18	8	-6	4.77	R	Putamen
221	-40	42	-12	4.52	L	Inferior Frontal Gyrus (p. Orbitalis)
	-32	54	-4	3.32	L	Middle Orbital Gyrus
189	-26	-6	-14	4.39	L	Amygdala
	-18	6	-8	3.67	L	Putamen
	-20	2	-6	3.46	L	Pallidum
169	48	42	0	3.86	R	Inferior Frontal Gyrus (p. Triangularis)
57	58	2	-16	3.84	R	Medial Temporal Pole
	54	-10	-12	3.36	R	Superior Temporal Gyrus
	54	8	-16	3.31	R	Temporal Pole
44	16	16	16	4.55	R	Caudate Nucleus
37	-42	4	-20	3.85	L	Temporal Pole
30	8	18	22	3.64	R	Anterior Cingulate Cortex
21	38	8	-2	3.6	R	Insula
17	46	22	-28	3.96	R	Temporal Pole
	50	20	-28	3.79	R	Medial Temporal Pole
12	-16	16	12	3.61	L	Caudate Nucleus
11	-12	-94	-2	3.35	L	Calcarine Gyrus

10	-26	-4	12	4.22	L	Putamen
10	42	0	-36	4.11	R	Inferior Temporal Gyrus
	44	4	-34	3.43	R	Medial Temporal Pole

Table7. Activation Table of (VideoFullResp-VideoSharedResp) - (FeedbackFullResp-FeedbackSharedResp) (p_{unc}<0.001, k>10, survived q_{FDR}<0.05).

Second, empathy for pain studies so far contrasted stimuli suggesting the pain of another against stimuli suggesting non-painful experiences – independently of responsibility. To explore if our painful movies trigger empathy in this traditional sense, we also performed a contrast between all painful videos and our non-painful video (i.e. VideoFullResp + VideoSharedResp + VideoNoResp - 3×VideoNoPain) (Figure 1e, blue), and overlapped this contrast with the Pain-localizer (Figure 1e, red). Results evidenced a network of brain regions consistent with those found in the literature, including the AI and ACC (Lamm et al., 2011) (Figure 1e, yellow; Table 8). Note that the contrast (VideoFullResp-VideoNoPain)-(VideoSharedResp-VideoNoPain) that would isolate the pain-specific part of empathy is mathematically identical to the contrast we report above (VideoFullResp-VideoSharedResp) because VideoNoPain is cancelled out. In addition, we extracted the mean signal in clusters common to VideoFullResp-VideoSharedResp and the Pain-localizer, calculated parameter estimates for all four conditions and found that the activation was always numerically lowest in the condition in which no pain was witnessed (Figure 1f), as expected if these ROIs encoded pain vicariously.

Cluster size	**Peak MIN coordinates (mm)**			**Peak T-Values**	**Hem**	**Peak anatomical location**
4592	-10	-70	2	6.34	L	Lingual Gyrus
	6	-66	6	5.96	R	Lingual Gyrus
	-18	-62	-14	5.87	L	Cerebellum
2897	-48	-38	22	5.44	L	Superior Temporal Gyrus
	-50	16	-12	5.02	L	Temporal Pole
	-52	20	-6	4.92	L	Inferior Frontal Gyrus (p. Orbitalis)
	-16	-24	4	4.9	L	Thalamus
	-16	8	12	4.79	L	Caudate Nucleus
	-32	-12	16	4.78	L	Insula Lobe
2634	-4	34	28	5.53	L	Anterior Cingulate Cortex
	-4	-16	40	4.89	L	Middle Cingulate Cortex
	14	36	26	4.6	R	Anterior Cingulate Cortex
	-20	-20	62	4.3	L	Precentral Gyrus
815	58	-32	20	5.73	R	Superior Temporal Gyrus
	36	-32	16	3.51	R	Heschls Gyrus
	56	-18	4	3.43	R	Superior Temporal Gyrus
516	32	6	10	4.85	R	Putamen
	20	2	6	3.94	R	Pallidum
	34	-4	10	3.71	R	Insula Lobe
184	50	22	-10	4.1	R	Inferior Frontal Gyrus (p. Orbitalis)
	52	14	-14	4.06	R	Temporal Pole
173	48	-66	0	5.76	R	Middle Temporal Gyrus

163	26	-32	60	3.57	R	Postcentral Gyrus
	20	-28	68	3.46	R	Precentral Gyrus
128	8	26	62	4.35	R	Superior Medial Gyrus
	-2	18	62	4.32	L	SMA
	-12	18	54	3.67	L	Superior Frontal Gyrus
	-8	28	48	3.59	L	Superior Medial Gyrus
	2	14	64	3.45	R	SMA
117	-44	-16	34	4.78	L	Postcentral Gyrus
102	16	14	8	3.83	R	Caudate Nucleus
89	-26	44	36	5.22	L	Middle Frontal Gyrus
81	16	14	8	3.83	R	Caudate Nucleus
51	30	54	18	4.13	R	Middle Frontal Gyrus
14	30	16	-14	3.73	R	Insula Lobe
11	-52	-8	14	3.43	L	Postcentral Gyrus

Table8. (VideoFullResp+VideoSharedResp+VideoNoResp)-3VideoNoPain overlapped with Pain-localizer (punc<0.001, k>10, survived qFDR<0.05). This table represents an approximation of traditional definitions of the neural basis for empathy: it identifies voxels for which the activation during the observation of painful shocks (independently of responsibility) exceeds that during the observation of non-painful shocks within regions involved in the experience of painfulness (Pain-localizer). Both contrast are calculated at (punc<0.001, k>10, survived qFDR<0.05), and only voxels common to both are listed. T-values from the contrast (VideoFullResp+VideoSharedResp+VideoNoResp)-3VideoNoPain.

DCM

Because the contrast VideoFullResp-VideoSharedResp evidenced differential processing in regions involved in visual processing (along the middle temporal gyrus and superior temporal sulcus - abbreviated as STS/MTG - and green dotted outline in Figure 1b) in addition to the core regions involved in empathy (AI and ACC; yellow and white dotted outline in Figure 1c respectively), it is unclear whether the differential activation primarily results from differential visual attention or differential empathy. To help differentiate these two scenarios, we used dynamic causal modeling (DCM). Because it has been recommended to keep DCM models as simple as possible to optimally contrast theoretical alternatives (Stephan et al., 2010),a simple three ROIs model was used. The three nodes were chosen to probe the nodes most representative of the two alternative accounts, including the STS/MTG cluster for the visual attention account, and AI and ACC for the empathy account (dotted outlines in Figure 1b and c). All models include a 'generic' visual input to the visual node (i.e. identical for all painful movies; gray arrows in Figure 2), and mutual and reciprocal connections between all nodes (for the known direct or indirect connections amongst these regions). We then compared 33 models (Figure 2) that represent variants of the two competing explanations, with the effect of responsibility (VideoFullResp -VideoSharedResp) entering through the STS/MTG, the AI or ACC. Variants had the effect of responsibility only influencing one node, one node and the connections flowing out, or a combination of multiple nodes (black arrows in Figure 2). Bayesian model selection showed that models 3 and 13 to 17 had the highest exceedance probability (red outlines in Figure 2). The significant coupling parameters compared to baseline are shown in Table 9. In all winning models responsibility first influenced activation in the AI, and this influence than spread to the other regions (Table 9).

A. instric connection parameters				**B. Generic Input to Visual Area**
	ACC	Insula	Visual	0.01
ACC	-0.50	0.03	0.03	

Insula	0.02	-0.50	0.03		
Visual	0.02	0.03	-0.50		
C. Responsbility Modulation					
	Direct into Insula	Insula->ACC	Insula->Visual	ACC->Visual	Visual->ACC
M3	0.03	0.82	NaN	NaN	NaN
M13	0.03	NaN	NaN	NaN	NaN
M14	0.03	NaN	0.65	NaN	NaN
M15	0.03	0.77	0.76	NaN	NaN
M16	0.03	0.82	NaN	0.14	NaN
M17	0.03	NaN	0.71	NaN	0.42

Table 9. Coupling parameters for the 6 winning DCM models. All connections shown in this table are different from zero at $p<0.001$. The coupling parameters represent connection strengths (Friston et al., 2003b). Positive coupling parameters suggest facilitation of neural activity and negative coupling parameters suggested inhibition of neural activity.

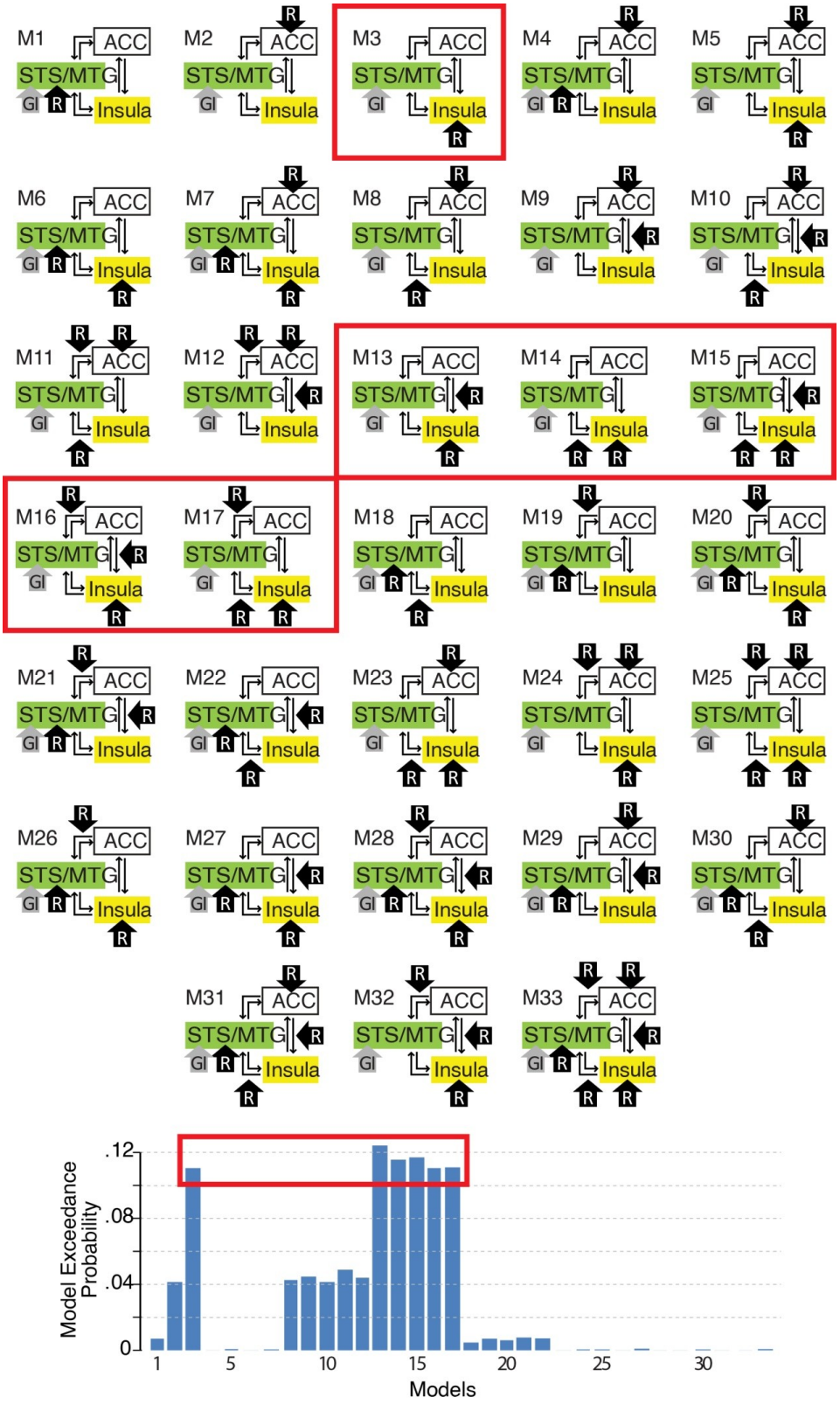

Figure2: DCM models All 33 models compared in the DCM analysis. Black arrows (R=Responsibility) represent modulations of nodes or connections by the factor responsibility. Gray arrows (GI=generic input) modulations of STS/MTG by the generic input. The graph below the models shows the results of the Bayesian Model Selection in DCM. The 6 winning models selected out of 33 tested models are marked with a red contour. The colored boxes around the anatomical description of the ROI reflect the colors of the dotted lines in figure 1b and 1c that show the location of that particular ROI.

Origin of the Effect or Responsibility

The DCM identified the AI ROI as the key node in the modulation of empathy by responsibility during the Video-Epoch. This raises the question of what brain region determines responsibility during the Feedback-Epoch maintains that information in memory until the Video-Epoch and then has the connectivity to modulate activity in the AI ROI during the Video-Epoch. To answer this question, we examined the existing literature to determine brain regions implicated in the cognitive regulation of emotional responses. The most relevant literature, is the one on cognitive reappraisal, in which people are shown emotional stimuli and asked to down- or up-regulate their emotional responses, which has been recently meta-analyzed, and the authors of that analysis sent us the z-map of their analysis (Buhle et al., 2013) , which we thresholded at z>2. Next, we used a probabilistic diffusion weighted imaging study of insula connectivity published by our lab (Cerliani et al., 2012), and extracted a map of regions connected to the AI ROI (thresholded at n>2 participants). Finally, we overlapped these two maps. This revealed a small number of regions consistently involved in reappraisal and connected to our AI ROI: the right SMA (119voxel, peak at 14/12/66), the left SMA (12voxel, peak at -4/16/64), the right inferior frontal gyrus (836voxels, peak 50/30/-12; 27voxels, peak 48/42/-12) and the right middle frontal gyrus (12voxel, 60/-36/-2). These peaks were then used for a small-volume correction (see below, 10mm spheres), as they represent our a-priori hypotheses of the regions that could influence the AI. Next, we identified regions in our data that indeed show sensitivity to responsibility during the Feedback-Epoch by calculating the contrast FeedbackFullResp-FeedbackSharedResp (punc<0.001, k>10, T>3.42), which revealed two clusters: the right SMA (64voxels, peak 8/8/64, T=4.18), and right precentral gurys (36voxels, peak 46/0/38, T=4.05). Only the SMA fell within regions connected with the AI and involved in emotional reappraisal (white in Figure 1g left panel), and survives the hypothesis driven small volume correction described above (pFWE=0.002). Next, we examined whether the responsibility-dependent signal in this SMA cluster (peak 8/8/64) during the Video-Epoch could predict (in the sense of a regression), the signal in the AI ROI during the same epoch. We therefore extracted, for each participant, the parameter estimates for VideoFullResp-VideoSharedResp contrast for the mean signal within the SMA cluster and the AI ROIs. These two signals were correlated (r=0.62, p<0,001, T (27)=4.1; graph in Figure 1g, right panel). Hence, the right SMA has been consistently involved in the cognitive modulation of emotional response(Buhle et al., 2013), is anatomically connected with the AI(Cerliani et al., 2012), is more active when the Feedback signals Full than Shared responsibility and predicts the Full-Shared responsibility specific modulation of the AI signal during the Video-Epoch.

Discussion

In contrast to most studies investigating the neural basis of empathy for pain, in which the witness witnesses a pain he did not cause (Lamm et al., 2011), we investigate how vicarious pain activations vary as a function of responsibility, a determining factor for morality. We find regions involved in the first hand pain experience, including the AI, ACC, the putamen and amygdala, are most strongly vicariously recruited (i.e. while witnessing someone else being in pain) when the participant has full responsibility. Shared or no responsibility lead to relatively reduced vicarious responses, an effect that a DCM analysis suggests to originate from the AI more than from visual attention acting on the STS/MTG during the actual Video-Epoch. Finally, we show the right SMA is likely to transform the performance feedback that determines responsibility into a modulation of empathy in the AI while viewing the video.

That having no responsibility for the pain reduces vicarious activations dovetails with a recent study (Koban et al., 2013) showing that the AI and dorsolateral prefrontal cortex differentiate between painful and non-painful stimulation to another individual when the participant caused the pain by erring, but not when the other individual had caused his own pain. Because in that study a task was performed by the witness in the full- but not in the no-responsibility condition, it could not determine the effect of sharing responsibility, and the modulation ascribed to

agency, could have been due to differences in attention: the participants could disengage attention during trials in which they were not required to perform a task. By having our participant always do the task together with the pain-taker, performing a DCM, and including a pain localizer, we were able to extend their results and (a) demonstrate a strong effect of sharing responsibility (b) make the attention explanation unlikely, and (c) show that some regions modulated by responsibility (AI, ACC, putamen and amygdala) fall within the pain-matrix while others (STS/MTG and dorsolateral prefrontal cortex) do not, thereby guiding the inferences, in terms of empathy, that can be drawn.

Three interpretations could explain why vicarious activations were maximal under full responsibility. First, for the witness, having caused the pain may magnify the sharing of the pain, in order to generate most vicarious pain in cases in which the witness should change his behavior because it harmed others. Second, an innocent victim might deserve pain the least (Decety et al., 2010a) and thus deserves most empathy to motivate more prosocial behavior. Because in our design the responsibility of the witness is inversely proportional to that of the victim, we cannot dissociate these alternatives. Experiments with two confederates (a passive victim and a second player) would help overcome this limitation. Third, because the AI is activated during a number of different emotions (Michl et al., 2012;Wicker et al., 2003;Jabbi et al., 2008), it is possible that increased activation in FullRespVideo does not reflect more sharing of the pain of the other (i.e. empathy), but other negative affects, that could also motivate prosocial behavior (e.g. guilt or concern), but which are not directly isomorphic to what the victim is thought to feel.
Why would evolution equip us (and our morality) with such a modulation of vicarious activation (and negative affect) by responsibility? One might speculate that our own pain is an adaptation to learn not to harm ourselves. By extension, vicarious pain would serve to learn not to harm others. This vicarious pain should then be maximal if I caused the pain, because I should then discontinue the behavior that I did to cause that pain. If my behavior has not caused the pain, there is no point in discouraging the behavior I was just performing, and thus, no reason for intense vicarious pain. If I share responsibility for that pain, it is not entirely certain who's behavior actually caused the pain, and my vicarious pain should thus be discounted by this uncertainty.

Should this responsibility-based magnification of vicarious activations be equally strong towards all victims? Evolutionarily, harming members of the in-group is worse than harming those of the out-group (Choi and Bowles, 2007), and one might therefore expect that the modulation of empathy by responsibility would be strongest for participants that belonged to the same group/race than the person in the movies (FC). This is in agreement with our finding: Chinese witnesses (same race as FC), modulated their empathic response more than Caucasians. However, future studies using participants and confederates of two races will need to assess whether the difference between our Chinese and Caucasian witnesses reflects an in-group out-group difference, or a properties of the witnesses independently of the pain-taker's race (e.g. differences in interdependence).

The brain regions we found to be modulated by responsibility fit with the existing literature on empathy and its modulation by other factor. The AI and ACC are the two most consistent regions across studies of empathy for pain (Lamm et al., 2011), and the AI has also been associated with empathy for disgust and happiness (Jabbi et al., 2007;Shamay-Tsoory, 2011;Moya-Albiol et al., 2010;Wicker et al., 2003), and with the unpleasantness and emotional arousal associated with nociception (Craig et al., 2000). Anatomically, the AI receives visual input from regions of the temporal lobe that encode facial pain expressions (Mesulam and Mufson, 1982a;Mufson and Mesulam, 1982;Mesulam and Mufson, 1982b), which allows it to respond to the pain of FC in the movies. Our DCM analysis supports a key role for the AI in the differential empathic response during the Video. In addition, this part of the AI has anatomical connectivity with the SMA (Cerliani et al., 2012) (Luppino et al., 1993), which is consistently involved in the cognitive reappraisal of emotional responses(Buhle et al., 2013), showed more

activation when the Feedback screen indicated Full compared to Shared responsibility, and predicted the modulation of empathy in the AI during the Video. Hence, the right SMA seems to have played a key role in transforming the performance feedback during the earlier Feedback Epoch into a modulation of empathy in the AI while viewing the Video. The ACC is also associated with the subjective unpleasantness of pain (Rainville et al., 1997;Vogt and Sikes, 2000;Sewards and Sewards, 2002), and patients following surgical ACC ablation loose the unpleasantness of pain and the motivation to avoid further damage (Gao and Ji, 2010). A reduction of vicarious activation in the ACC upon sharing responsibility could be a critical element of how this effect could reduce the motivation to help others. Furthermore, we found a modulation by responsibility in the amygdala and putamen, regions also found in the pain empathy literature when rich social stimuli, like our videos, were used (Lamm et al., 2011). The amygdala is widely activated during pain-related processing (Jelasic, 1966;Hebert et al., 1999;Rouwette et al., 2012) and thought to reflect the fear and anxiety associated with painful stimuli (Hebert et al., 1999;Narita et al., 2006). The putamen's is also involved in experiencing pain (Downar et al., 2003) and other negative emotions (Calder et al., 2000), has been associated with witnessing others in pain (Gu and Han, 2007), plays a key role in reinforcement learning (Packard and Knowlton, 2002), and its vicarious activation may thus be part of the learning signal that discourages us from repeating behaviors that harmed others.

That vicarious activations reflect responsibility suggests a mechanism that biases empathy in the service of learning and morality: rather than indiscriminately sharing all pains equally, evolution may have made us share those most that we can prevent because we caused them. Merely sharing responsibility was sufficient to decrease vicarious pain, and being the only responsible triggered the largest vicarious pain. This findings indirectly also shed light on the bystander effect(Darley and Latane, 1968), and advocates that if we want people to help others, it might be essential to maximize vicarious activations by actively emphasize each potential helper's personal responsibility.

Methods

Participants

Thirty-three volunteers participated in this study, but three were excluded from the analyses: one because felt claustrophobic and the other two because they said they didn't believe that the person in the movie received electroshocks in real time. Thirty participants (aged 24.8 y±4.37 s.d.; 15 Chinese, 15 Caucasians; 7 males in each race) were therefore included. All participants were healthy, right-handed, had no history of neurological or psychiatric disorders, and provided with written informed consent. This study was approved by the Ethics Committee of the University of Amsterdam, the Netherlands.

General experimental setup

A confederate design was used in this study, as described in the introduction. At the end of scanning, an anatomical scan was additionally acquired. After all the scanning, a debriefing was given, the participant was asked to fill out the Interdependent Self-Construal's Questionnaire (Theodore M.Singelis, 1994) and to indicate how much he/she believed that the FC was actually being shocked based on their joint performance during the experiment.

Flanker-Task in details

During the Flanker- epoch, one of the following five-letter-strings appeared on the screen randomly: "HHHHH", "LLLLL", "HHLHH" and "LLHLL". In order to achieve a similar task difficulty across participant, the duration of each string was initially set at 150 ms, and was changed to reach a minimum of 100 ms and a maximum of 200ms based on the participant's previous performance: if the participant gave two consecutive correct responses, the time of the next string was shortened by 10 ms; if the participant gave two consecutive incorrect

responses the time was prolonged of 10ms. The participant and author FC were instructed to simultaneously respond to the letter in the middle (H or L). To give the response the participant had to press one of two pre-assigned buttons on an MRI-compatible button-box. The faked setup for FC required her to press the "H" and "L" buttons on a keyboard. As mentioned above, in reality only the participant was running the task and he/she had 1.5 seconds to give a response. If no button press was recorded within this duration, the participant's performance in this trial would be considered incorrect, and indicated as such during Feedback-Epoch.

Videos preparation

The videos used in this study showed author FC seated by a table. Her face and upper body were clearly visible, and two electrodes, used to deliver the electroshock, were attached and visible on the back of her right hand, which was resting in front of her on the table (Supplementary information: Movie 1 and 2). During the video recording, we first tested FC's pain threshold (see section" Stimulation and Pain Threshold" for details). Afterwards 70 unique video-clips were recorded while FC received the painful or painless electroshocks (35 videos each). Each video was cut to last 1.5 s and started with 0.3s in which the experimenter was sitting still with a neutral face, followed by 0.5 second of electroshock to trigger FC's natural facial expression. All the settings, including the background and FC's look, were kept unchanged relative to the recording day during all the experimental days. For each of the 4 runs, at the end of each trial a movie was randomly picked (without replacement) from the 35 movies of the appropriate category (painful / painless), so that no movie would be seen twice per run.

Pain-localizer procedure

Sixteen painful and sixteen non-painful 0.5 s electroshocks were applied, in a pseudo-randomized order, on the participant's right hand using a MRI-compatible electrical stimulation system. The participant was asked to evaluate how painful each electroshock was by pressing buttons after each shock. The participant was instructed to use three buttons of a MRI compatible button-box placed next to their left hand. Two buttons were used to move the slider left and right on the visual scale on the screen and the third button was for confirmation. The pain intensity scale was a 10 point scale (1: not painful at all; 10: most imaginable pain), with the starting point set randomly for each trial to disentangle the number of button presses from the rating.

Electrical Stimulation and Pain Threshold

A 100 Hz train of electrical pulses (2ms each) was applied for 0.5 seconds through bipolar surface electrodes using an MRI-compatible electrical stimulator attached on the back of the right hand on the 4th musculus interossei (stimulation area: 16mm2). Before the scanning we measured the pain threshold from both FC and the participant. We started from a 0.2 mA current that was then increased until maximally 6.0 mA in 0.1 mA steps (Singer et al., 2004a). Participants were instructed to evaluate how painful the stimulation was on a 10-point scale (same as in Pain-localizer). We then chose the current corresponding to a rating of 7 for the painful condition and of 2 for the painless condition (Singer et al., 2004a). The current selected was 0.75±0.14mA (painless ± s.e.m) and 2.12±0.77mA (painful). The same procedure was used only on FC during the video recording session.

Data Acquisition

A Phillips Achieva 3.0 Tesla MRI scanner was used for image acquisition. We used a T2*-weighted echo-planar sequence with 32 interleaved 3.5 mm thick axial slices and a 0.35mm gap for functional imaging (TR=1700 ms, TE=27.6 ms, flip angle = 73°, FOV = 240 mm ×240 mm, 80×80 matrix of 3.5 mm isotropic voxels). At the end of the functional scanning, a T1-weighted anatomical image (1×1×1mm) covering the whole brain, was acquired.

Image pre-processing

FMRI data was preprocessed using SPM8 (www.fil.ion.ucl.ac.uk). All echo planar images (EPIs) were slice-time corrected and realigned to the participant's mean EPI. T1 images were then co-registered to the mean EPI, segmented, and the gray matter was used to estimate the normalization parameters which were then applied to all EPIs. Normalized (2×2×2) EPIs were smoothed with an 8 mm isotropic FWHM Gaussian kernel.

General linear models

Two separate general linear models (GLM) were applied at the single subject level, one for the four runs of the flanker-task and one for the pain localizer. Predictors were modeled using a standard boxcar function convolved with the hemodynamic response function (HRF). For each of the four runs of the flanker-task, we included the following predictors. First, because each run started with the participant indicating their readiness with a button press, one predictor collected this initial press. Another predictor contained all the Flanker-epochs from the appearance of the string until the end of the participants' button pressing, independently of performance. Four separate predictors, one for each experimental condition (NoPain, FullResp, SharedResp, NoResp, see Table 1), were then used for the Feedback-epoch. Four predictors finally captured the Video-epoch separately for each experimental condition. Each predictor lasted for as long as the epoch it represents. For the Pain-localizer session, we modeled one predictor for all 32 electrical stimulations with a parametric modulator for the subjective rating of pain intensity. A second predictor contained the rating period, from onset of the rating screen until the end of the button presses. Six additional predictors of no interest were entered for each of the five runs to account for translations and rotations of the head (none of the included participants had head motions parameters exceeding the acquired voxel-size). Data was then analyzed at the second level using t-tests within a repeated measurement ANOVA as described in the result section. Results were thresholded at punc <0.001 (uncorrected) with a minimum cluster size of 10. Unless specified otherwise, all results thresholded at that level were also found to survive qFDR <0.05 (false discovery rate).

Dynamic Causal Modeling (DCM)

Three ROIs were defined: "Insula", "ACC" and "STS" (Figure 1b and c, yellow, white and green dotted circles respectively). Because the differential activations in the insula and STS were strongest on the right hemisphere, we limited our DCM to that hemisphere. The "STS" ROI was extracted by selecting the anatomically appropriate cluster within the contrast VideoFullResp-VideoSharedResp (punc <0.001, k>10, T>3.42, and survived qFDR<0.05). This ROI was centered at MNI: 56/-2/-15 included 84voxels and was in the right middle temporal gyrus. The other two ROIs, "ACC" and "Insula", were extracted from the same contrast, but this time, after restriction to voxels also responding to first-hand pain experience in order to focus on empathy related responses (both contrasts at punc <0.001, k>10, T>3.42, and qFDR<0.05), masked further with the anatomical definition of ACC and Insula from the WFU_pickatlas toolbox (Lancaster et al., 2012;Maldjian et al., 2003;Lancaster et al., 2000) embedded in SPM8. The "Insula" ROI was centered at MNI: 39/9/-2 and included 45 voxels; the "ACC" ROI was centered at MNI: 0/33/22 and included 323 voxels. After defining the ROIs at the group level, the time courses for each individual subjects were extracted by deriving the first eigenvariate of the time course in all the voxels within the group ROI that also survive the contrast VideoFullResp-VideoSharedResp at the single subject level at punc <0.05. Then 33 models were built using these data (Figure 2). After defining candidate models, we used Bayesian model selection (BMS;(Penny et al., 2010)) implemented in SPM8 to identify the model that showing the highest exceedance probability in the applied Bayesian framework. After the best group of models was selected, we performed Bayesian model averaging (BMA) to estimate the connectivity parameters for this group of models.

Acknowledgements

VG was supported by a VENI grant 451-09-006 from the Netherlands Organization for Scientific Research (N.W.O.). CK and the research was supported by a VIDI grant of NWO 452-04-305 and a Marie Curie Excellence Grant MEXT-CT-2005-023253 and European Research Council grant 312511 of the European Commission. FC was supported by the China Scholarship Council for State Scholarship Fund. We thank Jennifer Silvers, Jason Buhle and Kevin Ochnser for sending us a z-map originated from her meta-analysis of reappraisal (Buhle et al., 2013). We thank Leonardo Cerliani for generating the diffusion weighted imaging maps specific for our AI ROI from the data and analyses reported in (Cerliani et al., 2012). We thank Claus Lamm for sending us the maps from their meta-analysis (reported in (Lamm et al., 2011)) in order to ascertain that our task activates the same regions as in their meta-analysis.

Author Contributions

FC, CK and VG conceived of the study. FC and AA acquired the data. FC, CK and VG analyzed the data and wrote the paper with comments from AA.

References Cited

Agnew Z, Wise RJ (2008) Separate areas for mirror responses and agency within the parietal operculum. J Neurosci 28:12268-12273.

Apkarian AV, Bushnell MC, Treede RD, Zubieta JK (2005) Human brain mechanisms of pain perception and regulation in health and disease. Eur J Pain 9:463-484.

Apkarian AV, Darbar A, Krauss BR, Gelnar PA, Szeverenyi NM (1999) Differentiating cortical areas related to pain perception from stimulus identification: temporal analysis of fMRI activity. J Neurophysiol 81:2956-2963.

Azevedo RT, Macaluso E, Avenanti A, Santangelo V, Cazzato V, Aglioti SM (2012) Their pain is not our pain: Brain and autonomic correlates of empathic resonance with the pain of same and different race individuals. Hum Brain Mapp.

Banerjee O, El Ghaoui L, d'Aspremont A, Natsoulis G (2006) Convex optimization techniques for fitting sparse Gaussian graphical models. In: Proceedings of the 23rd international conference on Machine learning.

Blair RJ (1995) A cognitive developmental approach to mortality: investigating the psychopath. Cognition 57:1-29.

Blakemore SJ, Frith CD, Wolpert DM (1999) Spatio-temporal prediction modulates the perception of self-produced stimuli. J Cogn Neurosci 11:551-559.

Blakemore SJ, Wolpert DM, Frith CD (1998) Central cancellation of self-produced tickle sensation. Nat Neurosci 1:635-640.

Buhle JT, Silvers JA, Wager TD, Lopez R, Onyemekwu C, Kober H, Weber J, Ochsner KN (2013) Cognitive Reappraisal of Emotion: A Meta-Analysis of Human Neuroimaging Studies. Cereb Cortex.

Calder AJ, Keane J, Manes F, Antoun N, Young AW (2000) Impaired recognition and experience of disgust following brain injury. Nat Neurosci 3:1077-1078.

Carter CS, Braver TS, Barch DM, Botvinick MM, Noll D, Cohen JD (1998) Anterior cingulate cortex, error detection, and the online monitoring of performance. Science 280:747-749.

Caspers S, Zilles K, Laird AR, Eickhoff SB (2010) ALE meta-analysis of action observation and imitation in the human brain. Neuroimage 50:1148-1167.

Cerliani L, Thomas RM, Jbabdi S, Siero JC, Nanetti L, Crippa A, Gazzola V, D'Arceuil H, Keysers C (2012) Probabilistic tractography recovers a rostrocaudal trajectory of connectivity variability in the human insular cortex. Hum Brain Mapp 33:2005-2034.

Cheng Y, Chen C, Lin CP, Chou KH, Decety J (2010) Love hurts: an fMRI study. Neuroimage 51:923-929.

Choi JK, Bowles S (2007) The coevolution of parochial altruism and war. Science 318:636-640.

Christensen MS, Lundbye-Jensen J, Geertsen SS, Petersen TH, Paulson OB, Nielsen JB (2007) Premotor cortex modulates somatosensory cortex during voluntary movements without proprioceptive feedback. Nat Neurosci 10:417-419.

Corradi-Dell'Acqua C, Hofstetter C, Vuilleumier P (2011) Felt and seen pain evoke the same local patterns of cortical activity in insular and cingulate cortex. J Neurosci 31:17996-18006.

Craig AD, Chen K, Bandy D, Reiman EM (2000) Thermosensory activation of insular cortex. Nat Neurosci 3:184-190.

Darley JM, Latane B (1968) Bystander intervention in emergencies: diffusion of responsibility. J Pers Soc Psychol 8:377-383.

de Vignemont F, Singer T (2006) The empathic brain: how, when and why? Trends Cogn Sci 10:435-441.

Decety J, Echols S, Correll J (2010) The blame game: the effect of responsibility and social stigma on empathy for pain. J Cogn Neurosci 22:985-997.

Desmurget M, Reilly KT, Richard N, Szathmari A, Mottolese C, Sirigu A (2009) Movement intention after parietal cortex stimulation in humans. Science 324:811-813.

Downar J, Mikulis DJ, Davis KD (2003) Neural correlates of the prolonged salience of painful stimulation. Neuroimage 20:1540-1551.

Eisenberg N (2000) Emotion, regulation, and moral development. Annu Rev Psychol 51:665-697.

Friedman J, Hastie T, Tibshirani R (2008) Sparse inverse covariance estimation with the graphical lasso. Biostatistics 9:432-441.

Friston KJ, Harrison L, Penny W (2003a) Dynamic causal modelling. Neuroimage 19:1273-1302.

Friston KJ, Harrison L, Penny W (2003b) Dynamic causal modelling. Neuroimage 19:1273-1302.

Gao YJ, Ji RR (2010) Targeting astrocyte signaling for chronic pain. Neurotherapeutics 7:482-493.

Gazzola V, Aziz-Zadeh L, Keysers C (2006) Empathy and the somatotopic auditory mirror system in humans. Curr Biol 16:1824-1829.

Gazzola V, Keysers C (2009a) The observation and execution of actions share motor and somatosensory voxels in all tested subjects: single-subject analyses of unsmoothed fMRI data. Cereb Cortex 19:1239-1255.

Gazzola V, Keysers C (2009b) The observation and execution of actions share motor and somatosensory voxels in all tested subjects: single-subject analyses of unsmoothed fMRI data. Cereb Cortex 19:1239-1255.

Gray K, Wegner DM (2012) Morality takes two: Dyadic morality and mind perception. In: The social psychology of morality: Exploring the causes of good and evil. Herzliya series on personality and social psychology. (Mikulincer M, Shaver PR, eds), pp 109-127. Washington, DC, US: American Psychological Association.

Gu X, Han S (2007) Attention and reality constraints on the neural processes of empathy for pain. Neuroimage 36:256-267.

Haggard P, Whitford B (2004) Supplementary motor area provides an efferent signal for sensory suppression. Brain Res Cogn Brain Res 19:52-58.

Hebert MA, Ardid D, Henrie JA, Tamashiro K, Blanchard DC, Blanchard RJ (1999) Amygdala lesions produce analgesia in a novel, ethologically relevant acute pain test. Physiol Behav 67:99-105.

Hein G, Silani G, Preuschoff K, Batson CD, Singer T (2010) Neural responses to ingroup and outgroup members' suffering predict individual differences in costly helping. Neuron 68:149-160.

Heldmann M, Russeler J, Munte TF (2008) Internal and external information in error processing. BMC Neurosci 9:33.

Hoffman ML (2000) Empathy and Moral Development: Implications for caring and Justice. Cambridge University Press.

Iannetti GD, Mouraux A (2010) From the neuromatrix to the pain matrix (and back). Exp Brain Res 205:1-12.

Jabbi M, Bastiaansen J, Keysers C (2008) A common anterior insula representation of disgust observation, experience and imagination shows divergent functional connectivity pathways. PLoS One 3:e2939.

Jabbi M, Swart M, Keysers C (2007) Empathy for positive and negative emotions in the gustatory cortex. Neuroimage 34:1744-1753.

Jackson PL, Rainville P, Decety J (2006) To what extent do we share the pain of others? Insight from the neural bases of pain empathy. Pain 125:5-9.

Jelasic F (1966) Relation of the lateral part of the amygdala to pain. Confin Neurol 27:53-55.

Johansson RS, Flanagan JR (2009) Coding and use of tactile signals from the fingertips in object manipulation tasks. Nat Rev Neurosci 10:345-359.

Jones EG, Coulter JD, Hendry SH (1978) Intracortical connectivity of architectonic fields in the somatic sensory, motor and parietal cortex of monkeys. J Comp Neurol 181:291-347.

Kawato M (1999) Internal models for motor control and trajectory planning. Curr Opin Neurobiol 9:718-727.

Keysers C, Gazzola V (2009) Expanding the mirror: vicarious activity for actions, emotions, and sensations. Curr Opin Neurobiol 19:666-671.

Keysers C, Kaas JH, Gazzola V (2010) Somatosensation in social perception. Nat Rev Neurosci 11:417-428.

Keysers C, Wicker B, Gazzola V, Anton JL, Fogassi L, Gallese V (2004) A touching sight: SII/PV activation during the observation and experience of touch. Neuron 42:335-346.

Koban L, Corradi-Dell'Acqua C, Vuilleumier P (2013) Integration of error agency and representation of others' pain in the anterior insula. J Cogn Neurosci 25:258-272.

Lamm C, Decety J, Singer T (2011) Meta-analytic evidence for common and distinct neural networks associated with directly experienced pain and empathy for pain. Neuroimage 54:2492-2502.

Lancaster JL, Laird AR, Eickhoff SB, Martinez MJ, Fox PM, Fox PT (2012) Automated regional behavioral analysis for human brain images. Front Neuroinform 6:23.

Lancaster JL, Woldorff MG, Parsons LM, Liotti M, Freitas CS, Rainey L, Kochunov PV, Nickerson D, Mikiten SA, Fox PT (2000) Automated Talairach atlas labels for functional brain mapping. Hum Brain Mapp 10:120-131.

London BM, Miller LE (2013) Responses of somatosensory area 2 neurons to actively and passively generated limb movements. J Neurophysiol 109:1505-1513.

Luppino G, Matelli M, Camarda R, Rizzolatti G (1993) Corticocortical connections of area F3 (SMA-proper) and area F6 (pre-SMA) in the macaque monkey. J Comp Neurol 338:114-140.

Maldjian JA, Laurienti PJ, Kraft RA, Burdette JH (2003) An automated method for neuroanatomic and cytoarchitectonic atlas-based interrogation of fMRI data sets. Neuroimage 19:1233-1239.

Marrelec G, Krainik A, Duffau H, Pelegrini-Issac M, Lehericy S, Doyon J, Benali H (2006) Partial correlation for functional brain interactivity investigation in functional MRI. Neuroimage 32:228-237.

Mathalon DH, Whitfield SL, Ford JM (2003) Anatomy of an error: ERP and fMRI. Biol Psychol 64:119-141.

Meffert H, Gazzola V, den Boer JA, Bartels AA, Keysers C (2013) Reduced spontaneous but relatively normal deliberate vicarious representations in psychopathy. Brain 136:2550-2562.

Mesulam MM, Mufson EJ (1982a) Insula of the old world monkey. I. Architectonics in the insulo-orbito-temporal component of the paralimbic brain. J Comp Neurol 212:1-22.

Mesulam MM, Mufson EJ (1982b) Insula of the old world monkey. III: Efferent cortical output and comments on function. J Comp Neurol 212:38-52.

Michl P, Meindl T, Meister F, Born C, Engel RR, Reiser M, Hennig-Fast K (2012) Neurobiological underpinnings of shame and guilt: a pilot fMRI study. Soc Cogn Affect Neurosci.

Monfardini E, Gazzola V, Boussaoud D, Brovelli A, Keysers C, Wicker B (2013) Vicarious neural processing of outcomes during observational learning. PlosOne Accpeted.

Mouraux A, Diukova A, Lee MC, Wise RG, Iannetti GD (2011) A multisensory investigation of the functional significance of the "pain matrix". Neuroimage 54:2237-2249.

Moya-Albiol L, Herrero N, Bernal MC (2010) The neural bases of empathy. Rev Neurol 50:89-100.

Mufson EJ, Mesulam MM (1982) Insula of the old world monkey. II: Afferent cortical input and comments on the claustrum. J Comp Neurol 212:23-37.

Narita M, Kaneko C, Miyoshi K, Nagumo Y, Kuzumaki N, Nakajima M, Nanjo K, Matsuzawa K, Yamazaki M, Suzuki T (2006) Chronic pain induces anxiety with concomitant changes in opioidergic function in the amygdala. Neuropsychopharmacology 31:739-750.

Packard MG, Knowlton BJ (2002) Learning and memory functions of the Basal Ganglia. Annu Rev Neurosci 25:563-593.

Penny WD, Stephan KE, Daunizeau J, Rosa MJ, Friston KJ, Schofield TM, Leff AP (2010) Comparing families of dynamic causal models. PLoS Comput Biol 6:e1000709.

Poldrack RA (2006) Can cognitive processes be inferred from neuroimaging data? Trends Cogn Sci 10:59-63.

Pons TP, Kaas JH (1986) Corticocortical connections of area 2 of somatosensory cortex in macaque monkeys: a correlative anatomical and electrophysiological study. J Comp Neurol 248:313-335.

Rainville P, Duncan GH, Price DD, Carrier B, Bushnell MC (1997) Pain affect encoded in human anterior cingulate but not somatosensory cortex. Science 277:968-971.

Ramnani N (2012) Frontal lobe and posterior parietal contributions to the cortico-cerebellar system. Cerebellum 11:366-383.

Rouwette T, Vanelderen P, Roubos EW, Kozicz T, Vissers K (2012) The amygdala, a relay station for switching on and off pain. Eur J Pain 16:782-792.

Rozzi S, Calzavara R, Belmalih A, Borra E, Gregoriou GG, Matelli M, Luppino G (2006) Cortical connections of the inferior parietal cortical convexity of the macaque monkey. Cereb Cortex 16:1389-1417.

Schippers MB, Renken R, Keysers C (2011) The effect of intra- and inter-subject variability of hemodynamic responses on group level Granger causality analyses. Neuroimage 57:22-36.

Sewards TV, Sewards MA (2002) The medial pain system: neural representations of the motivational aspect of pain. Brain Res Bull 59:163-180.

Shamay-Tsoory SG (2011) The neural bases for empathy. Neuroscientist 17:18-24.

Shane MS, Stevens M, Harenski CL, Kiehl KA (2008) Neural correlates of the processing of another's mistakes: a possible underpinning for social and observational learning. Neuroimage 42:450-459.

Singer T, Seymour B, O'Doherty J, Kaube H, Dolan RJ, Frith CD (2004) Empathy for pain involves the affective but not sensory components of pain. Science 303:1157-1162.

Singer T, Seymour B, O'Doherty JP, Stephan KE, Dolan RJ, Frith CD (2006) Empathic neural responses are modulated by the perceived fairness of others. Nature 439:466-469.

Smith SM, Miller KL, Salimi-Khorshidi G, Webster M, Beckmann CF, Nichols TE, Ramsey JD, Woolrich MW (2011) Network modelling methods for FMRI. Neuroimage 54:875-891.

Stephan KE, Penny WD, Moran RJ, den Ouden HE, Daunizeau J, Friston KJ (2010) Ten simple rules for dynamic causal modeling. Neuroimage 49:3099-3109.

Taylor SF, Stern ER, Gehring WJ (2007) Neural systems for error monitoring: recent findings and theoretical perspectives. Neuroscientist 13:160-172.

Theodore M.Singelis (1994) The Measurement of Independent and Interdependent Self-Construals. Pers Soc Psychol Bull 20:580-591.

Ullsperger M, von Cramon DY (2003) Error monitoring using external feedback: specific roles of the habenular complex, the reward system, and the cingulate motor area revealed by functional magnetic resonance imaging. J Neurosci 23:4308-4314.

Vogt BA, Sikes RW (2000) The medial pain system, cingulate cortex, and parallel processing of nociceptive information. Prog Brain Res 122:223-235.

Weber DJ, London BM, Hokanson JA, Ayers CA, Gaunt RA, Torres RR, Zaaimi B, Miller LE (2011) Limb-state information encoded by peripheral and central somatosensory neurons: implications for an afferent interface. IEEE Trans Neural Syst Rehabil Eng 19:501-513.

Weiller C, Juptner M, Fellows S, Rijntjes M, Leonhardt G, Kiebel S, Muller S, Diener HC, Thilmann AF (1996) Brain representation of active and passive movements. Neuroimage 4:105-110.

Wicker B, Keysers C, Plailly J, Royet JP, Gallese V, Rizzolatti G (2003) Both of us disgusted in My insula: the common neural basis of seeing and feeling disgust. Neuron 40:655-664.

Wolpert DM, Flanagan JR (2001) Motor prediction. Curr Biol 11:R729-R732.

Wolpert DM, Ghahramani Z (2000) Computational principles of movement neuroscience. Nat Neurosci 3 Suppl:1212-1217.

Wolpert DM, Miall RC (1996) Forward Models for Physiological Motor Control. Neural Netw 9:1265-1279.

Does Monetary Compensation for physical pain buffer empathic response or induce jealousy?

Fang Cui[1,2], Judith Suttrup[1] , Christian Keysers[2,1], Valeria Gazzola[1,2*]

1 Department of Neuroscience, University Medical Center Groningen, University of Groningen

2 Netherlands Institute for Neuroscience, Royal Netherlands Academy for Arts and Sciences, Amsterdam

Abstract

Money has been widely used as compensation for physical pain and injury. In the current study, we compare the subjective reports of participants that observe the pain of a victim with or without getting monetary compensation. Results were twofold. First, observers attribute less unpleasantness to victims that received money for a painful shock. Second, observers themselves, felt more unpleasant when victims received money for a non-painful shock, possibly reflecting jealousy. These results provide novel insights into the social impact of monetary compensation to victims.

Introduction

When you see a man break his arm during work you may feel bad for him. But if you hear that he is entitled to 5000 Euro compensation, you may feel better. Similar situation often happen in our 'insured' societies. Money is the most common token used to compensate the physical pain of victims. The aim of such compensation is primarily to help the victim. However, a question that has received little attention is what impact such compensation would have on witnesses of the incident. Would the compensation change how witnesses would feel about the incident? Empathy is the ability to experience and understand what others feel while being aware of the external source of emotions(Jackson et al., 2005). Studies show that empathy for others' pain is a flexible phenomena which can be modulated by many social factors, for example, the relationship between the observer and the pain-taker(Meyer et al., 2012) , if the observer likes the pain-taker or not (Singer et al., 2006b), if the other's pain is in the focus of the observer's attention (Fan and Han, 2008), if the pain-taker and the observer are of the same race (Avenanti et al., 2010;Forgiarini et al., 2011); and so on (Decety et al., 2010b;Li and Han, 2010). Money is powerful, not only economically but also psychologically. Studies found that money can decrease physical pain (Zhou et al., 2009;Vohs, 2010;Vohs et al., 2006), but would money also influence empathy for pain? One fMRI study supports this idea by finding that the empathic response towards rich people is reduced compared to the response towards people that are not rich(Guo et al., 2011).

In the present study we tested the effect of monetary compensation to a victim on empathy for that victim's pain. In the experimental setup an observer witnessed another person (the pain-taker) receiving painful or non-painful electrical shocks. Independently of the intensity of the shock, the pain-taker received monetary compensation in half the trials. The dependent variables were four subjective ratings given by the observer: Two relate to the observers perception of the experience of the pain-taker, and include (1) the pain intensity and (2) the unpleasantness the observer perceives the pain-taker to have experienced; two relate to the observer's own emotional state, and include 3) the observer's emotional arousal and 4) the unpleasantness the observer experienced while witnessing the pain. Our main hypothesis is that the effect of the monetary compensation on empathy will demonstrate itself in the observer's ratings of the pain-taker's experienced unpleasantness.

Materials and Method

Participants

Data were collected from 37 right-handed Chinese participants who reported no history of neurological or psychiatric disorders (19 female, ages: 26.3+4.6 s.d.). All participants were healthy, right-handed, had no history of neurological or psychiatric disorders, and provided written informed consent. This study was approved by the Ethics Committee of the University of Amsterdam, the Netherlands. Only Chinese participants were chosen, because the movies were of the first author (FC), who is Chinese, and empathy is known to depend on whether observer and pain-taker belong to the same race(Avenanti et al., 2010), with the most ecologically frequent condition being one in which observer and pain-taker are of the same race.

Experimental Procedures

Stimuli

Video clips showing a female Chinese adult (author FC) receiving an electrical stimulation on the back of her right hand were used as visual stimuli. There were two categories of videos, with 25 different takes of each. Painfull (P+) videos showing the pain-taker receive a painful stimulation and non-Painfull (P-) videos showing the pain-taker receive a non painful but detectable stimulation. Each video lasts 1500ms. The pain-taker's upper body with her right hand resting on a desk with electrodes attached on it and her facial expression during the applying of stimulation were clearly visible. Her eyes were fixed on her hand direction.

We chose electrical stimulation to induce physical pain - a commonly used approach in empathy research (Singer et al., 2004a;Singer et al., 2006b;Hein et al., 2010). The electrical stimulation we used was a 100 HZ train of electrical pulses of 4 ms pulse duration delivered by a bipolar concentric surface electrode (stimulation areas:16mm2). Each stimulus lasted 500ms. The intensity of the stimulation was modulated by changing current intensity. The range of the current intensity was from 0.2 mA to 6.0 mA.

Before the recording of the videos we measured the pain threshold of FC (the pain-taker in the videos). We started from a 0.2 mA current that was then increased until maximally 6.0 mA in 0.1 mA steps. She was instructed to evaluate how painful the stimulation was on a 10-point scale. We then chose the current corresponding to a rating of 8 for P+ and of 2 for P- videos. The current selected was 2.6mA (P+) and 1.2mA (P-). During the recording, we applied the two selected levels 25 times each randomly. There is a 10 to 15 seconds interval between each stimulus in order to minimize the influence of repetition. The videos were cut into 1500 ms clips including the starting and ending point of the 500 ms electrical stimulation.

In order validate the videos we recruited 12 participants to evaluate the videos. All these validators did not participate in the main experiment. In the validation, each participant observed all 50 videos in random order and rated the intensity of the pain F.C felt in the movie on a 1 to 9 scale. Results showed that the participants rated the P+ videos significantly higher than the P- videos (Mean (P+) = 7.5±0.32 s.e, Mean(P-)=2.12±0.56 s.e.; $p<0.001$). The average rating was thus also quite close to the actual experience of FC.

Experimental Setup

A confederate design was used. The participant was informed that he/she would be paired with another participant and there were two roles in the study: the "observer "and the "pain-taker". The pain-taker would receive the electrical stimulation and the observer would see video showing the pain-taker receiving the stimulation and then evaluate the videos. He/she was told that the roles would be decided randomly by drawing

lots on the experimental day. Author FC was actually the 'other participant' and during the lots were manipulated so that FC always was assigned to the pain-taker role and the real participant to the observer role.

After deciding the roles FC was placed in the "Electrical stimulation space" and the real participant in the "Evaluation space". The two spaces were in the same room separated by an opaque barrier (Figure 1). The real participant was misled to believe that FC would receive electrical stimulation during the experiment and he/she would observe it on the monitor of the Computer_B connected with the video camera placed in front of FC to create a CCTV. Actually, the real participant would be shown the pre-recorded videos described above. FC's clothes and hair style matched her appearance in the video and the participant wore earplugs so that the silence of the pain-taker during the electrical stimulation won't cause suspicion.

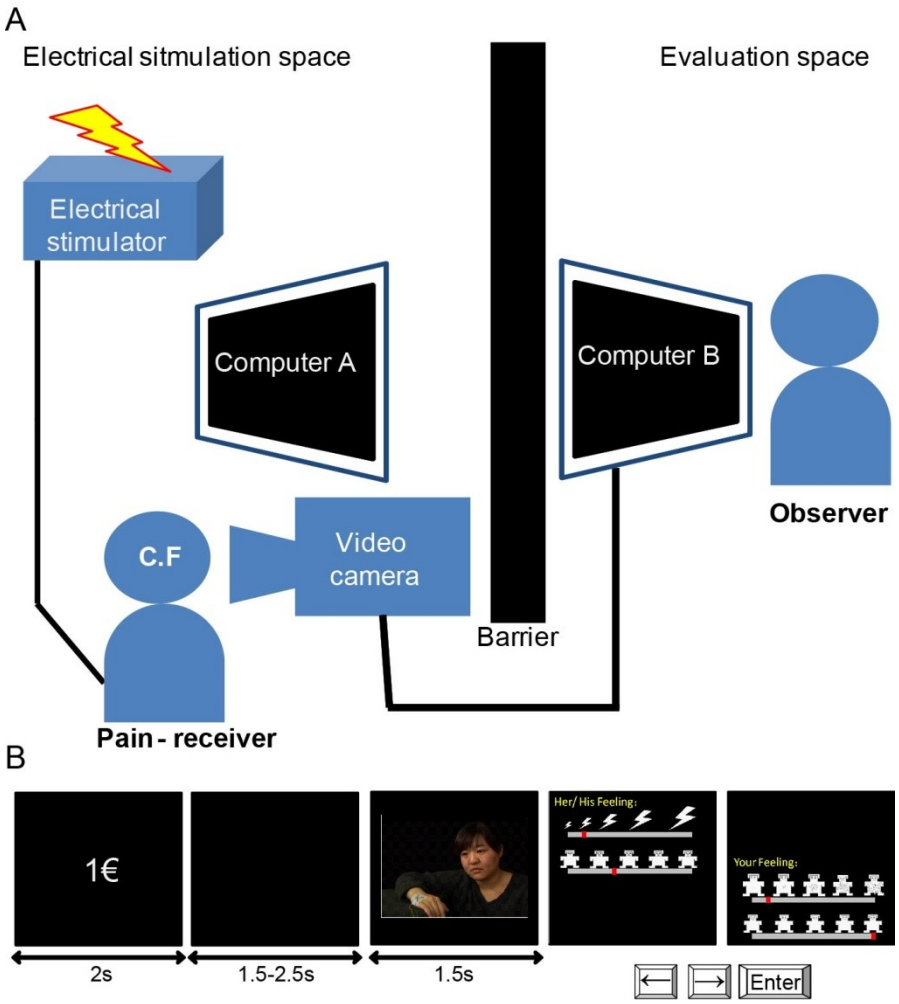

Figure 1. Experimental Setup The Observer (the real participant) and the Pain-taker (confederate CF) were seated in two space "Electical stimulation space" and "Evaluation space", separated by an opaque divider. The pain-taker's right hand was attached to an electrical stimulator and a video camera was pointed towards the pain-taker and connected to the computer facing the Observer. During the study, the Observer saw videos showing the Pain-taker receiving shocks on the computer in front of the observer (Computer B). The observer was lead to believe that this was a life video-feed from the camera, but in reality, they were prerecorded movies. Both participants saw the monetary information before each shock on their respective computer.

Experimental design

This study is a 2x2 within-subject design. The first factor is the painfulness of the stimulation to the pain-taker (P+/P-). The second factor is Monetray Compensation (€+/€-): in half the trials of each painfulness, the pain-taker (supposedly) received either 1€ (€+) or 0€ (€-) for the electrical stimulation. In each trial, the real participant first saw the monetary information on the monitor. If he/she saw a "1€" the pain-taker will be paid 1€ for the following stimulation no matter whether it was painful or not. If he/she saw a "0€" the pain-taker will not be paid for the following stimulation. The observer was informed that the pain-taker would see the monetary information on Computer_A before each stimulus, which meant that the participant thought that the pain-taker knew whether she would or not receive money for the shock while experiencing the shock. The monetary information lasted 2 s and after a 1.5 to 2.5s interval, a video showing the pain-taker receiving an electrical stimulation displayed on Computer B. The observer was told to watch the video carefully and to answer questions afterwards.

There were four conditions in this design differing in what the pain taker received: (A) P+€+: a painful stimulation and 1€; (B) P+€-: a painful stimulation and 0€; (C)P-€+; a non-painful stimulation and 1€; (D) P-€-: a non-painful stimulation and 0€. Each condition was repeated in 25 trials leading to a total of 100 trials. The trials were divided into 4 runs. The four conditions appeared in random order. The participants had 2 minutes rest between runs.

Data Collecting

Evaluation Scales

There were four questions about each video that the observers had to answer on a numeric rating scale.

(1) Two about what they perceived the pain-taker to have experienced: (a) "How painful was the stimulus for the pain-taker?", from 1 (very weak feeling) to 9 (very strong painful feeling) and (b) "How does this stimuli make the pain-taker feel?", from 1 (makes her/him feel very pleasant) to 9 (makes him/her feel very unpleasant).

(2) Two self-oriented questions: (c) "How alert/aroused did this scene make you feel?" from 1 (makes me want to sleep) to 9 (draws a lot of attention and makes me feel strongly influenced). (d) "How was your experience of watching this scene?" from 1 (makes me feel very pleasant) to 9 (makes me feel very unpleasant).

The two categories of questions appeared in a random order for each trail. The observer was instructed to answer fast and honestly.

Questionnaires

All participants were asked to fill out the Davis's Interpersonal reactivity Index(Davis, 1980;Davis, 1983), Money Attitude Scale(Yamauchi and Templer, 1982) and a feedback questionnaire including 10 questions after the task(See the Feedback Questionaire attached). In the feedback questionnaire all questions were stated as a declarative sentence. The participants answered them by rating on a 7 point scale from "strongly disagree "to "strongly agree". The questions were mainly about how the participants felt during the experiment.

Data Analysis

Because the answers to the four questions after each movie were not normally distributed, for further analysis, the non-parametric Wilcoxon paired test was used. Then, for question (b) and question (d) we subtracted a value of 4.5 from all rating values to simplify the interpretation of the value, with zero now representing a neutral, and positive values unpleasantness. Statistical tests were applied to all conditions separately for all four questions. Correction for repeated measurement was used. Pearson correlation is used here. To explore the impact of

individual differences, the IRI and MAS scores were correlated (pearson) with the difference between ratings in P+€+ and P+€- and between P-€+ and P-€-.

Result

For all four categories we found higher rating in P+ than in P- conditions ($p<0.001$). Hence, the pain-taker in P+ videos was perceived to experience the shock as more intense and unpleasant than in P- videos, and seeing the P+ movies made the observer feel more aroused and more unpleasant.

In question (a), rating in P+€+ condition (Mdn=6.19) was higher than rating in P-€+ (Mdn=1.48) ($z=-5.304$, $p<0.001$, $r=-0.17$); rating in P+€- (Mdn=6.18) condition was higher than rating in P-€- (Mdn=1.7) ($z=-5.303$, $p<0.001$, $r=-0.17$). In question (b), rating in P+€+ condition (Mdn=1.5) was higher than rating in P-€+ (Mdn=-0.34) ($z=-5.107$, $p<0.001$, $r=-0.17$); rating in P+€- condition (Mdn=1.6) was higher than rating in P-€- (Mdn=-0.43) ($z=-5.243$, $p<0.001$, $r=-0.17$). In question (c), rating in P+€+ condition (Mdn=6.5) was higher than rating in P-€+ (Mdn=2.6) ($z=-5.303$, $p<0.001$, $r=-0.17$); rating in P+€- condition (Mdn=6.23) was higher than rating in P-€- (Mdn=2.41) ($z=-5.288$, $p<0.001$, $r=-0.17$). In question (d), rating in P+€+ condition (Mdn=1.27) was higher than rating in P-€+ (Mdn=-0.23) ($z=-3.677$, $p<0.001$, $r=-0.12$); rating in P+€- condition (Mdn=1.82) was higher than rating in P-€- (Mdn=-0.35) ($z=-4.177$, $p<0.001$, $r=-0.14$).

The result supported our hypothesis: monetary compensation reduced the observer's perception of how unpleasant the pain-taker felt. The rating of the pain-taker's unpleasantness in P+€+ condition (Mdn=1.50) was significantly lower than P+€- condition (Mdn=1.60) ($z=-1.696$, $p<0.05$, one-tailed, $r=-0.06$).

Unexpectedly, the monetary compensation of non-painful shocks triggered an increase in self-unpleasantness in the observers: observers reported that the P-€+ movies made them feel less pleasant (Mdn=-0.23) than P-€- (Mdn=-0.35) ($z=-4.421$, $p<0.001$, $r=-0.15$). And the difference of rating on these two conditions (P-€+-P-€-) was positively correlated with the jealousy rating in the feedback questionnaire($r=0.42$, $p<0.001$). This result showed that observers felt worse when the pain-taker received money for a non-painful stimulation than when the pain-taker did not receive money for that non-painful stimulation. This effect was positively correlated with the intensity of jealousness the observers felt for the pain-taker.

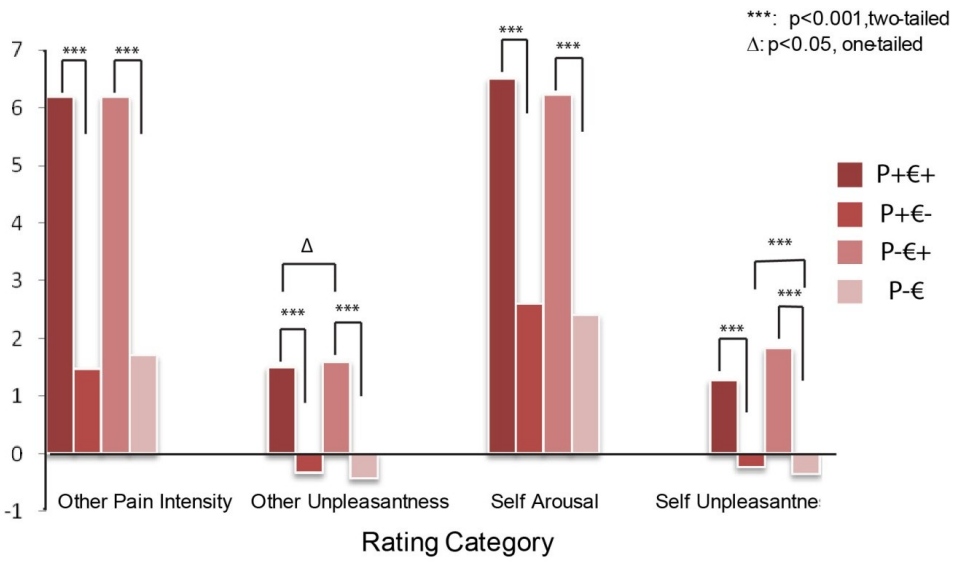

Figure 2. Main Results There was a very clear effect of painfulness of stimulation on all four questions: P+ movies lead to significantly higher ratings than P- conditions (***: $p<0.001$, two-tailed) in all cases. The effect of monetary compensation was more subtle and restricted, with only two significant differences. First, monetary compensation reduced other-unpleasantness

for painful electroshocks ("Other Unpleasantness" rating, P+€+ is significantly lower than P+€-, △: $p<0.05$, one-tailed). Second, in the "Self Unpleasantness" rating, P-€+ is significantly higher than P-€- ($p<0.001$, two-tailed). Note that for questions (b) and (d), a rating above zero indicated unpleasantness. The bars show the Median of all the ratings. And the positive error bars shows the (third quartile- median) and the negative error bars show the (median-first quartile).

Discussion

Our result supports the idea that the monetary compensation commonly used to help victims also has a social function: it reduces, in the eye of observers of the incident, how unpleasant the event must be for the victim. So, if observers know that a victim was insured, and receives compensation for its damage, the observer will be left with the feeling that things are a little less unpleasant for the victim. We also found that when a 'victim' turned out not to receive a painful shock, but a painless one, monetary compensation made the observer feel worse about the event. This might reflect a kind of jealousy for gains that the victim did not really 'earn' through pain.

Monetary Compensation reduce perceived unpleasantness of pain

Pain is an experience including physiological and psychological aspects (Kut et al., 2007) .The subjective feelings of physical pain are not necessarily the same for the same person each time. It can be influenced by psychological factors like: mood (Villemure and Bushnell, 2009a;Loggia et al., 2008) , attention (Cioffi and Holloway, 1993;de and Verbaten, 2001;Villemure and Bushnell, 2009b) and self-perception (Roy et al., 2011;Kut et al., 2007). Studies show that physical pain increases the desire for money; money loss exacerbates physical pain and even only the idea of money can ease physical pain (Vohs, 2010;Zhou et al., 2009;Rohling et al., 1995). Money enables people to obtain resource from the social system and gives them the feeling of strength and self-sufficiency, thereby reducing the aversive feelings induced by physical pain (Zhou et al., 2009). An fMRI study found that people shows less empathy to rich people compared to less rich people, providing evidence that money can also influence empathy for pain (Guo et al., 2011). Here we wanted to investigate if the widely-used monetary compensation for suffering that is part of our legal system and insurance culture, would also serve a social purpose by influencing how bystanders perceive the distress of a victim. We found that when observers are informed that the pain-taker will be compensated with money for a painful event the observer rates the unpleasantness experienced by the pain-taker as reduced compared to conditions without compensation. Importantly, this reduction of perceived unpleasantness occurred although the actual victim, in the movies, was not really receiving any compensation, and was blind, during movie recording, to whether that trial would include monitory compensation or not. The perceived reduction of unpleasantness therefore cannot be driven by changes in the reaction of the victim, but derives from the observer's belief about the presence of a monetary compensation alone. Importantly, the perceived intensity of the stimulation was not affected by the monetary compensation, suggesting that observers still perceive that the victim is experiencing an intense nociceptive stimulus, but discount the affective unpleasantness that the victim must have experienced. Our data cannot directly speak to how monetary compensation specifically reduces perceived unpleasantness. A possibility might however be, that physical pain normally reduces fitness, and that would cause psychological distress. Money allows buying resources that could compensate this loss of fitness, and would thus alleviate the distress caused by worring about resources. Our study is the first one to directly show that monetary compensation for a specific painful event reduces perceived unpleasantness. In the only similar study we are aware of,(Guo et al., 2011), it had been shown that empathy is reduced if a person receives a very substantial lump sum, that makes that person 'rich'. The richness then becomes a characteristic of the victim, not of the specific incident. By having a design in which the same victim sometimes receives and sometimes does not receive compensation for a shock, we study a related but different effect, that measures the impact of compensation on a specific event, while keeping the status of the victim constant. Notice that our result only prove that monetary compensation can buffers the perceived unpleasantness of other people's painful experiences, but the neurobiological mechanism

remains unclear. Further neuroscience researches including brain imaging techniques need to be done on the basis of this behavioral result (and we are currently undertaking this research). An interesting finding in this regard is that the observers report perceiving the victim as experiencing less unpleasantness if a painful shock was compensated compared with the same shock uncompensated, but that this did not entirely translate into a change of how unpleasant the observer's felt while witnessing these events (self-unpleasantness).

No pain, no gain: "Undeserved" monetary compensation triggers jealousy

An unexpected result is that when the pain-taker receives 1€ for a non-painful stimulus the observer felt worse about the event, than if the pain-taker did not receive money for this non-painful stimulus. It is important to note, that in terms of median ratings, observers reported feeling slightly positive whenever the pain-taker turned out not to get a painful shock, but that this positive affect was reduced, if the 'spared' victim received money. Studies show that human beings are extremely sensitive to social comparison. For instance, they not only care about absolute values of money but the relative value of money, which is decided by the social context (Dvash et al., 2010). When people think there is a unfairness or the other does not deserve certain monetary contributions they are even willing to pay to reduce other people's earnings out of jealousy, an effect sometimes called the "Envious Brain" (Andrew J.Oswald and Daniel J.Zizzo, 2001). Envy or jealousy is defined as a subjectively unpleasant emotion that can arise in response to social comparison with advantaged others in domain of personal relevance. It is experienced as a complex mix of unpleasant psychological states (Hill et al., 2011;Takahashi et al., 2009a;Shamay-Tsoory et al., 2007). In the context of this study, the observers believed that the pain-taker was paid by randomized monetary compensation per stimulus and the observers were paid simply on the basis of how long they participate in the study. In total, the observers' were led to believe that they received less money than the pain-taker (Actually, the pain-taker didn't receive any payment as a confederate, but participants do not know that). When the pain-taker received 1€ for a non-painful stimulus, the money was not a compensation for suffering and was thus not 'earned'. We assume that from a social comparison perspective, the observer might resent the pain-taker's opportunity to make money without painfulness. This would be less the case, in trials in which the pain-taker suffered, which is why we believe this effect to have been specific to the non-painful condition. The positive correlation between the self-unpleasantness rating and the jealousy rating in the feedback questionnaire gives further support to associating this effect with jealousy.

References Cited

Andrew J.Oswald, Daniel J.Zizzo (2001) Are People Willing to Pay to Reduce Others'Incomes? Annales d'Economie et de Statistique04.

Avenanti A, Sirigu A, Aglioti SM (2010) Racial bias reduces empathic sensorimotor resonance with other-race pain. Curr Biol 20:1018-1022.

Cioffi D, Holloway J (1993) Delayed costs of suppressed pain. J Pers Soc Psychol 64:274-282.

Davis MH (1980) A multidimensional approach to individual differences in empathy. JSAS Catalog of Selected Documents in Psychology 10.

Davis MH (1983) Measuring individual differences in empathy: Evidence for a multidimensional approach. Journal of Personality and Social Psychology 44:113-126.

de WM, Verbaten MN (2001) Affective pictures processing, attention, and pain tolerance. Pain 90:163-172.

Decety J, Echols S, Correll J (2010) The blame game: the effect of responsibility and social stigma on empathy for pain. J Cogn Neurosci 22:985-997.

Dvash J, Gilam G, Ben-Ze'ev A, Hendler T, Shamay-Tsoory SG (2010) The envious brain: the neural basis of social comparison. Hum Brain Mapp 31:1741-1750.

Fan Y, Han S (2008) Temporal dynamic of neural mechanisms involved in empathy for pain: an event-related brain potential study. Neuropsychologia 46:160-173.

Forgiarini M, Gallucci M, Maravita A (2011) Racism and the empathy for pain on our skin. Front Psychol 2:108.

Guo X, Zheng L, Zhang W, Zhu L, Li J, Wang Q, Dienes Z, Yang Z (2011) Empathic neural responses to others' pain depend on monetary reward. Soc Cogn Affect Neurosci.

Hein G, Silani G, Preuschoff K, Batson CD, Singer T (2010) Neural responses to ingroup and outgroup members' suffering predict individual differences in costly helping. Neuron 68:149-160.

Hill SE, DelPriore DJ, Vaughan PW (2011) The cognitive consequences of envy: attention, memory, and self-regulatory depletion. J Pers Soc Psychol 101:653-666.

Jackson PL, Meltzoff AN, Decety J (2005) How do we perceive the pain of others? A window into the neural processes involved in empathy. Neuroimage 24:771-779.

Kut E, Schaffner N, Wittwer A, Candia V, Brockmann M, Storck C, Folkers G (2007) Changes in self-perceived role identity modulate pain perception. Pain 131:191-201.

Li W, Han S (2010) Perspective taking modulates event-related potentials to perceived pain. Neurosci Lett 469:328-332.

Loggia ML, Mogil JS, Bushnell MC (2008) Experimentally induced mood changes preferentially affect pain unpleasantness. J Pain 9:784-791.

Meyer ML, Masten CL, Ma Y, Wang C, Shi Z, Eisenberger NI, Han S (2012) Empathy for the social suffering of friends and strangers recruits distinct patterns of brain activation. Soc Cogn Affect Neurosci.

Rohling ML, Binder LM, Langhinrichsen-Rohling J (1995) Money matters: A meta-analytic review of the association between financial compensation and the experience and treatment of chronic pain. Health Psychol 14:537-547.

Roy M, Lebuis A, Peretz I, Rainville P (2011) The modulation of pain by attention and emotion: a dissociation of perceptual and spinal nociceptive processes. Eur J Pain 15:641-10.

Shamay-Tsoory SG, Tibi-Elhanany Y, Aharon-Peretz J (2007) The green-eyed monster and malicious joy: the neuroanatomical bases of envy and gloating (schadenfreude). Brain 130:1663-1678.

Singer T, Seymour B, O'Doherty J, Kaube H, Dolan RJ, Frith CD (2004) Empathy for pain involves the affective but not sensory components of pain. Science 303:1157-1162.

Singer T, Seymour B, O'Doherty JP, Stephan KE, Dolan RJ, Frith CD (2006) Empathic neural responses are modulated by the perceived fairness of others. Nature 439:466-469.

Takahashi H, Kato M, Matsuura M, Mobbs D, Suhara T, Okubo Y (2009) When your gain is my pain and your pain is my gain: neural correlates of envy and schadenfreude. Science 323:937-939.

Villemure C, Bushnell MC (2009a) Mood influences supraspinal pain processing separately from attention. J Neurosci 29:705-715.

Villemure C, Bushnell MC (2009b) Mood influences supraspinal pain processing separately from attention. J Neurosci 29:705-715.

Vohs KD (2010) The mere thought of money makes you feel less pain. Harv Bus Rev 88:28-29.

Vohs KD, Mead NL, Goode MR (2006) The psychological consequences of money. Science 314:1154-1156.

Yamauchi KT, Templer DJ (1982) The development of a Money Attitude Scale. J Pers Assess 46:522-528.

Zhou X, Vohs KD, Baumeister RF (2009) The symbolic power of money: reminders of money alter social distress and physical pain. Psychol Sci 20:700-706.

Supplementary Materials

Feedback Questionnaire

Below you will find some statements about your feelings towards the study. Please indicate how well these statements describe you by choosing the appropriate answer from the scale at the top of the page. READ EACH ITEM CAREFULLY BEFORE RESPONDING. Answer as honestly as you can. Thank you.

		Strongly disagree	Disagree	Somewhat disagree	Neither agree nor disagree	Somewhat agree	Agree	Strongly agree
1.	You felt sleepy during the study.	□	□	□	□	□	□	□
2.	You thought it was unfair that the other participant received more money than you did.	□	□	□	□	□	□	□
3.	You felt uncomfortable when you saw the other person getting painful stimulation.	□	□	□	□	□	□	□
4.	You think the experimental setup was realistic enough to believe it.	□	□	□	□	□	□	□
5.	You feel relieved when you know that nobody really got electrical stimulation during the study.	□	□	□	□	□	□	□
6.	You feel angry because you were misled in the study for scientific reasons.	□	□	□	□	□	□	□
7.	You had strong physically painful experiences in the past.	□	□	□	□	□	□	□
8.	You would like to ask your friends to attend our study.	□	□	□	□	□	□	□
9.	You feel unhappy because of the study.	□	□	□	□	□	□	□
10.	You liked the experience of participating in this study	□	□	□	□	□	□	□

Future implications

How our brains differentiate self-generated actions and other-generated actions has been studied using different technologies, like SEP, PET and fMRI. But no consistent conclusion has been drawn from these results. One reason could be that the difference in regional brain activation is spatially too small and temporally too short to be detect (Weiller et al., 1996b). It has been suggested that it would be helpful to differentiate active and passive conditions as much as possible in the tasks to ensure that the participant does not imagine or accidently executes actions during the passive condition. One method used in the study in Chapter 2 is to train the participant to achieve minimal EMG signal using EMG feedback before the task. Secondly, instead of simply comparing active movement and passive movement conditions, we quantified EMG in each trial to better account for variance in motor signals across and within conditions. We hope that this approach might be helpful not just for our own study that allowed us to detect motor modulations of BA2 activity but also for future experiments in the field.

In the studies focused on the mirror neuron system, two main techniques have been used: EEG and fMRI. Mu-suppression and shared voxels are used as indices of the activity of the mirror neuron system in these two different techniques(for mu-suppression studies, see: (Pineda et al., 2000;Oberman et al., 2005;Southgate et al., 2009;Perry et al., 2011;Muthukumaraswamy and Johnson, 2004;Muthukumaraswamy et al., 2004)); (for sVx studies see: (Dinstein et al., 2007;Gazzola and Keysers, 2009b;Grezes et al., 2003;Iacoboni and Mazziotta, 2007). Do these two indices measure activity in the same set of brain regions? The result from our second study shows that μ-suppression is a valid indicator of MNS activity in BA2, IPL and dPM, but not in BA44. We hope that this finding will help bridge the gap that had existed between experiments using these two different techniques by providing empirical evidence for their common neural basis.

The interpersonal faculties of human beings, especially our ability to cooperate and understand others, strongly support our species' success in cross-species competition with animals faster, stronger and bigger than us (Zaki and Ochsner, 2012). These abilities are supported by empathy (Preston and de Waal, 2002;Decety, 2011;Hoffman, 1977;Eisenberg, 2007;Hoffman, 2000). For the past two decades, neuroscientists have devoted substantial effort to investigate the neural bases of human empathy. The "shared network" theory states that overlapping neural systems are activated when a person executes an action, feels an emotion or sensation and observes another person doing the same action, feeling the same emotion or sensation, respectively. Thereby, the observer could understand how the executer feels and predict future behaviour accordingly (Wicker et al., 2003;Jabbi et al., 2007;Gazzola and Keysers, 2009b;Keysers et al., 2004;Singer et al., 2004b;Corradi-Dell'Acqua et al., 2011) In action perception, voxels in brain areas including PM, IPL, IFG are found to activated during both first hand action execution and second hand action perception, these regions form the MNS in human brain(Iacoboni et al., 2005;Dinstein et al., 2007;Grezes et al., 2003;Gazzola and Keysers, 2009b;Arnstein et al., 2011) Also for sensation perception and experiences sVx have been reported(Blakemore et al., 2005;Ebisch et al., 2008;Keysers et al., 2004). For others' emotion like disgust and pain, studies also found that AI are activated during both first hand and second hand disgust experience (Wicker et al., 2003); AI and ACC are constantly activated during first hand and second hand pain across different experimental paradigms and stimuli (Corradi-Dell'Acqua et al., 2011;Singer et al., 2004b;Lamm et al., 2011;Fan et al., 2011).

Human beings empathize with others often, but not always. Whether we will empathize with others and how much we will empathize heavily depends on many factors (see reviews: (Engen and Singer, 2012;Singer and Lamm, 2009;Hein and Singer, 2008;de Vignemont and Singer, 2006)). The modulation of empathy for pain has been extensively studied. However, most of these studies suffer from a big pitfall: Artificiality. By "Artificiality" I

mean the artificial stimuli and artificial contextual setups. In nearly all paradigms, the stimuli used are either a cue indicating a person is receiving painful stimuli (Singer et al., 2004b;Singer et al., 2006a;Bird et al., 2010;Hein et al., 2010) or static picture showing a body part under a situation that might cause pain (Jackson et al., 2005;Lamm et al., 2007a;Han et al., 2009;Guo et al., 2012); both of them are far away from reality. In our daily life, the stimuli that trigger our empathy are often real-time multifaceted information formed by dynamic facial expression, body movement, and the context where the painful scenes happen. In studies presented in this thesis (Chapter 4 and 5), a more realistic scenario has been chosen. A video showing the whole process of applying a painful stimulation was used as a visual stimulus and a misleading strategy was applied to make the empathizers believed these videos were presented in real time through a CCTV. The degree of authenticity is therefore improved. We believe that this trend to making paradigms more involving is important in improving the validity of the neural findings.

Another implication this thesis suggests is the importance of investigating the empathizer's involvement in the pain scene. In most studies focusing on empathy for pain, the empathizers were mere bystanders: they were shown the cue or pictures indicating another person's painful state. However, in real life our limited attention usually focuses on persons who interact with us. The people whose emotions or sensations are caused by our own behaviours usually draw more of our attention and influence our own emotional states more. In one study presented here (Chapter 4), we investigate how the involvement of the empathizer in causing the other's pain modulates the empathic brain response. We found that an actual involvement of the witness in causing the pain indeed had a large effect on the neural basis of empathy, and we therefore suggest that involving real causal interactions in empathy paradigms is another interesting point that might inspire new research.

There are now many studies showing that a number of factors, of which the responsibility modulation we show is only one, can modulate the amplitude of activations in empathy related brain regions (Lamm et al., 2007b;Hein and Singer, 2008;Engen and Singer, 2012). How does this modulation happen? Some studies found that the reduction of AI activation during empathizing was correlated with increased activation of the ventral striatum/nucleus accumbens(NAcc), which are regions often related with reward processing and desire for revenge and Schadenfreude (Singer et al., 2006a;Takahashi et al., 2009b;de Quervain et al., 2004). Studies also found that the modulation of empathy was associated with activation of a number of regions implicated in metalizing such as TPJ, vmPFC/orbitofrontal cortex, and executive control and emotion regulation such as lateral middle frontal gyrus, genual ACC and orbital IFG (Wager et al., 2008;Mitchell, 2009;Rossi et al., 2009;Ochsner et al., 2012;Engen and Singer, 2012). These results imply that our preconceptions about others' emotional states modulate our empathic response and this modulation may work in a similar fashion to the one seen in emotion regulation. On the other hand, studies show that in the empathy circuits, the insula is most likely the entry hub of the modulation. Anatomically, the insula is a hub that integrates many sources of information. In Craig's influential model, the insula plays a key role in integrating sensory information with emotional states (Craig, 2009;Craig, 2009). The insula projects to the amygdala, ACC and high-level visual areas like STS, allowing it to influence sensory processing, autonomic states and behaviour. It also receives inputs from orbitfrontal, olfactory cortex, ACC and STS, allowing it to combine a wide range of information (Mesulam and Mufson, 1982a;Mesulam and Mufson, 1982b;Mufson and Mesulam, 1982). Our work also supports this notion of the insula as the hub of empathy modulation (Chapter 4). A model extracted from the literature and our current work is that the regions involved in emotion regulation shape the observer's emotional information and modulate the whole activity of empathy via the insula. More work should to be done to test this model and to figure out the dynamic connections in this modulation.

References Cited

Agnew Z, Wise RJ (2008) Separate areas for mirror responses and agency within the parietal operculum. J Neurosci 28:12268-12273.

Andrew J.Oswald, Daniel J.Zizzo (2001) Are People Willing to Pay to Reduce Others'Incomes? Annales d'Economie et de Statistique04.

Apkarian AV, Bushnell MC, Treede RD, Zubieta JK (2005) Human brain mechanisms of pain perception and regulation in health and disease. Eur J Pain 9:463-484.

Apkarian AV, Darbar A, Krauss BR, Gelnar PA, Szeverenyi NM (1999) Differentiating cortical areas related to pain perception from stimulus identification: temporal analysis of fMRI activity. J Neurophysiol 81:2956-2963.

Arnstein D, Cui F, Keysers C, Maurits NM, Gazzola V (2011) mu-suppression during action observation and execution correlates with BOLD in dorsal premotor, inferior parietal, and SI cortices. J Neurosci 31:14243-14249.

Avenanti A, Sirigu A, Aglioti SM (2010) Racial bias reduces empathic sensorimotor resonance with other-race pain. Curr Biol 20:1018-1022.

Azevedo RT, Macaluso E, Avenanti A, Santangelo V, Cazzato V, Aglioti SM (2012) Their pain is not our pain: Brain and autonomic correlates of empathic resonance with the pain of same and different race individuals. Hum Brain Mapp.

Banerjee O, El Ghaoui L, d'Aspremont A, Natsoulis G (2006) Convex optimization techniques for fitting sparse Gaussian graphical models. In: Proceedings of the 23rd international conference on Machine learning.

Bird G, Silani G, Brindley R, White S, Frith U, Singer T (2010) Empathic brain responses in insula are modulated by levels of alexithymia but not autism. Brain 133:1515-1525.

Blair RJ (1995) A cognitive developmental approach to mortality: investigating the psychopath. Cognition 57:1-29.

Blakemore SJ, Bristow D, Bird G, Frith C, Ward J (2005) Somatosensory activations during the observation of touch and a case of vision-touch synaesthesia. Brain 128:1571-1583.

Blakemore SJ, Frith CD, Wolpert DM (1999) Spatio-temporal prediction modulates the perception of self-produced stimuli. J Cogn Neurosci 11:551-559.

Blakemore SJ, Wolpert DM, Frith CD (1998) Central cancellation of self-produced tickle sensation. Nat Neurosci 1:635-640.

Buhle JT, Silvers JA, Wager TD, Lopez R, Onyemekwu C, Kober H, Weber J, Ochsner KN (2013) Cognitive Reappraisal of Emotion: A Meta-Analysis of Human Neuroimaging Studies. Cereb Cortex.

Calder AJ, Keane J, Manes F, Antoun N, Young AW (2000) Impaired recognition and experience of disgust following brain injury. Nat Neurosci 3:1077-1078.

Carter CS, Braver TS, Barch DM, Botvinick MM, Noll D, Cohen JD (1998) Anterior cingulate cortex, error detection, and the online monitoring of performance. Science 280:747-749.

Caspers S, Zilles K, Laird AR, Eickhoff SB (2010) ALE meta-analysis of action observation and imitation in the human brain. Neuroimage 50:1148-1167.

Cerliani L, Thomas RM, Jbabdi S, Siero JC, Nanetti L, Crippa A, Gazzola V, D'Arceuil H, Keysers C (2012) Probabilistic tractography recovers a rostrocaudal trajectory of connectivity variability in the human insular cortex. Hum Brain Mapp 33:2005-2034.

Cheng Y, Chen C, Lin CP, Chou KH, Decety J (2010) Love hurts: an fMRI study. Neuroimage 51:923-929.

Choi JK, Bowles S (2007) The coevolution of parochial altruism and war. Science 318:636-640.

Christensen MS, Lundbye-Jensen J, Geertsen SS, Petersen TH, Paulson OB, Nielsen JB (2007) Premotor cortex modulates somatosensory cortex during voluntary movements without proprioceptive feedback. Nat Neurosci 10:417-419.

Cioffi D, Holloway J (1993) Delayed costs of suppressed pain. J Pers Soc Psychol 64:274-282.

Corradi-Dell'Acqua C, Hofstetter C, Vuilleumier P (2011) Felt and seen pain evoke the same local patterns of cortical activity in insular and cingulate cortex. J Neurosci 31:17996-18006.

Craig AD (2009) How do you feel--now? The anterior insula and human awareness. Nat Rev Neurosci 10:59-70.

Craig AD, Chen K, Bandy D, Reiman EM (2000) Thermosensory activation of insular cortex. Nat Neurosci 3:184-190.

Darley JM, Latane B (1968) Bystander intervention in emergencies: diffusion of responsibility. J Pers Soc Psychol 8:377-383.

Davis MH (1980) A multidimensional approach to individual differences in empathy. JSAS Catalog of Selected Documents in Psychology 10.

Davis MH (1983) Measuring individual differences in empathy: Evidence for a multidimensional approach. Journal of Personality and Social Psychology 44:113-126.

de Quervain DJ, Fischbacher U, Treyer V, Schellhammer M, Schnyder U, Buck A, Fehr E (2004) The neural basis of altruistic punishment. Science 305:1254-1258.

de Vignemont F, Singer T (2006) The empathic brain: how, when and why? Trends Cogn Sci 10:435-441.

de WM, Verbaten MN (2001) Affective pictures processing, attention, and pain tolerance. Pain 90:163-172.

Decety J (2011) The neuroevolution of empathy. Ann N Y Acad Sci 1231:35-45.

Decety J, Echols S, Correll J (2010a) The blame game: the effect of responsibility and social stigma on empathy for pain. J Cogn Neurosci 22:985-997.

Decety J, Echols S, Correll J (2010b) The blame game: the effect of responsibility and social stigma on empathy for pain. J Cogn Neurosci 22:985-997.

Desmurget M, Reilly KT, Richard N, Szathmari A, Mottolese C, Sirigu A (2009) Movement intention after parietal cortex stimulation in humans. Science 324:811-813.

di Pellegrino G, Fadiga L, Fogassi L, Gallese V, Rizzolatti G (1992) Understanding motor events: a neurophysiological study. Exp Brain Res 91:176-180.

Dinstein I, Hasson U, Rubin N, Heeger DJ (2007) Brain areas selective for both observed and executed movements. J Neurophysiol 98:1415-1427.

Downar J, Mikulis DJ, Davis KD (2003) Neural correlates of the prolonged salience of painful stimulation. Neuroimage 20:1540-1551.

Dvash J, Gilam G, Ben-Ze'ev A, Hendler T, Shamay-Tsoory SG (2010) The envious brain: the neural basis of social comparison. Hum Brain Mapp 31:1741-1750.

Ebisch SJ, Perrucci MG, Ferretti A, Del GC, Romani GL, Gallese V (2008) The sense of touch: embodied simulation in a visuotactile mirroring mechanism for observed animate or inanimate touch. J Cogn Neurosci 20:1611-1623.

Eisenberg N (2000) Emotion, regulation, and moral development. Annu Rev Psychol 51:665-697.

Eisenberg N (2007) Empathy-related responding and prosocial behaviour. Novartis Found Symp 278:71-80.

Engen HG, Singer T (2012) Empathy circuits. Curr Opin Neurobiol.

Fan Y, Duncan NW, de GM, Northoff G (2011) Is there a core neural network in empathy? An fMRI based quantitative meta-analysis. Neurosci Biobehav Rev 35:903-911.

Fan Y, Han S (2008) Temporal dynamic of neural mechanisms involved in empathy for pain: an event-related brain potential study. Neuropsychologia 46:160-173.

Forgiarini M, Gallucci M, Maravita A (2011) Racism and the empathy for pain on our skin. Front Psychol 2:108.

Friedman J, Hastie T, Tibshirani R (2008) Sparse inverse covariance estimation with the graphical lasso. Biostatistics 9:432-441.

Friston KJ, Harrison L, Penny W (2003a) Dynamic causal modelling. Neuroimage 19:1273-1302.

Friston KJ, Harrison L, Penny W (2003b) Dynamic causal modelling. Neuroimage 19:1273-1302.

Gallese V, Fadiga L, Fogassi L, Rizzolatti G (1996) Action recognition in the premotor cortex. Brain 119 (Pt 2):593-609.

Gao YJ, Ji RR (2010) Targeting astrocyte signaling for chronic pain. Neurotherapeutics 7:482-493.

Gazzola V, Aziz-Zadeh L, Keysers C (2006) Empathy and the somatotopic auditory mirror system in humans. Curr Biol 16:1824-1829.

Gazzola V, Keysers C (2009a) The observation and execution of actions share motor and somatosensory voxels in all tested subjects: single-subject analyses of unsmoothed fMRI data. Cereb Cortex 19:1239-1255.

Gazzola V, Keysers C (2009b) The observation and execution of actions share motor and somatosensory voxels in all tested subjects: single-subject analyses of unsmoothed fMRI data. Cereb Cortex 19:1239-1255.

Gray K, Wegner DM (2012) Morality takes two: Dyadic morality and mind perception. In: The social psychology of morality: Exploring the causes of good and evil. Herzliya series on personality and social psychology. (Mikulincer M, Shaver PR, eds), pp 109-127. Washington, DC, US: American Psychological Association.

Grezes J, Armony JL, Rowe J, Passingham RE (2003) Activations related to "mirror" and "canonical" neurones in the human brain: an fMRI study. Neuroimage 18:928-937.

Gu X, Han S (2007) Attention and reality constraints on the neural processes of empathy for pain. Neuroimage 36:256-267.

Guo X, Zheng L, Zhang W, Zhu L, Li J, Wang Q, Dienes Z, Yang Z (2011) Empathic neural responses to others' pain depend on monetary reward. Soc Cogn Affect Neurosci.

Guo X, Zheng L, Zhang W, Zhu L, Li J, Wang Q, Dienes Z, Yang Z (2012) Empathic neural responses to others' pain depend on monetary reward. Soc Cogn Affect Neurosci 7:535-541.

Haggard P, Whitford B (2004) Supplementary motor area provides an efferent signal for sensory suppression. Brain Res Cogn Brain Res 19:52-58.

Han S, Fan Y, Xu X, Qin J, Wu B, Wang X, Aglioti SM, Mao L (2009) Empathic neural responses to others' pain are modulated by emotional contexts. Hum Brain Mapp 30:3227-3237.

Hebert MA, Ardid D, Henrie JA, Tamashiro K, Blanchard DC, Blanchard RJ (1999) Amygdala lesions produce analgesia in a novel, ethologically relevant acute pain test. Physiol Behav 67:99-105.

Hein G, Silani G, Preuschoff K, Batson CD, Singer T (2010) Neural responses to ingroup and outgroup members' suffering predict individual differences in costly helping. Neuron 68:149-160.

Hein G, Singer T (2008) I feel how you feel but not always: the empathic brain and its modulation. Curr Opin Neurobiol 18:153-158.

Heldmann M, Russeler J, Munte TF (2008) Internal and external information in error processing. BMC Neurosci 9:33.

Hill SE, DelPriore DJ, Vaughan PW (2011) The cognitive consequences of envy: attention, memory, and self-regulatory depletion. J Pers Soc Psychol 101:653-666.

Hoffman ML (1977) Empathy, its development and prosocial implications. Nebr Symp Motiv 25:169-217.

Hoffman ML (2000) Empathy and Moral Development: Implications for caring and Justice. Cambridge University Press.

Iacoboni M, Mazziotta JC (2007) Mirror neuron system: basic findings and clinical applications. Ann Neurol 62:213-218.

Iacoboni M, Molnar-Szakacs I, Gallese V, Buccino G, Mazziotta JC, Rizzolatti G (2005) Grasping the intentions of others with one's own mirror neuron system. PLoS Biol 3:e79.

Iannetti GD, Mouraux A (2010) From the neuromatrix to the pain matrix (and back). Exp Brain Res 205:1-12.

Jabbi M, Bastiaansen J, Keysers C (2008) A common anterior insula representation of disgust observation, experience and imagination shows divergent functional connectivity pathways. PLoS One 3:e2939.

Jabbi M, Swart M, Keysers C (2007) Empathy for positive and negative emotions in the gustatory cortex. Neuroimage 34:1744-1753.

Jackson PL, Meltzoff AN, Decety J (2005) How do we perceive the pain of others? A window into the neural processes involved in empathy. Neuroimage 24:771-779.

Jackson PL, Rainville P, Decety J (2006) To what extent do we share the pain of others? Insight from the neural bases of pain empathy. Pain 125:5-9.

Jelasic F (1966) Relation of the lateral part of the amygdala to pain. Confin Neurol 27:53-55.

Johansson RS, Flanagan JR (2009) Coding and use of tactile signals from the fingertips in object manipulation tasks. Nat Rev Neurosci 10:345-359.

Jones EG, Coulter JD, Hendry SH (1978) Intracortical connectivity of architectonic fields in the somatic sensory, motor and parietal cortex of monkeys. J Comp Neurol 181:291-347.

Kawato M (1999) Internal models for motor control and trajectory planning. Curr Opin Neurobiol 9:718-727.

Keysers C, Gazzola V (2009a) Expanding the mirror: vicarious activity for actions, emotions, and sensations. Curr Opin Neurobiol 19:666-671.

Keysers C, Gazzola V (2009b) Expanding the mirror: vicarious activity for actions, emotions, and sensations. Curr Opin Neurobiol 19:666-671.

Keysers C, Kaas JH, Gazzola V (2010) Somatosensation in social perception. Nat Rev Neurosci 11:417-428.

Keysers C, Wicker B, Gazzola V, Anton JL, Fogassi L, Gallese V (2004) A touching sight: SII/PV activation during the observation and experience of touch. Neuron 42:335-346.

Koban L, Corradi-Dell'Acqua C, Vuilleumier P (2013) Integration of error agency and representation of others' pain in the anterior insula. J Cogn Neurosci 25:258-272.

Krach S, Cohrs JC, de Echeverria Loebell NC, Kircher T, Sommer J, Jansen A, Paulus FM (2011) Your flaws are my pain: linking empathy to vicarious embarrassment. PLoS One 6:e18675.

Kut E, Schaffner N, Wittwer A, Candia V, Brockmann M, Storck C, Folkers G (2007) Changes in self-perceived role identity modulate pain perception. Pain 131:191-201.

Lamm C, Batson CD, Decety J (2007a) The neural substrate of human empathy: effects of perspective-taking and cognitive appraisal. J Cogn Neurosci 19:42-58.

Lamm C, Decety J, Singer T (2011) Meta-analytic evidence for common and distinct neural networks associated with directly experienced pain and empathy for pain. Neuroimage 54:2492-2502.

Lamm C, Nusbaum HC, Meltzoff AN, Decety J (2007b) What are you feeling? Using functional magnetic resonance imaging to assess the modulation of sensory and affective responses during empathy for pain. PLoS One 2:e1292.

Lancaster JL, Laird AR, Eickhoff SB, Martinez MJ, Fox PM, Fox PT (2012) Automated regional behavioral analysis for human brain images. Front Neuroinform 6:23.

Lancaster JL, Woldorff MG, Parsons LM, Liotti M, Freitas CS, Rainey L, Kochunov PV, Nickerson D, Mikiten SA, Fox PT (2000) Automated Talairach atlas labels for functional brain mapping. Hum Brain Mapp 10:120-131.

Li W, Han S (2010) Perspective taking modulates event-related potentials to perceived pain. Neurosci Lett 469:328-332.

Loggia ML, Mogil JS, Bushnell MC (2008) Experimentally induced mood changes preferentially affect pain unpleasantness. J Pain 9:784-791.

London BM, Miller LE (2013) Responses of somatosensory area 2 neurons to actively and passively generated limb movements. J Neurophysiol 109:1505-1513.

Luppino G, Matelli M, Camarda R, Rizzolatti G (1993) Corticocortical connections of area F3 (SMA-proper) and area F6 (pre-SMA) in the macaque monkey. J Comp Neurol 338:114-140.

Maldjian JA, Laurienti PJ, Kraft RA, Burdette JH (2003) An automated method for neuroanatomic and cytoarchitectonic atlas-based interrogation of fMRI data sets. Neuroimage 19:1233-1239.

Marrelec G, Krainik A, Duffau H, Pelegrini-Issac M, Lehericy S, Doyon J, Benali H (2006) Partial correlation for functional brain interactivity investigation in functional MRI. Neuroimage 32:228-237.

Mathalon DH, Whitfield SL, Ford JM (2003) Anatomy of an error: ERP and fMRI. Biol Psychol 64:119-141.

Meffert H, Gazzola V, den Boer JA, Bartels AA, Keysers C (2013) Reduced spontaneous but relatively normal deliberate vicarious representations in psychopathy. Brain 136:2550-2562.

Mesulam MM, Mufson EJ (1982a) Insula of the old world monkey. I. Architectonics in the insulo-orbito-temporal component of the paralimbic brain. J Comp Neurol 212:1-22.

Mesulam MM, Mufson EJ (1982b) Insula of the old world monkey. III: Efferent cortical output and comments on function. J Comp Neurol 212:38-52.

Meyer ML, Masten CL, Ma Y, Wang C, Shi Z, Eisenberger NI, Han S (2012) Empathy for the social suffering of friends and strangers recruits distinct patterns of brain activation. Soc Cogn Affect Neurosci.

Michl P, Meindl T, Meister F, Born C, Engel RR, Reiser M, Hennig-Fast K (2012) Neurobiological underpinnings of shame and guilt: a pilot fMRI study. Soc Cogn Affect Neurosci.

Mitchell JP (2009) Inferences about mental states. Philos Trans R Soc Lond B Biol Sci 364:1309-1316.

Monfardini E, Gazzola V, Boussaoud D, Brovelli A, Keysers C, Wicker B (2013) Vicarious neural processing of outcomes during observational learning. PlosOne Accpeted.

Mouraux A, Diukova A, Lee MC, Wise RG, Iannetti GD (2011) A multisensory investigation of the functional significance of the "pain matrix". Neuroimage 54:2237-2249.

Moya-Albiol L, Herrero N, Bernal MC (2010) The neural bases of empathy. Rev Neurol 50:89-100.

Mufson EJ, Mesulam MM (1982) Insula of the old world monkey. II: Afferent cortical input and comments on the claustrum. J Comp Neurol 212:23-37.

Muthukumaraswamy SD, Johnson BW (2004) Primary motor cortex activation during action observation revealed by wavelet analysis of the EEG. Clin Neurophysiol 115:1760-1766.

Muthukumaraswamy SD, Johnson BW, McNair NA (2004) Mu rhythm modulation during observation of an object-directed grasp. Brain Res Cogn Brain Res 19:195-201.

Narita M, Kaneko C, Miyoshi K, Nagumo Y, Kuzumaki N, Nakajima M, Nanjo K, Matsuzawa K, Yamazaki M, Suzuki T (2006) Chronic pain induces anxiety with concomitant changes in opioidergic function in the amygdala. Neuropsychopharmacology 31:739-750.

Oberman LM, Hubbard EM, McCleery JP, Altschuler EL, Ramachandran VS, Pineda JA (2005) EEG evidence for mirror neuron dysfunction in autism spectrum disorders. Brain Res Cogn Brain Res 24:190-198.

Oberman LM, Ramachandran VS, Pineda JA (2008) Modulation of mu suppression in children with autism spectrum disorders in response to familiar or unfamiliar stimuli: the mirror neuron hypothesis. Neuropsychologia 46:1558-1565.

Ochsner KN, Silvers JA, Buhle JT (2012) Functional imaging studies of emotion regulation: a synthetic review and evolving model of the cognitive control of emotion. Ann N Y Acad Sci 1251:E1-24.

Packard MG, Knowlton BJ (2002) Learning and memory functions of the Basal Ganglia. Annu Rev Neurosci 25:563-593.

Penny WD, Stephan KE, Daunizeau J, Rosa MJ, Friston KJ, Schofield TM, Leff AP (2010) Comparing families of dynamic causal models. PLoS Comput Biol 6:e1000709.

Perry A, Stein L, Bentin S (2011) Motor and attentional mechanisms involved in social interaction--evidence from mu and alpha EEG suppression. Neuroimage 58:895-904.

Pineda JA, Allison BZ, Vankov A (2000) The effects of self-movement, observation, and imagination on mu rhythms and readiness potentials (RP's): toward a brain-computer interface (BCI). IEEE Trans Rehabil Eng 8:219-222.

Poldrack RA (2006) Can cognitive processes be inferred from neuroimaging data? Trends Cogn Sci 10:59-63.

Pons TP, Kaas JH (1986) Corticocortical connections of area 2 of somatosensory cortex in macaque monkeys: a correlative anatomical and electrophysiological study. J Comp Neurol 248:313-335.

Preston SD, de Waal FB (2002) Empathy: Its ultimate and proximate bases. Behav Brain Sci 25:1-20.

Rainville P, Duncan GH, Price DD, Carrier B, Bushnell MC (1997) Pain affect encoded in human anterior cingulate but not somatosensory cortex. Science 277:968-971.

Ramnani N (2012) Frontal lobe and posterior parietal contributions to the cortico-cerebellar system. Cerebellum 11:366-383.

Rizzolatti G, Fadiga L, Gallese V, Fogassi L (1996) Premotor cortex and the recognition of motor actions. Brain Res Cogn Brain Res 3:131-141.

Rohling ML, Binder LM, Langhinrichsen-Rohling J (1995) Money matters: A meta-analytic review of the association between financial compensation and the experience and treatment of chronic pain. Health Psychol 14:537-547.

Rossi AF, Pessoa L, Desimone R, Ungerleider LG (2009) The prefrontal cortex and the executive control of attention. Exp Brain Res 192:489-497.

Rouwette T, Vanelderen P, Roubos EW, Kozicz T, Vissers K (2012) The amygdala, a relay station for switching on and off pain. Eur J Pain 16:782-792.

Roy M, Lebuis A, Peretz I, Rainville P (2011) The modulation of pain by attention and emotion: a dissociation of perceptual and spinal nociceptive processes. Eur J Pain 15:641-10.

Rozzi S, Calzavara R, Belmalih A, Borra E, Gregoriou GG, Matelli M, Luppino G (2006) Cortical connections of the inferior parietal cortical convexity of the macaque monkey. Cereb Cortex 16:1389-1417.

Schippers MB, Renken R, Keysers C (2011) The effect of intra- and inter-subject variability of hemodynamic responses on group level Granger causality analyses. Neuroimage 57:22-36.

Sewards TV, Sewards MA (2002) The medial pain system: neural representations of the motivational aspect of pain. Brain Res Bull 59:163-180.

Shamay-Tsoory SG (2011) The neural bases for empathy. Neuroscientist 17:18-24.

Shamay-Tsoory SG, Tibi-Elhanany Y, Aharon-Peretz J (2007) The green-eyed monster and malicious joy: the neuroanatomical bases of envy and gloating (schadenfreude). Brain 130:1663-1678.

Shane MS, Stevens M, Harenski CL, Kiehl KA (2008) Neural correlates of the processing of another's mistakes: a possible underpinning for social and observational learning. Neuroimage 42:450-459.

Singer T, Lamm C (2009) The social neuroscience of empathy. Ann N Y Acad Sci 1156:81-96.

Singer T, Seymour B, O'Doherty J, Kaube H, Dolan RJ, Frith CD (2004a) Empathy for pain involves the affective but not sensory components of pain. Science 303:1157-1162.

Singer T, Seymour B, O'Doherty J, Kaube H, Dolan RJ, Frith CD (2004b) Empathy for pain involves the affective but not sensory components of pain. Science 303:1157-1162.

Singer T, Seymour B, O'Doherty JP, Stephan KE, Dolan RJ, Frith CD (2006a) Empathic neural responses are modulated by the perceived fairness of others. Nature 439:466-469.

Singer T, Seymour B, O'Doherty JP, Stephan KE, Dolan RJ, Frith CD (2006b) Empathic neural responses are modulated by the perceived fairness of others. Nature 439:466-469.

Smith SM, Miller KL, Salimi-Khorshidi G, Webster M, Beckmann CF, Nichols TE, Ramsey JD, Woolrich MW (2011) Network modelling methods for FMRI. Neuroimage 54:875-891.

Southgate V, Johnson MH, Osborne T, Csibra G (2009) Predictive motor activation during action observation in human infants. Biol Lett 5:769-772.

Stephan KE, Penny WD, Moran RJ, den Ouden HE, Daunizeau J, Friston KJ (2010) Ten simple rules for dynamic causal modeling. Neuroimage 49:3099-3109.

Takahashi H, Kato M, Matsuura M, Mobbs D, Suhara T, Okubo Y (2009a) When your gain is my pain and your pain is my gain: neural correlates of envy and schadenfreude. Science 323:937-939.

Takahashi H, Kato M, Matsuura M, Mobbs D, Suhara T, Okubo Y (2009b) When your gain is my pain and your pain is my gain: neural correlates of envy and schadenfreude. Science 323:937-939.

Taylor SF, Stern ER, Gehring WJ (2007) Neural systems for error monitoring: recent findings and theoretical perspectives. Neuroscientist 13:160-172.

Theodore M.Singelis (1994) The Measurement of Independent and Interdependent Self-Construals. Pers Soc Psychol Bull 20:580-591.

Ullsperger M, von Cramon DY (2003) Error monitoring using external feedback: specific roles of the habenular complex, the reward system, and the cingulate motor area revealed by functional magnetic resonance imaging. J Neurosci 23:4308-4314.

Villemure C, Bushnell MC (2009a) Mood influences supraspinal pain processing separately from attention. J Neurosci 29:705-715.

Villemure C, Bushnell MC (2009b) Mood influences supraspinal pain processing separately from attention. J Neurosci 29:705-715.

Vogt BA, Sikes RW (2000) The medial pain system, cingulate cortex, and parallel processing of nociceptive information. Prog Brain Res 122:223-235.

Vohs KD (2010) The mere thought of money makes you feel less pain. Harv Bus Rev 88:28-29.

Vohs KD, Mead NL, Goode MR (2006) The psychological consequences of money. Science 314:1154-1156.

Wager TD, Davidson ML, Hughes BL, Lindquist MA, Ochsner KN (2008) Prefrontal-subcortical pathways mediating successful emotion regulation. Neuron 59:1037-1050.

Warreyn P, Ruysschaert L, Wiersema JR, Handl A, Pattyn G, Roeyers H (2013) Infants' mu suppression during the observation of real and mimicked goal-directed actions. Dev Sci 16:173-185.

Weber DJ, London BM, Hokanson JA, Ayers CA, Gaunt RA, Torres RR, Zaaimi B, Miller LE (2011) Limb-state information encoded by peripheral and central somatosensory neurons: implications for an afferent interface. IEEE Trans Neural Syst Rehabil Eng 19:501-513.

Weiller C, Juptner M, Fellows S, Rijntjes M, Leonhardt G, Kiebel S, Muller S, Diener HC, Thilmann AF (1996a) Brain representation of active and passive movements. Neuroimage 4:105-110.

Weiller C, Juptner M, Fellows S, Rijntjes M, Leonhardt G, Kiebel S, Muller S, Diener HC, Thilmann AF (1996b) Brain representation of active and passive movements. Neuroimage 4:105-110.

Wicker B, Keysers C, Plailly J, Royet JP, Gallese V, Rizzolatti G (2003) Both of us disgusted in My insula: the common neural basis of seeing and feeling disgust. Neuron 40:655-664.

Wolpert DM, Flanagan JR (2001) Motor prediction. Curr Biol 11:R729-R732.

Wolpert DM, Ghahramani Z (2000) Computational principles of movement neuroscience. Nat Neurosci 3 Suppl:1212-1217.

Wolpert DM, Miall RC (1996) Forward Models for Physiological Motor Control. Neural Netw 9:1265-1279.

Yamauchi KT, Templer DJ (1982) The development of a Money Attitude Scale. J Pers Assess 46:522-528.

Zaki J, Ochsner K (2012) The neuroscience of empathy: progress, pitfalls and promise. Nat Neurosci 15:675-680.

Zhou X, Vohs KD, Baumeister RF (2009) The symbolic power of money: reminders of money alter social distress and physical pain. Psychol Sci 20:700-706.

Abbreviations

ACC	-	Anterior cingulated cortex
AI	-	Anterior insula
ASD	-	Autism spectrum disorder
BEES	-	Balanced Emotional empathy Scale
BOLD	-	Blood-oxygen-level-dependent
BA	-	Broadman Area
DCM	-	Dynamic Causal Modelling
EEG	-	Electroencephalography
EQ	-	Empathy Quotient
fMRI	-	Functional magnetic resonance iamgeing
EPIs	-	Functional MRI images
GLM	-	General Linear Models
HRF	-	Hemodynamic response function
IFG	-	Inferior frontal gyrus
IRI	-	Interpersonal Reactivity Index
MTG	-	Middle temporal gyrus
MNS	-	Mirror neuron system
PET	-	Positron emission tomography
pACC/aMCC	-	Posterior anterior and anterior medial cingulate cortex
S1	-	Primary somatosensory cortices
M1	-	Primary motor cortex
PM	-	Promoter cortex
PPI	-	Psycho-Physiological Interaction
ROI	-	Region of Interest
S2	-	Secondary somatosensory cortices
sVx	-	Shared voxels
S2	-	Secondary somatosensory cortices
SPM	-	Statistical Parametric Mapping
STS	-	Superior temporal sulcus
SMA	-	Supplementary motor areas

TPJ - Temporoparietal junction

VMPFC - Ventromedial prefrontal cortex

English Summary

Human beings are born as social animals. To successfully perform social interactions, our brain needs to "distinguish between self and others" as well as "connect self and others".

A nice example of "distinguish between self and others" is tickling. When you are tickled by another person, you cannot help but giggle. Instead, when you attempt to tickle yourself, you don't feel the same tickle that makes you giggle. The dominant explanation of this difference is that when you tickle yourself, the motor command to move your hand is sent to your body, but a copy of that motor command, called efference copy, is also sent to the somatosensory areas to cancel the sensations caused by the action. This efference copy will not be there if you are tickled by others and the ticke will thus not be cancelled by the efference copy. To better understand this phenomenon, in one of the studies presented in this thesis we tried to localize the origin of this efference copy. We imaged brain activity while people squeezed their hand voluntarily (active condition) and while their hand was moved in a similar way by another person (passive condition) in order to localize the origin of the efference copy. We used functional magnetic resonance imaging (fMRI) to capture the brain activity of our participants. When a brain area becomes activated by a task, it requires more oxygen, which will cause a change in the local oxygenation of the blood that in turn influences the local magnetic field and can be measured as a proxy of neural activity using magnetic resonance imaging (MRI). Subjects were lying in the scanner wearing a thin rubber glove on their right hand. Another glove was attached to the back of this glove and was worn by the experimenter. During one of the two conditions the subjects would squeeze a ball of soft material (comparable to self-tickling action of the example). In the other condition the subjects would keep their hands completely relaxed and the experimenter will squeeze the soft ball by gently pressing the subject's hand (comparable to someone else tickling; Figure 1).

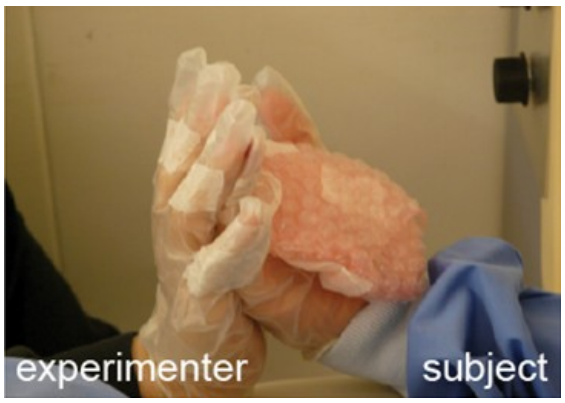

Figure 1

Electromyography (EMG) was used to measure the muscle activity of the subjects' hand during the two conditions and was correlated with the fMRI signal. EMG activity measured while the subject moves the hand can be considered a proxy of the efference copy. Brain areas correlated with the EMG will therefore likely be a source or a recipient of the efference copy. We found that the EMG signal can predict activity in primary somatosensory regions, particularly BA2. This result confirmed that during voluntary movement a copy of the motor command used to perform the action is sent to the somatosensory cortices, probably to make prediction on how that action will feel like. Importantly, we could also identify that the likely sources of this efference copy lie in the supplementary motor cortex, and transits through the cerebellum and/or premotor cortex via the posterior parietal

lobe, to the somatosensory cortex. This predictive efference copy will not happen when someone else is moving parts of our own body: when someone tickles us, will therefore not easily be able to suppress our reactions.

We human beings are also surprisingly good at understanding and predicting other people's actions. Just by looking at how a person reaches for a teacup we often know if he/she will drink tea from it or just wants to wash it. The discovery of mirror neurons in the monkey in 1990s sheds lights on how our brain works to do so: when we observe others performing an action, we activate the same brain areas that are also activated when we perform that action ourselves. In humans, this system of areas is named after the mirror neurons found in monkeys as the "mirror neuron system" (MNS). Since in human beings, we cannot directly record single neuron activities as systematically as in monkeys, most evidence for the existence of the MNS comes from indirect measurements like fMRI or electroencephalography (EEG). Different indices are used in fMRI and EEG studies to proxy MNS activity. In fMRI, the activity of voxels (the 3D equivalent of a pixel; i.e. a volume element representing a value on a regular grid in a space) that are active both during action execution and action observation is taken to reflect the activity of the MNS. In EEG studies, the power suppression in the alpha band recorded in somatosensory areas on the scalp (mu suppression) is assumed to proxy the same underlying mechanism. Whether the two really measure the same processes was so far unknown. In the second study presented in this thesis, subjects performed hand actions and observed videos showing others performing similar hand actions (Figure 2), while both EEG and fMRI signals were recorded - at the same time.

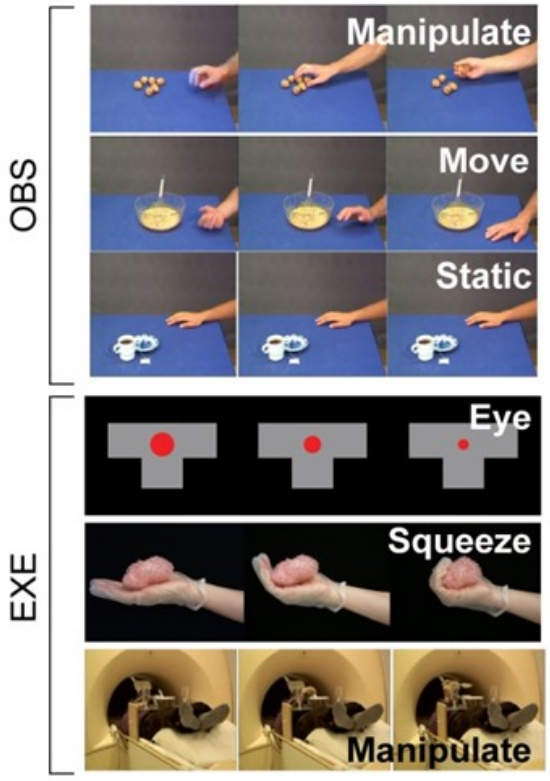

Figure 2 The OBS part shows still images of the videos presented to the subjects. The EXE part shows the action execution part, during which subjects performed hand actions inside the scanner.

We found that the EEG index (i.e. how much mu-suppression happened at a given trial) co-varied with the fMRI index (how much fMRI signal occurred in regions involved in both action observation and execution) in most typical MNS regions including inferior parietal lobule (IPL), dorsal premotor (dPM) and BA2, but not BA44 (Pink

color in Figure 3). These results provide a basis for integrating more closely the flourishing but often separate literatures on the MNS using fMRI and EEG.

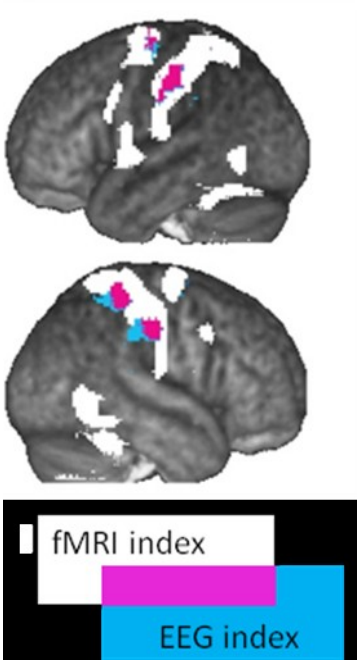

Figure 3 The White areas represent the MNS, localized using fMRI. The blue areas are correlating with mu suppression in the EEG signal. The pink areas are the overlapping areas.

Besides understanding other's actions, we human beings also have an excellent ability in empathizing with other's sensations and emotions. The sight of a suffering person makes us feel bad, to the point where we sometimes also feel the pain ourselves. Part of the brain areas activated when we feel the pain ourselves are also activated when we observe other's in pain. However, we do not always empathize to the same degree. We can even feel the pleasure of revenge when we see a person we hate in pain, but we will suffer together with our lovers or close friends. In the third study presented here we tried to test if the responsibility in causing other's pain can modulate the empathy for this pain. For example, will you fell more empathic to a person that broke his leg if a) he is hit by your car or b) he fell down from the stairs himself? To investigate the role of responsibility in causing others' pain we recruited two subjects each time: one is in the MRI scanner and the other is outside the scanner (the latter is actually always me). They performed an attention task together. If both of them did the task correctly, the subject outside the scanner (i.e. I) receives a painless, weak electrical shock on the right hand. Otherwise (i.e. if either the participant and/or I made a mistake), I would receive a painful electrical shock. So we have four conditions in total. The subject in the scanner' responsibility in causing my pain was modulated accordingly (Table1).

Subject's response In the Scanner	**my response**	**Electrical Shock Applied to me**	**Responsbilty for Pain of the Subject in Scanner**
Right	Right	Not painful	No Pain
Wrong	Right	Painful	No Responsibility
Wrong	Wrong	Painful	Shared Responsibility
Right	Wrong	Painful	Full Responsibility

Table 1

Then we compared the brain activation under different conditions. We found that regions of the functionally localized pain matrix of the subjects (the anterior insula in particular) were activated most strongly when seeing me receive a shock when only the subject had erred (and hence had full responsibility). When both or only I had erred (i.e. subject's shared or no responsibility), significantly weaker vicarious pain-matrix activations were measured (Figure 4). The supplementary motor area played a key role in transforming performance feedback into this modulation of vicarious activation.

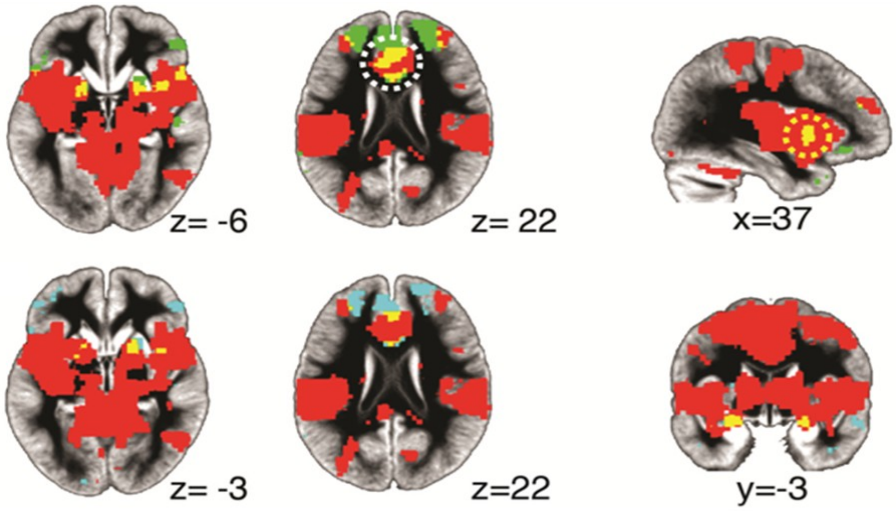

Figure 4 Green = (Full Responsibility) – (Shared Responsibility); Cyan = (Full Responsibility)-(No Responsibility). Red = First-hand painful experience. The white circle is the anterior cingulated cortex; the yellow circle is the insula.

Another factor that we assumed to influence empathy for pain is monetary compensation. Imagine you know that a person who broke his arm during work receives a substantial amount of money from insurance for his injury; will you feel better when you see his painful face? Might such compensation, in addition to helping the victim, also serve a social function of comforting the observers? A behavioral study was conducted to test this hypothesis. We recruited subjects and showed them another person (the victim – me again!) receiving electrical shocks. Before each electrical shock the subject was informed whether I will receive money for the coming shock or not. After observing the applying of the electrical shock, the subjects were asked to evaluate their feelings and the victim's feelings about the shock. Results were twofold. First, subjects attribute less unpleasantness to victims that received money for a painful shock. Second, subjects themselves, felt more unpleasant when victims received money for a non-painful shock, possibly reflecting jealousy. These results provide novel insights into the social impact of monetary compensation to victims. An fMRI study is under preparation to dig the neural mechanism under this effect.

For these four years of researching, I went from self to others, from action to emotion, from EEG to fMRI, trying to discover the mystery of the social aspect of human nature. There are millions of questions out there, and I am heading to them with curiosity and determination.

Dutch Summary

Mensen worden geboren als sociale wezens. Voor succesvolle sociale interactie moeten onze hersenen in staat zijn om onderscheid te maken tussen jezelf en anderen maar ook om contact te maken tussen jezelf met anderen.

Een goed voorbeeld van onderscheid maken tussen jezelf en anderen is kietelen. Wanneer iemand jou kietelt, ga je vanzelf giechelen. Maar als je probeert jezelf te kietelen, voel je niet dat gevoel waardoor je gaat giechelen. De overheersende verklaring voor dit verschil is dat wanneer je jezelf kietelt, je lichaam de opdracht krijgt om met je hand die beweging te maken, maar een kopie van die opdracht, de zogenaamde efferente kopie, wordt ook verzonden naar de somatosensorische gebieden die ervoor zorgen dat het gevoel dat veroorzaakt wordt door deze handeling wordt uitgeschakeld. Deze efferente kopie ontbreekt als je gekieteld wordt door iemand anders en het gevoel van het kietelen wordt hierdoor ook niet uitgeschakeld. Om dit verschijnsel beter te kunnen begrijpen hebben we in een van de hoofdstukken van dit proefschrift geprobeerd het gebied van deze efferente kopie te localiseren. Met behulp van fMRI werd de hersenactiviteit vastgelegd van proefpersonen die vrijwillig in hun hand knepen (actieve conditie) of door een ander in hun hand werden geknepen (passieve conditie). Wanneer een gebied in de hersenen wordt geactiveerd door het uitvoeren van een bepaalde taak is er meer zuurstof nodig; hierdoor ontstaat een verandering in de lokale concentratie van de zuurstof in het bloed die dan weer van invloed is op het lokale magnetische veld en gemeten kan worden als bewijs van neurale activiteit bij MRI gebruik. De proefpersonen lagen in een scanner en droegen een dunne rubberen handschoen aan hun rechterhand. Een andere handschoen zat vast aan de achterkant van deze handschoen en werd gedragen door degene die het experiment uitvoerde. Bij de ene conditie knepen de proefpersonen in een bal van zacht materiaal (te vergelijken met het jezelf kietelen uit het voorbeeld hierboven). Bij de andere conditie hielden de proefpersonen hun handen helemaal stil en kneep degene die het experiment uitvoerde in de bal door zachtjes op de hand van de proefpersoon te drukken (vgl. iemand anders kietelen; Figuur 1).

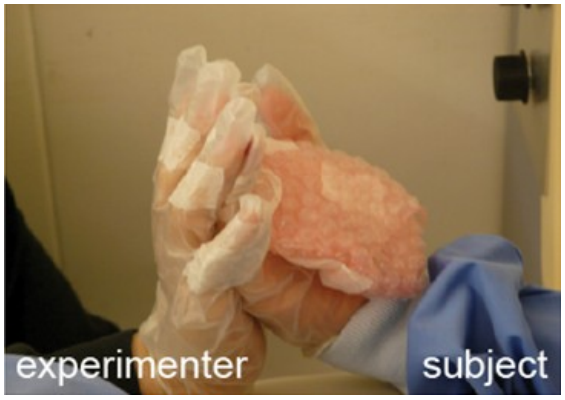

Figuur 1

Door middel van elektromyografie (EMG) werd de spieractiviteit van de hand van de proefpersonen gemeten tijdens deze twee condities en gecorreleerd met het fMRI signaal. Het meten van EMG activiteit terwijl de proefpersoon zijn hand beweegt kan beschouwd worden als een bewijs van de efferente kopie. Als gevolg hiervan kunnen hersengebieden die correleren met EMG zowel bron of ontvanger zijn van de efferente kopie. Wij hebben aangetoond dat het EMG signaal activiteit in primaire somatosensorische gebieden kan voorspellen,

bijvoorbeeld in BA2. Dit resultaat bevestigde onze aanname dat gedurende een vrijwillige beweging een kopie van de opdracht om een bepaalde beweging te maken wordt verzonden naar de somatosensorische schors, waarschijnlijk met de bedoeling om aan te geven hoe die beweging zal aanvoelen. Bovendien kon worden aangetoond dat de oorsprong van deze efferente kopie gelegen is in de supplementaire motorschors, vervolgens het cerebellum en/of de premotor schors doorkruist via de posterior pariëtale kwab en doorloopt naar de somatosensorische schors. Deze voorspellende efferente kopie treedt niet op wanneer iemand anders delen van ons lichaam beweegt: bij kietelen zal het echter niet eenvoudig zijn een reactie te onderdrukken.

Mensen zijn ook bijzonder goed in het begrijpen en voorspellen van andermans handelingen. Uit de manier waarop iemand een theekopje pakt, weten we of hij/zij de thee gaat opdrinken of het kopje pakt om het af te wassen. De ontdekking van spiegelneuronen in de aap in de jaren negentig verschafte ons inzicht in hoe onze hersenen in deze situatie functioneren: wanneer we observeren hoe anderen een bepaalde handeling uitvoeren, worden tegelijkertijd bij ons diezelfde hersengebieden geactiveerd. Bij de mens wordt dit systeem het “spiegelneuronen systeem”(MNS) genoemd naar de spiegelneuronen die bij de aap werden gevonden. Omdat het bij de mens niet mogelijk is om, zoals bij de aap, systematisch en rechtstreeks single neuron activiteit te meten, wordt het bestaan van MNS grotendeels aangetoond door het uitvoeren van indirecte metingen met behulp van fMRI en elektroencephalografie (EEG). Bij deze studies wordt van verschillende indices gebruik gemaakt om MNS activiteit aan te tonen. Bij fMRI wordt de activiteit van voxels (de 3D equivalent van een pixel d.w.z. een voxel geeft een waarde aan die aan een volumecel in een driedimensionale ruimte gebonden is) die actief zijn zowel tijdens het uitvoeren van een handeling als bij het observeren van een handeling beschouwd als een weerspiegeling van MNS activiteit. In EEG studies wordt aangenomen dat de kracht onderdrukking in de alfaband gemeten in somatosensorische gebieden van de schedel (mu-onderdrukking) het bewijs is van hetzelfde onderliggende mechanisme. Tot nu toe was niet duidelijk of deze twee technieken dezelfde processen meten. In de tweede studie die in dit proefschrift wordt beschreven gaat het om proefpersonen die handelingen uitvoeren met hun hand en naar een video kijken waarop andere personen dezelfde handelingen uitvoeren (Figuur 2) terwijl tegelijkertijd EEG en fMRI signalen worden geregistreerd.

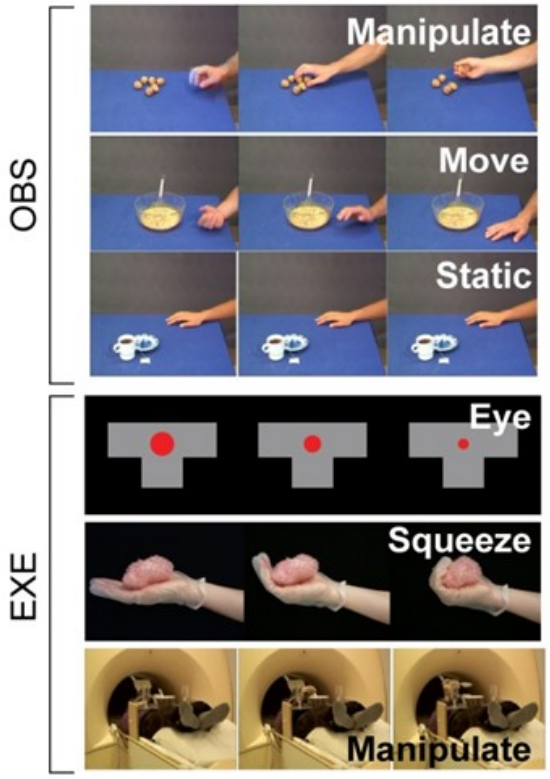

Figuur 2 Het OBS gedeelte laat een statische afbeelding zien van de video's die aan de proefpersonen getoond zijn. Het EXE gedeelte laat het actie executie gedeelte zien, waarbij de proefpersonen hand acties hebben uitgevoerd in de scanner.

Wij ontdekten dat de EEG index (d.w.z. de mate van mu-onderdrukking tijdens een bepaalde test) co-varieerde met de fMRI index (de hoeveelheid fMRI signaal in de gebieden betrokken bij observatie en uitvoering van bepaalde handelingen) in de meest kenmerkende MNS gebieden zoals de inferior pariëtale kwab (IPL), dorsale premotor (dPM) en BA2, maar niet inBA44 (roze kleur in Figuur 3). Deze resultaten geven zeker aanleiding tot een meer geïntegreerde benadering van de interessante literatuur over MNS en het gebruik van fMRI en EEG.

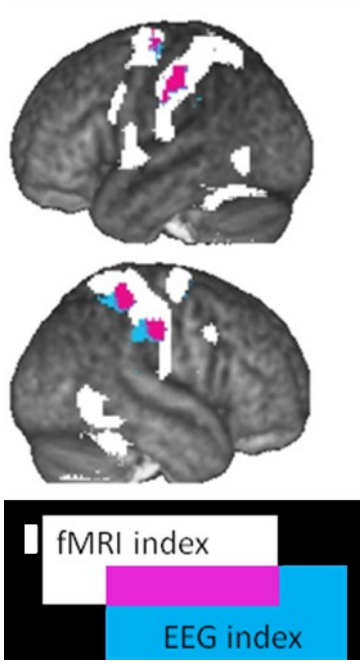

Figuur 3 De witte gebieden vertegenwoordigen het spiegelneuronensysteem, gelokaliseerd door middel van fMRI. De blauwe gebieden correleren aan mu suppressie in het EEG signaal. De roze gebieden zijn de overlappende gebieden.

Figure 4 Green = (Full Responsibility) – (Shared Responsibility); Cyan = (Full Responsibility)-(No Responsibility). Red = First-hand painful experience. The white circle is the anterior cingulated cortex; the yellow circle is the insula.

Naast het begrijpen van andermans handelingen, beschikt de mens ook over een groot talent om zich in te leven in de gevoelens en emoties van de ander. Als we iemand zien lijden voelen we ons ongelukkig, zozeer soms dat we de pijn bijna zelf voelen/ervaren. Een gedeelte van de hersengebieden die geactiveerd worden als we zelf pijn lijden zijn ook geactiveerd als we naar de pijn van een ander kijken. Echter, we ervaren die pijn niet op dezelfde wijze. We kunnen zelfs wraakgevoelens koesteren bij het zien van pijn in een persoon die we niet mogen, maar leven darentegen wel mee met geliefden en vrienden. De derde studie die hier beschreven wordt richt zich op de vraag in hoeverre de verantwoordelijkheid voor het veroorzaken van de pijn in iemand anders de empathie voor die pijn kan moduleren. Bijvoorbeeld, is je inlevingsvermogen groter voor iemand die zijn been heeft gebroken doordat hij (a) is aangereden door een auto of (b) zelf van de trap is gevallen? Bij ons onderzoek naar de mate waarin verantwoordelijkheid een rol speelt bij het veroorzaken van pijn bij een ander, werden steeds twee personen gebruikt: een persoon in de MRI scanner en de ander buiten de scanner (deze persoon was ikzelf). Beiden voerden tegelijkertijd een aandachtstaak uit. Als ze allebei de taak goed hadden uitgevoerd, kreeg de persoon buiten de scanner een pijnloze, zwakke elektrische schok toegediend op de rechterhand. In het andere geval (d.w.z. als de proefpersoon en/of ikzelf een fout hadden gemaakt) kreeg ik een pijnlijke elektrische schok toegediend. Er zijn dus in totaal 4 condities. De verantwoordelijkheid van de proefpersoon in de scanner werd op dezelfde wijze gemoduleerd (Tabel 1).

Respons Proefpersoon in scanner	Mijn Respons	Toediening elektrische schok aan mij	Verantwoordelijkheid voor pijn proefpersoon in scanner
Goed	Goed	Pijnloos	Geen oijn
Fout	Goed	Pijnlijk	Geen verantwoordelijkheid
Fout	Fout	Pijnlijk	Gedeelde verantwoordelijkheid
Goed	Fout	Pijnlijk	Volledige verantwoordelijkheid

Tabel 1

Vervolgens werd de hersenactiviteit onder andere condities vergeleken. Geconstateerd kon worden dat bepaalde gebieden van de functioneel gelocaliseerde pijn matrix van de proefpersonen (de anterior insula in het bijzonder) zeer sterk waren geactiveerd als ze zagen dat ik een schok kreeg terwijl de proefpersoon een fout had gemaakt (en de volledige verantwoordelijkheid had). Als we allebei of alleen ik een fout maakten (d.w.z. gedeelde of geen verantwoordelijkheid) werd er significant zwakkere pijn matrix activatie gemeten (Figuur 4). Het naastgelegen motorisch schorsgebied speelt kennelijk een sleutelrol bij het omzetten van performance feedback naar de modulatie van imaginaire / plaatsvervangende activatie.

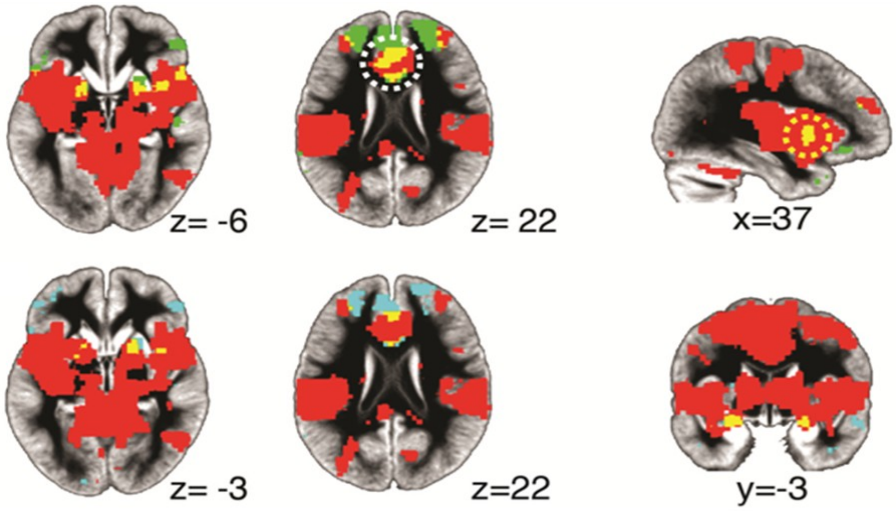

Figuur 4 Groen = (Volle Verantwoordelijkheid) – (Gedeelde Verantwoordelijkheid); Cyaan = (Volle Verantwoordelijkheid) – (Geen Verantwoordelijkheid); Rood = Directe Pijnlijke Ervaring. De Witte cirkel is de Cortex Cingularis Anterior; de Gele cirkel is de Insula.

Een andere factor die hoogstwaarschijnlijk empathie kan beïnvloeden is financiële compensatie. Stel je voor dat je iemand kent die tijdens zijn werk een arm heeft gebroken en daarvoor een aanzienlijk geldbedrag van de verzekering heeft ontvangen: voel je je dan beter als je zijn van pijn verwrongen gezicht ziet? Zou deze (financiële) compensatie, naast het helpen van het slachtoffer, ook een sociaal effect kunnen hebben op de toeschouwers, namelijk een gevoel van troost. Om deze hypothese te testen werd een gedragsstudie uitgevoerd. De proefpersonen moesten kijken naar een persoon (het slachtoffer was ik) aan wie elektrische schokken werden toegediend. Voor elke elektrische schok die werd toegediend werd vooraf aan de proefpersoon verteld of ik voor die schok wel of geen geld zou ontvangen. Na het kijken naar het toedienen van de elektrische schok, werd de proefpersonen gevraagd hun gevoelens en die van het slachtoffer te evalueren. De evaluatie leidde tot twee constateringen: proefpersonen vonden het toedienen van een pijnlijke schok niet zo erg voor slachtoffers die hiervoor geld kregen en proefpersonen voelden zich een stuk minder prettig wanneer slachtoffers geld

ontvingen voor een pijnloze schok, waarschijnlijk uit een gevoel van jaloezie. Deze resultaten leiden tot nieuwe inzichten in de sociale impact van financiële compensatie voor slachtoffers. Een fMRI studie om uit te zoeken wat het neurale mechnisme is wat ten grondslag ligt aan dit effect wordt momenteel voorbereid.

De afgelopen vier jaar ben ik tijdens mijn onderzoek gegaan van mijzelf naar anderen, van actie naar emotie, van EEG naar fMRI, in de hoop het mysterie van de sociale aspecten van de menselijke natuur te ontdekken. Er zijn nog miljoenen vragen waar ik me in de toekomst over wil buigen vol van nieuwsgierigheid en vastberadenheid.

中文摘要 (Chinese Summary)

人类生来就是社会动物。为了顺利进行社会交流，我们的大脑必须掌握两个技能：“区别自我和他人”以及“连接自我和他人”。

我们的大脑是如何区分自我和他人的呢？一个有趣的例子是，我们无法胳肢自己。别人胳肢我们的时候，我们会忍不住哈哈笑，可是当我们自己胳肢自己的时候，即使用同样的力度和动作，去挠同一个地方，我们也无法令自己发笑。这是为什么呢？这是因为但我们准备要胳肢自己的时候，我们大脑的前动作区会对动作区发出一个动作指令，与这个动作指令同时发出的，还有一个指令的拷贝，这个拷贝不会发到动作区，而会发到躯体感觉区。当躯体感觉区接受到这个指令拷贝，它就会自动抵消掉胳肢这个动作可能诱发的躯体感觉。这样我们就不会觉得痒了。而当我们被别人胳肢的时候，躯体感觉不会被抵消，所以我们就忍不住大笑了。

在本论文第二章的研究中，我们尝试探索大脑是如何区分“自主动作”和“被动动作”的。所谓“自主动作”是指我们自己主动做出的动作。“被动动作”是指我们肢体放松，由于受到外力而被动做出的动作。我们采用了功能磁共振（fMRI）这一技术来捕捉大脑的活动。功能磁共振的原理是这样的：当大脑某一区域被激活的时候，这一区域的需氧量变大，血流量也随之变大。功能磁共振正是通过捕捉血流量的变化让我们得以一窥大脑活动的秘密。在实验中，志愿者躺在磁共振机中，他/她的左手上戴着一个薄橡胶手套。在手套的手心部位固定着一个泡沫塑料制作的球状物。在手背部固定着另一个相同的橡胶手套，由实验者佩戴（见图 1）。在“自主动作”条件下，志愿者自己跟随指令做出挤压塑料球的动作。在“被动动作“条件下，志愿者放松自己的左手肌肉。由实验者握住志愿者的手指做出相同的挤压动作。在使用功能磁共振记录大脑活动的同时，我们使用肌电图（EMG）记录了志愿者左手肌肉活动的电生理信号。肌电信号反映了志愿者在自主动作的时候，大脑的前运动区对躯体感觉区发出的动作指令拷贝信号。结果显示，肌电信号预测了初级躯体感觉区，特别是 BA2 脑区的激活程度。这个结果告诉我们，当我们解释初级躯体感觉区（BA2）的活动时，不仅仅要考虑单纯的体感编码，还要考虑与躯体感觉相关的动作方面的信息。

人类在理解和预测他人动作方面能力惊人。当我们看到一个人伸手去拿一个茶杯时，我们很容易判断他下一步的动作。九十年代，科学家在恒河猴大脑里发现一种特殊的神经元。这种神经元在恒河猴伸手抓花生的时候被激活。而当恒河猴看到研究者伸手抓花生的时候，也会被激活。仿佛一面镜子，反映出它看到的别人做的动作。这类神经元被称为“镜像神经元”。这一发现给我们解密人类大脑如何理解他人动作带来了一线曙光。研究发现，在人类的大脑中也有一套类似的系统，这套系统不仅在我们自己做动作的时候被激活，在我们看到他人做动作的时候也会被激活，从而让我们利用对自己动作系统的理解去迅速地理解他人。这套系统被随之称为“镜像神经系统”（MNS）。在以人类为研究对象的实验中。我们很难像在恒河猴研究中，可以直接开颅记录单个神经元活动，所以大部分对人脑中镜像神经系统的研究是来自于间接的，无创性技术，比如脑电图和功能磁共振。在功能磁共振研究中，“共同体素” (Shared Voxel)被用来作为研究指标。体素是指磁共振三维图像里的一个小立方体单位。一般大小为 2 立方毫米。一个体素内包含上万个神经元。所谓“共同体素”是指，在人自己做动作的时候，和在他/她看到其他人做相同动作的时候，都被激活的体素。在脑电图的研究中，人们发现在颅骨的躯体感觉区记录到的一种 8～13 赫兹的脑电波（这一特定脑电成分被称为 mu rhythm）会在人自己做动作和看到他人做动作的时候波幅减小。Mu 波的抑制被作为对镜像神经系统的脑电研究中使用的指标。但是这两种指标是否都如我们所猜测的那样，反映了相同脑区（MNS）的活动呢？第三章中的实验就验证了这一假设。在这个实验中，我们让志愿者观看他人做动作的影片，或者让他们自己做一些类似的动作。志愿者观看动作和自己做动作时，他们的大脑活动被磁共振机器记录，同时他们的脑电活动也被记录了下来（图 2）。

之后我们将两种数据结合分析发现。脑电指标（Mu 波的抑制）与核磁指标（共同体素）在大部分 MNS 脑区是共变的。这些脑区包括下顶叶（Inferior Parietal Lobule）, 背外侧运动前皮层(Dorsal Premotor)和 BA2，但是不包括 BA44 区（图 3 的粉色区域）。这一结果为更好的整合使用功能磁共振和脑电图两类研究方法获得的结果提供了基础。

除了理解他人的动作，人类也很擅长理解和感知他人的感觉和情绪。当我们看到一个痛苦的人，我们可能会随之感到痛苦。这就是疼痛共情。研究发现，一部分在我们自身感到疼痛时被激活的脑区在我们看到他人疼痛时也会被激活（主要包括脑岛，扣带前回等区域）。有趣的是，我们并不是一直都在与他人共情的。比如我们看到一个自己非常厌恶的人疼痛时，不仅不会感到痛苦，相反还会感到复仇的愉悦。而当我们的爱人，亲友疼痛时，我们感同身受。在本论文第四章的实验中，我们研究了“造成他人疼痛的责任”这一因素对疼痛共情的影响。例如，一个人腿骨折了。A) 是因为你开车不小心撞到了他。B)因为他自己喝醉了摔下了楼梯。在 A) 中，你对他的疼痛负有责任，而在 B) 中，你没有造成他的疼痛。这两种情况下，当你看到他痛苦的表情，你是否会有不同的感受呢？ 在实验中，我们每次招募两名志愿者。一名在核磁机内被扫描，另一名在机外的房间里。两人在电脑上同时做一个注意力测试游戏。每一次，如果有一个人做错了，或者两人都做错了，在机外的人就会受到疼痛电击一次。在核磁机内的人会通过闭路电视看到另一个人被电击。这样，核磁机内的人在造成机外人的疼痛中，有三种不同程度的责任。第一种，零责任（机外的人做错了,核磁机内的人没有做错）； 第二种，部分责任（两人都做错了）；第三种，全责（只有核磁机内的人做错了）。我们比较不同责任情况下，核磁机内的人看到机外的人被电击时候的大脑活动，发现当核磁机内的人负全责的时候，与疼痛共情相关的脑区（如脑岛等）被强烈激活了，而在部分责任和零责任情况下，激活则微弱的多（图 4）。我们还发现辅助运动区（Supplementary motor area）在将责任信息转换为疼痛共情的过程中起了重要作用。

另外一个我们认为可能影响疼痛共情的因素是“金钱补偿”。比如当你了解到一个因为工作摔断腿的人获得了一大笔经济补偿的时候，当你看到他痛苦的表情，你是不是会感觉不那么难受了呢 ？事实上，除了帮助受害者，金钱补偿的另一个重要社会作用就是减轻这种负性刺激给旁观者带来的压力和不快。为了验证这一假设，我们进行了一个行为实验。我们招募志愿者，之后通过闭路电视给他们观看一个人被电击。在每次电击前，他们会被告知，下一次电击是否会给予被电击者经济补偿。看完电击后，他们被要求对被电击者和自己的感受做出主观评价。结果有两方面，其一，我们确实发现当疼痛电击得到经济补偿时，观看者会认为被电击者感受到较低的不愉悦感。另一方面，我们发现，当被电击者得到了金钱，但是没有受到疼痛电击的时候，观看者会觉得不满，这种不满程度与嫉妒相关。目前我们在进行一项功能磁共振的实验，以便进一步探索金钱补偿效应的脑机制。

在这四年的时间里，我的研究课题从动作跨越到情绪，研究方法从脑电图，肌电图，跨越到功能磁共振，一直在尝试着解开人脑社会性的秘密。未来有无数的问题在等待着研究者们的努力，我将满怀好奇心和决心坚定的继续下去。

Acknowledgments

It has never been part of my plan to come to the Netherlands. I happened to get a scholarship from the Chinese government then I was somehow pushed overseas. Now, after over 4 years, I would like to say that it is the best thing happened to me.

It completely changed my life. A brand new world is opened in front of me. Here, I found the direction of my career, I determined what I want to dedicate to for the rest of my life and I am changed to a person I like more.

Valeria, you are the first person I want to say Thanks (with a big hug). You are the person I spent most time with during these years, the support and care you generously offered are extremely important for a girl 5,000 km away from home. You are the person who taught me how to be a serious, devoted scientist and be a passionate, lovely woman. You did change me from many aspects.

Christian, thank you for giving me the chance to come to this new world; thank you for leading me through all these years; thank you for showing me how to make science and thank you for all the teaching, sharing and supporting. Your encouragements and praises gave me confidence and motivations. You will always be my supervisor and my dear friend.

All my group members in Amsterdam: Leo, Lawrie, Nienke, Maria, Rajat and Fillippo. Actually, you guys are not only my colleges but also “my friends” and “my family members”. You guys make me expect to come to work every morning and leave the office with a smile every evening. Every hug, every joke, every comfort, every smile of yours will stay in my heart.

My friends in Groningen, Luca, Marc, I cannot quickly adjust to European life and without your help and support. You guys helped me overcome the worries and fears to be aboard and started to open myself to the new place. A lot of Thanks to you!

My co-workers, Dan, Judith and Abdel, it is my pleasure to have the chance to work with you. All of you are brilliant, nice and funny. We learned, worked and improved together, what wonderful experiences!

All my Chinese friend in Netherlands, Xinrui Qi, Xin Jin, Ning Chen, Juan Zhao, Ling Shan, Jing Zhao, Xiangfei Chai, Xiaofei Li, Shangfeng Gao, Yan Su, Zhi Zhang and Jason Liu. My life became more colourful and happier because of you. Friendships with you guys are the best bonus I got!

My supervisor in Graduate School and my future boss: Yuejia Luo: you are the first person took me into this field. Without your help I won’t even start working on science. What you gave me is not only academic help and support but also care and encouragements. You are like a father to me for all these 7 years. Thank you!

My dear Dad, Mum, I always feel blessed to have such a perfect family. The love and cares we give to each are unconditional and pressure-less. You are always my shore. I know that I can be nobody outside, but always the best in your eyes.

Finally, I want to dedicate this thesis to my Grandpa and Grandma. We spent nearly 30 years together, how lucky we are. You raised me, taught me, loved me and shaped me. You are always the most important persons in my life and I know I am the same in your life. I miss you.

亲爱的爸爸，妈妈，我一直觉得自己非常幸运能拥有一个如此完美的家庭。你们给我的爱一直是如此的温暖，没有条件，没有压力。你们一直是我的坚实后盾和温暖的港湾。我一直知道即使我在外面不名一文，我在你们的眼中也永远是最好的。

最后，我要把这篇论文献给我的姥爷和姥姥。我们是如此幸运得以彼此陪伴 30 年。你们二老抚养了我，教育了我，塑造了我。你们永远是我人生中最重要的人，我知道，我也是你们生命最重要的人。我很想你们。

Publication List

Publications

Arnstein D, Cui F, Keysers C, Maurits NM, Gazzola V (2011) μ-suppression during action observation and execution correlates with BOLD in dorsal premotor, inferior parietal, and SI cortices. Journal of Neuroscience.31, 14243-14249 (Shared first authorship)

Cui F, Luo YJ (2009) Facial Expression Processing of People with Different Empathic Abilities: An ERP study. Chinese Journal of Clinical Psychology Vol.17.No.4.

Cui F, Luo YJ (2008) A Review of Cognitive Neuroscience Studies on Empathy. Advances in Psychological Science. 2008, 16(2):250-254.

Papers in Prepration

Cui F, Arnstein D, Keysers C, Maurits NM, Gazzola V (2013) Functional Magnetic Resonance Imaging Connectivity Analyses Reveal Efference-Copy to Primary Somatosensory Area, BA2. (Shared first authorship)

Cui F., Keysers C., Abdelgaba A., Gazzola V. (2013) Responsibility Increases Vicarious Activations to the Pain of Others.

Cui F., Suttrup J., Keysers C., Gazzola V. (2013) Does Monetary Compensation for physical pain buffer empathic response or induce jealousy?

Posters& Presentations

Cui F (2013) Responsibility modulates empathy for pain. Neuroscience& Vision symposium, Netherlands Institute for Neuroscience, Amsterdam, the Netherlands (Oral)

Arnstein D., Cui F., Keysers C., Maurits N.M., Gazzola V. (2011) Mu-suppression during action observation and execution correlates with BOLD activity in dorsal premotor, inferior parietal and somatosensory cortices. Opportunities and challenges in social neuroscience. Utrecht, the Netherlands (Poster)

Cui F., Keysers C., Gazzola V. (2012) Responsibility modulates empathy for pain. Human Brain Mapping (HBM). Beijing, China (Poster)

Distinguishing and Connecting Self and Other:
A social neuroscience perspective

If you have seen the movie starred by Will Smith "I am legend" you might be shocked by the feeling of desperation and loneliness.
Born as social animals, it is curial for our survival to be able to distinguish and connect self and others. "How does our brain work when performing these social functions?" This is the question we want to answer in this thesis using a combination of functional Magnetic Resonance Imaging (fMRI), ElectroEncephaloGraphy (EEG) and ElectroMyoGraphy (EMG) technologies.
Here, you will find out how our brain differentiates active and passive body movement; how fMRI and EEG were used to discover how you share the actions of others; why you feel the pain of others more when you are fully responsible for their suffering compared to when you are not or partly responsible; and why knowing that the suffering person receives monetary compensation makes you feel better.
This thesis will shed light on some of the mystery of our social nature.

Fang Cui

Fang Cui is born in Taiyuan, China in 1982. She studies computer science from 2001 to 2005 at University of Science and Technology in Beijing. From 2006 to 2009, she studied neuroscience in Beijing Normal University, National Key Laboratory of Cognitive Neuroscience and Learning. She graduated with a Master degree of Science in June, 2009.After graduated, she determined to continue her interest in research. She came to Univeristy of Groningen with a Chinese National Scholarship and became a PhD student in Prof. Christian Keysers lab. From September, 2009 till now, she worked with Christian Keysers and Valeria Gazzola on the topic of mirror neuron system and empathy. After the completion of her PhD, she will go back to China and continue her research in Institute of Affective and Social Neuroscience (IASN) in Shenzhen University.